HYDRAULIC ANALYSIS OF THIBA MAIN CANAL REACH IN MWEA IRRIGATION SCHEME, KENYA

IMBENZI JAIRUS SEREDE

A Thesis Submitted to the Graduate School in Partial Fulfillment for the Requirement of the Degree of Master of Science in Water Resources and Environmental Management (WREM) of Egerton University

EGERTON UNIVERSITY

OCTOBER, 2015

DECLARATION AND RECOMMENDATION

DECLARATION

I, Imbenzi Jairus Serede do declare that this thesis is my original work and that it has not been submitted to any other University for award of any degree.

Signature: …… Date: ……

IMBENZI JAIRUS SEREDE

BM13/2768/10

RECOMMENDATION

This thesis is the candidate's original work and has been prepared with our guidance and assistance as supervisors. It is submitted for examination with our approval as official University supervisors.

Signature: …….. Date: ……

Prof. Benedict M. Mutua

Department of Agricultural Engineering,

Egerton University

Signature: …….. Date: ……

Dr. (Eng). James M. Raude

Soil, Water and Environmental Engineering Department,

Jomo Kenyatta University of Agriculture and Technology

COPYRIGHT

DEDICATION

To Almighty GOD for making all things be. Secondly, to the cherished memory of my beloved father Mr. Japheth Miheso Silingi (1954 - 2011), whose promising life was untimely nipped in the bud before witnessing fulfillment of my academic ambitions.

To my friends Siele, Lolming'ani and Lokwaliwa for their moral, material and financial support they offered. Finally to my beloved wife Davine, daughter Branice and son Bradley, who endured my inadequate attention during the study period. May you live long to reap benefits that will accrue from the study.

ACKNOWLEDGEMENT

The success of this research and preparation of this thesis is attributed to the support received from varied sources. Special thanks to the Almighty God for His guidance, faithfulness and sufficient grace that enabled me to remain determined to this moment.

Sincere gratitude is to my employer, National Irrigation Board, who granted me time to complete this program despite the tough work schedule, which I am grateful. More so, I express my deepest appreciation to my supervisors Prof. Benedict M. Mutua and Dr. (Eng.). James M. Raude for their encouragement, guidance and patience in realization of this work. The success of this research and production of the thesis is attributed to their invaluable ideas, support, constructive criticism, guidance and improvement of its logical flow.

Special thanks to Mr. Tutsuo Morishita and Abdullahi M. Juma of RiceMAPP project and Mr. Peter Orwa of Mwea Irrigation Scheme (MIS) for their support during data collection which was pivotal for analysis of this work. I would also like to thank Eng. Donald Wasike of GIBB Africa International for his guidance and ideas on development and interpretation of the as-built canal profiles for Thiba Main Canal (TMC). Further appreciations to all technical staff at Mwea Irrigation Agricultural Development Centre (MIAD) and all the lecturers from Faculty of Engineering and Technology, Egerton University, who were involved in disseminating the knowledge that made me, complete my research work. I believe that the materials and academic ideas gathered and their input into my thesis will remain to be a reminder of my being at Egerton University.

Further, I salute Water Resources and Environmental Management (WREM) class of 2010 (3 students all from different Counties in the Country) for their camaraderie and limitless support that always left me appreciating the meaning of teamwork during our course work; you were simply wonderful!

Last but not the least, my sincere thanks to my dear wife; Davine Minayo for her encouragement and lovely support during the study period. Her moral contribution is highly appreciated particularly during data collection and thesis writing. Furthermore, special thanks to my family for their continued support in my quest for knowledge and for their unwavering love and affection that, always gave me a cause to keep going.

ABSTRACT

As population continues to increase especially in African and Asian countries, demand for more food is equally increasing. There have been challenges in meeting the food security needs in most countries especially those depending on rain-fed agriculture. Although a number of countries are addressing the shortfall by investing heavily on irrigated agriculture, the availability of irrigation water still remains one of the major challenges. Irrigation has been ranked as one of the activities that utilize huge amounts of water with global values estimated between 70-80% of the available fresh water. Kenya is one such country facing the challenge of having enough water available for irrigation. To supplement rain-fed agriculture in Kenya, a number of food crops are grown under irrigation. One of these food crops whose demand as a staple food has continuously increased is rice which in Kenya is grown in irrigation schemes. Mwea Irrigation Scheme (MIS) continue to face various challenges that include; high irrigation water demand, vandalism, inadequate system calibration and minimal measuring devices. Due to water shortage in addition to poor operation and maintenance of hydraulic structures within irrigation schemes, rice production is far below the required quantity. To address these challenges, this research focused on a number of strategies which include; improved design of the main canals, proper management and operation of hydraulic structures and proper scheduling of water release to the farmers. In order to realize these strategies, Hydrologic Engineering Center - River Analysis System model (HEC-RAS) was applied. The model was calibrated and validated using two sets of observed discharges and water levels. In addition the model was used to simulate the hydraulic behaviour of Thiba Main Canal (TMC) reach in MIS. The model was used to simulate different flows in the main canal for varied design discharges through the sluice gates and drop structures. Statistical and graphical techniques were used to assess the model against its performance. The model was finally used to estimate the potential capacity of the main canal reach. The results show that HEC-RAS model is capable of evaluating the canal hydraulics under steady state conditions. The results from this study further show that increasing the hydraulic resistance of Link Canal II (LCII) from 0.022 to 0.027 resulted in a decrease in estimated maximum capacity by 10.97%. In the case of Thiba Main Canal, increasing the roughness coefficient from 0.015 to 0.016 resulted in a decrease in estimated maximum capacity by 11.61%. The Link canal II and TMC were capable of only allowing flows of 9.9 m^3/s and 5.7 m^3/s respectively. These research findings would therefore be a basis for the scheme management and operators to improve on the operation, management and maintenance of the irrigation system for effective and efficient water delivery to the farmers.

TABLE OF CONTENTS

LIST OF TABLES

LIST OF FIGURES

LIST OF ABBREVIATIONS AND ACRONYMS

Abbreviations	Description
1-D	One Dimensional flow
2-D	Two Dimensional flow
ASAE	American Society of Agricultural Engineers
ASCE	American Society of Civil Engineers
CANALMAN	Canal Management Model
DEM	Digital Elevation Model
DSS	Decision Support System
DUFLOW	Dutch Flow Model
FAO	Food and Agriculture Organization
FLOP	Flow Profiles Model
GDP	Gross Domestic Product
HEC-RAS	Hydrologic Engineering Center - River Analysis System
JICA	Japanese International Cooperation Agency
MIAD	Mwea Irrigation Agricultural Development Centre
MODIS	Modelling Drainage and Irrigation System model
NERICA	New Rice for Africa
O & M	Operation and Maintenance
OCF	Open Channel Flow
RiceMAPP	Rice-based Market-oriented Agriculture Promotion Project
SAPROF	Special Assistance for Project Formulation
SIC	Simulation of Irrigation canal model
SRI	System of Rice Intensification
SSARR	Stream flow Synthesis and Reservoir Regulation
TBC-1	Thiba Branch Canal 1
TBC-2	Thiba Branch Canal 2
TBC-3	Thiba Branch Canal 3
TBC-4	Thiba Branch Canal 4
USM	Unsteady Model
WARDA	West Africa Rice Development Association
WREM	Water Resources and Environmental Management
MASSCOTE	Mapping Systems and Services for Canal Operation Techniques

CHAPTER ONE
INTRODUCTION

1.1 Background information

Water use and competition among different users has been growing at more than twice the rate of population increase over the last century. For instance, water use for irrigation accounts for about 70-80% of the total freshwater available worldwide and irrigation has been ranked as one of the activities that utilize huge amounts of fresh water in many countries. In the near future, less water will be available for agricultural production due to competition with other sectors (Molden, 2007). At the same time, food production will have to be increased to feed the growing world population rate estimated at 81 million persons per year (UN, 2013) or about 9 billion people by 2050 (Munir and Qurreshi, 2010). As a result of population growth and rising incomes, worldwide demand for cereals such as rice has been projected to increase by 65% (de Fraiture *et al*., 2007). For instance, Seck *et al*. (2012) projects that global rice consumption will rise to 496 million tonnes by 2020 and further increase to 555 million tonnes by 2035. These authors further state that aggregate global rice consumption is still expected to increase through 2035 due to increased demand in Africa, Latin America and parts of Asia.

It has been further estimated that the world will need to feed 1.5 to 2 billion extra people by 2025 (Rosegrant *et al.*, 2002). Thus, agricultural sector which is considered to be the largest water user may face a serious challenge in producing more food with less water (FAO, 2011). Although the expansion of land for agricultural activities has continued to increase over the years, there is still a demand for more food to match the population. This is associated with insufficient water for irrigation to match the increased expansion of agricultural land. However, considerable efforts have been devoted over time to introduce new technologies and policies aimed at increasing efficient water resources management especially for irrigation.

To improve on irrigation systems so as to supplement rain-fed agriculture and realize increased yields per unit area, many countries in the world are investing more resources in irrigation. The demand for food in many African countries has overshot production since most of these countries depend on rain-fed agriculture. Some of these countries have opted to import food to bridge the deficit. For instance, the demand for rice which is a staple food and constitutes a major part of the diet has consistently increased overshooting its production

(FAO, 2006). High quantities of food are being imported at the expense of local production in an attempt to meet these deficits. For example in 2006, the Sub-Saharan African countries consumed a total of 14.7 million tonnes of milled rice (WARDA, 2007). Among identified constraints to local food production is adequate availability of water resources. Further, low overall irrigation efficiencies associated with improper irrigation systems' operation and maintenance are additional factors linked to low rice production (Maghsoud *et al.*, 2013).

Rice is the third most important food after maize and wheat especially for the urban population in Kenya (Keya, 2013). It is mainly grown under surface irrigation where water is applied in basins by flooding the paddy fields. To meet the high water requirements, proper water management is inevitable. However, most irrigation schemes in Kenya continue to experience chronic water shortages. For example, in Mwea irrigation scheme (MIS), rotational water application method has been introduced due to constrained water supply. Farmers have thus been divided into three rotational groups on the cropping calendar that falls between the months of August and April (CMC, 2011).

Due to water shortage for irrigation in MIS, it is inevitable that the little available water needs to be utilized more efficiently. This can be achieved through several strategies that include; proper design of canals, hydraulic structures and proper scheduling for water release to farmers. To achieve this, a total change in operation and maintenance of the systems is required (Maghsoud *et al.*, 2013). In addition, further efforts have been developed to manage the limited available irrigation water such as the introduction of New Rice for Africa (NERICA) varieties which thrive in the uplands areas. Further, the use of System of Rice Intensification (SRI) which allows rice paddy to be grown in straight lines at a specified spacing leading to higher yields of rice is also another strategy being used (Omwenga *et al*., 2014).

Maintenance of irrigation scheme infrastructure consisting of canals, roads and water management structures requires substantial amount of funds. Furthermore, preparation of a workable maintenance schedule may lead to disruption of the cropping programme leading to exorbitant losses to farmers. In order to address this challenge, proper understanding of the irrigation canal hydraulics and water management within the scheme can be assessed by use of HEC-RAS model as was the case in this study.

1.2 Statement of the problem

Mwea Irrigation Scheme (MIS) currently directs every effort to supply irrigation water to command 9,080 ha. This water was originally available to the nuclear farm with a command area of 6,600 ha only. This corresponds to an additional increase of 37.6% in command area (Koei, 2008). Further, over the last two decades, the out-growers whose farms were originally not part of the command area have expanded their own land from 1,200 ha to 3,100 ha and yet, still rely on the MIS irrigation water supply infrastructure. The corresponding water requirements showed that the combined peak demand was more than the supply from the three headworks at Nyamindi, Thiba and Rubble weir on Thiba River. The available flow during the peak demand period was 11.81 m^3/s against the peak irrigation demand of 15.02 m^3/s (Gibb, 2010). Intensive use of land and water together with rapid expansion of the scheme, for instance, expansion to Mutithi area located at the south west border of the existing MIS and inclusion of the out-growers into the cropping programme has over stretched the existing scheme infrastructure. Despite recent rehabilitation efforts that involved lining of the conveyance canals, no recalibration of the system has been done. Water is still applied with minimal measurements to ascertain if the irrigation infrastructure is under or over loaded in its utilization. However, most of the irrigation systems have only minimal facilities for water measurement. The combination of all these challenges from manual operation of canals with a number of controls, lack of adequate and reliable data from both the main and on-farm systems, has culminated to unreliable decisions making process. These have greatly affected accurate operations of the scheme. Hydraulic calibration of canals is considered a prerequisite in effective canal management and an important activity in improving the performance of an irrigation system. Canal simulation models offer unlimited opportunities of achieving this by studying the flow behaviour in large and complex canal network under a variety of design and management scenarios. These models are being adopted for efficient water management in large irrigation schemes in developed countries (Ochieng *et al.,* 2010). Therefore, there was need to carry out hydraulic analysis of the Thiba main canal reach to determine its potential capacity and realize efficient water management.

1.3 Objectives

1.3.1 Main Objective

The main objective of this study was to carry out hydraulic analysis of Thiba main canal reach in Mwea Irrigation Scheme, using HEC-RAS model as a decision support tool for effective operation and management of the irrigation system.

1.3.2 Specific objectives

The specific objectives of this study were to:

i. Evaluate the effect of hydraulic and structural variations on Thiba main canal reach potential capacity using the HEC-RAS model
ii. Formulate improved operational and maintenance procedures for Thiba main canal system using HEC-RAS model as a decision support tool

1.4 Research questions

i. How does the variation of the hydraulic and structural parameters affect canal discharge capacity?
ii. How does HEC-RAS model assist in formulation of operational and maintenance procedures for Thiba main canal reach?

1.5 Justification

Rice has been considered as a food crop that takes a shorter time of three months to mature (Trimmer, 2010). Adequate production of rice can thus make a country food secure hence a key way of achieving the Sustainable Development Goal (SDG) number two on ending hunger, achieving food security, improved nutrition and promotion of sustainable agriculture (John and Fielding, 2014). The Kenyan Government therefore targets to double rice production under irrigation as per the National Irrigation Board's (NIB's) 2014-2018 Strategic Plan. The NIB 2014-2018 strategic plan is also in line with the country's Vision 2030 targeting food production through development and rehabilitation of existing irrigation systems especially in Arid and Semi-arid Lands (ASALs) (GoK, 2013). Improving the performance of major irrigation projects is one of the economically viable options in meeting the growing demands and sustaining the productivity of irrigated agriculture under the present financial, environmental, and physical constraints (Islam *et al.,* 2008). Achievement of these targets, require development of strategies to manage the limited irrigation water. Among these strategies is by planting rice varieties that are less water consuming and

promotion of research and innovation. This can also be complimented with water storage and the system of rice intensification (SRI). In addition to these strategies, this study focused more on efficient procedures for proper canal system operation and maintenance of existing irrigation schemes in addition to development of new irrigation schemes in the country.

1.6 Scope and limitation of the study

This study covered Mwea Irrigation Scheme in the upper Tana River basin of Kirinyaga County, Kenya. The focus was on the Thiba main canal reach which comprises Thiba head works, Link Canal II and Thiba main canal. Although the study focused on improved irrigation water management, it did not consider the water loss through canal seepage and evaporation. In addition, very limited research work was carried out on sediment transport and water quality simulations due to limited resources. However, preliminary insights on these parameters were taken into account.

CHAPTER TWO
LITERATURE REVIEW

2.1 Open channel flow

Open channels are conduits for flow with a free surface. The free surface rises and falls in response to flow perturbations caused by changes in channel slope or width (Chanson, 2004). The fluid in these channels flow under hydrostatic pressure produced under action of the fluid weight. Open flow channels can thus be classified as either natural or artificial. Natural channels refer to those developed by natural processes and have not been significantly improved by human. Artificial channels on the other hand refer to those which have been developed by human effort. Examples of artificial channels include navigation and irrigation canals, drainage ditches, culverts flowing partially full and spillways.

The main parameters linked with Open Channel Flow (OCF) include; canal geometry, properties of flowing fluid and flow properties (Chanson, 2004). Water flow in a single or network of canals has always been a major interest for irrigation engineers (Novak *et al.*, 2010). Many studies have been carried out on open channels using hydraulic models. One of these hydraulic models that has been widely applied especially in relation to flood denudation severity studies is the HEC-RAS (Gautum and Kharbaja, 2006; Shahrokhnia *et al.*, 2008).

2.2 Classification of open channel flow

Open channel flow is classified as steady, unsteady, uniform or non-uniform flow, although the flow can also be classified as steady uniform, steady-non uniform or varied flow. Flow in open channels is referred to as steady if all flow properties such as velocity and depth are independent of time. For a given channel, steady flow consists of various fetches considered as uniform, gradually varied or rapidly varied flows, while examples of unsteady flow include; waves, surges and tidal flows (Nalluri *et al.*, 2009).

In uniform flow, the depth and cross stream velocity profile are independent of downstream distance. This can only occur in a long channel of uniform cross-section, constant slope and no side streams. Steady uniform flow is also called normal flow. In uniform channels, all flows tend to normal flow if there is sufficient fetch.

In gradually varied flow, the water depth changes slowly with streamwise distance (usually over distances of hundreds or thousands of times the flow depth) because of an imbalance

between gravitational and frictional forces. This may occur as a result of a change in channel conditions which include; slope, cross-section, and roughness or as an adjustment brought about by the upstream or downstream disturbances such as weirs and sluices. Since the variation is gradual, the flow can still be treated as one dimensional (1-D) where it varies in the direction of flow alone and the pressure is hydrostatic (Chadwick *et al.*, 2013).

Rapidly varied flow occurs when the flow adjusts over relatively short distances (a few times the flow depth). Classic examples are hydraulic jumps, as well as flow conditions induced by construction of hydraulic structures such as weirs, venturi flumes and sluice gates. Because the streamwise distance is relatively short, the rapid changes to flow properties can often be obtained by neglecting bed friction. In many situations, the flow in an open channel is of non-uniform depth along the channel. This type of flow conditions comes about because of changes in the channel cross-section, slope, and obstructions such as gates in the stream path (Chanson, 2004).

2.3. Flow conditions in open channels

Flow conditions in open channels are essentially governed by gravity, inertia and viscous forces. The Froude Number indicates the effect of gravity on the state of flow and it is computed using Equation 2.1. It is represented by a ratio of inertial forces to gravitational forces (Chow, 1959).

$$F_r = \frac{V}{\sqrt{g h_d}} \tag{2.1}$$

Where,

F_r = froude number

g = acceleration due to gravity (m/s^2)

h_d = hydraulic depth (m)

V = average velocity (m/s)

For non-rectangular channel,

$$h_d = \frac{\mathrm{A}}{b} \tag{2.2}$$

Where,

A = cross-sectional area normal to the direction of flow (m^2)

b = surface width (m)

The dimensionless Froude number is used to characterize the flow regime. When the Froude number is equal to one, the flow is termed critical flow. Analysis of flow in open channels begins with a point where critical depth occurs. When the depth of flow in a given channel is equal to the critical depth, the flow is referred to as critical. This is the condition where simple waves can no longer spread upstream (Bitner, 2003). When the Froude number is greater than one, the flow is termed supercritical flow. This flow is characterized by high velocities where inertial forces become dominant at a cross-section. If the Froude number is less than one, the flow is termed subcritical flow. Subcritical flow is characterized by low velocities and is dominated by gravitational forces (Chow, 1959).

The rise of water level, which occurs during the transformation from supercritical to subcritical flow is called hydraulic jump. These phenomena occur frequently in canals where a steep channel bottom slope suddenly changes to a flat slope. Subcritical flow scenarios are very common in natural and man-made channels. In subcritical flow, direct step computations would begin at the downstream end of the reach, and progress upstream between adjacent cross-sections. Gradually varied flow (GVF) and rapidly varied flow (RVF) conditions are summarized in Figure 2.1 which was adopted from Chow (1959). However, steady state flow conditions are always considered in irrigation canal design and canal simulation.

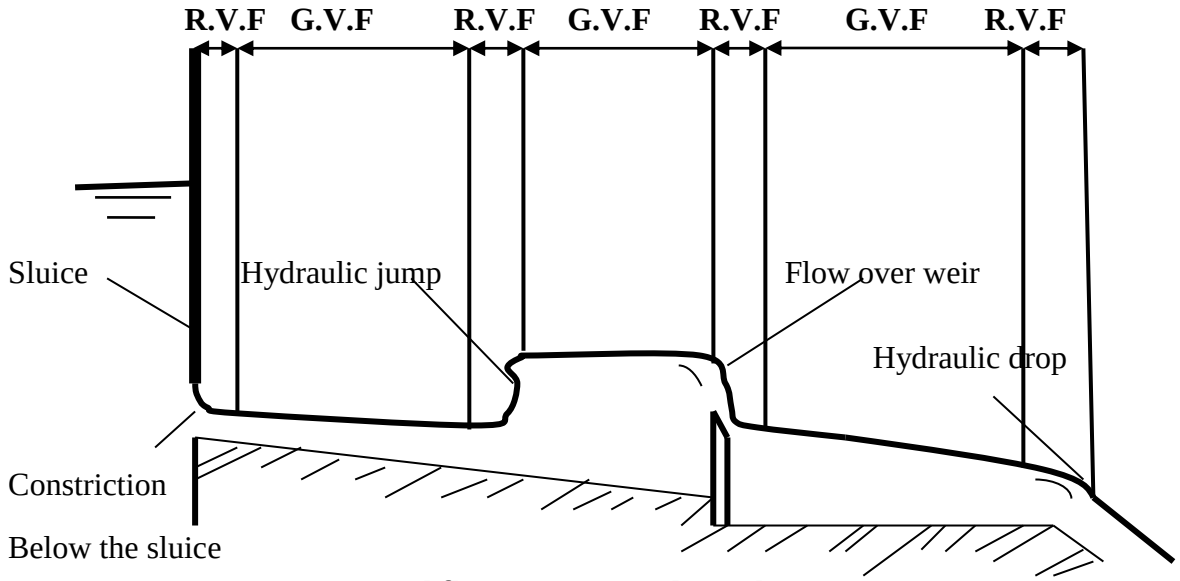

Figure 2.1: Varied flow in an open channel

2.3.1 Computational methods

There are two commonly used procedures in the design and analysis of Open Channel Flow (OCF). The two procedures are the direct and the standard step methods. The direct method is a procedure in which the water depth is known at two locations and the distance between the two locations is considered (Kragh, 2011). Standard step method on the other side applies the hydraulic equations to iteratively calculate water surface profiles and energy grade lines. This method applies the conservation of energy phenomenon in the calculation of water-surface elevations and energy lines along the reach between cross-sections as illustrated in Figure 2.2.

Standard step method is one of the coded algorithms in hydraulic models such as HEC-RAS model which is one of the commonly used hydraulic models in analyzing flow behaviour of open channels. Depending on the nature of the flow, the model iteratively calculates a water surface profile and energy grade line beginning with a certain cross-section upstream or downstream. For instance, if the flow is supercritical, HEC-RAS model can be used to calculate the profiles beginning with the most upstream cross-section. If the flow is subcritical, the profiles are calculated beginning with the most downstream cross-section (USACE, 2001).

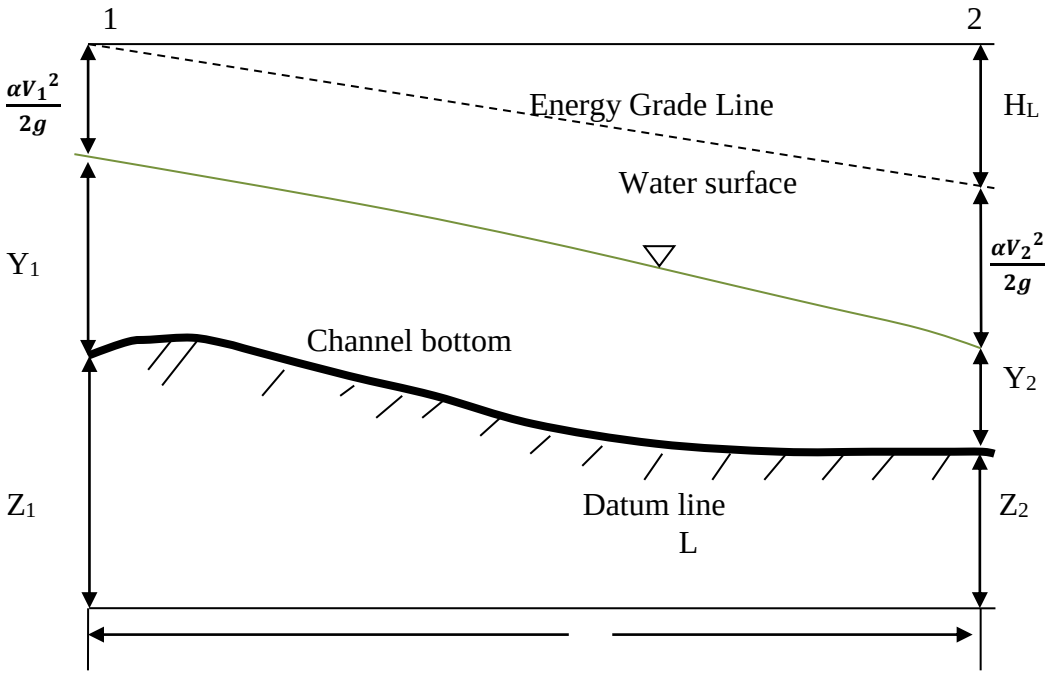

Figure 2.2: Water surface profiles and energy lines between two points

2.4 Irrigation canals

Irrigation canals are mainly man made channels and are used to convey water from an intake to the command area. Canals have been used for irrigation since the ancient Roman times (Mays, 2010). Over the years, improvements of conveyance efficiencies have been achieved through enhanced designs and construction. This has been through use of different materials for canal lining. Such materials include; clay, concrete, wood, rocks and plastic. Existing streams can also be canalized by widening the banks and regulating the flows to serve end users according to need. Irrigation canals are thus classified according to type, use, construction materials, length, size and nature (Sharma and Sharma, 2007). Some of the commonly used classification types include; earth canals, concrete, main, drain, feeder, primary, secondary, tertiary and either lined or unlined canals.

2.4.1 Causes of canal malfunctioning

Irrigation canals are ideally designed to ensure water is conveyed without scouring the bed or depositing sediment in the channel. Well designed and newly compacted earth lined canals have reduced seepage losses similar to concrete lined canals. However, regular and consistent maintenance is required to minimize seepage losses (Hill, 2002).

Canals can deteriorate in functional use due to different causes. Some of these causes include; sediment deposition, canal erosion and frequent overtopping of the canal banks, vandalism of structures especially stop gates, excessive loading of the canal, poor workmanship during construction and floods. As a routine in irrigation schemes, maintenance is often delayed until the end of a cropping season leading to costly rehabilitation due to over grown weeds which endanger the lined sections and thus resulting to inaccurate estimation of flows into the feeder canals as it is in the case of this study.

2.5 Hydraulic structures

Hydraulic structures are facilities constructed to divert, restrict, stop, or otherwise manage the natural flow of water. The hydraulic structures include; weirs, orifices, flumes and gates. Among the many uses of these hydraulic structures, flow measurement is the most common. The structures are made from materials ranging from large rock and concrete to obscure items such as wooden timbers or tree trunks (Khatib, 2009). A dam, for instance, is a type of hydraulic structure used to hold water in a reservoir as potential energy, just as a weir is a type of hydraulic structure which can be used to pool water for irrigation, establish control of the bed or to divert flow away from eroding banks or into diversion channels for flood control (Kay, 2007). In Kenya, majority of these canals are earth lined leading to excessive losses of water through seepage.

2.5.1 Weirs

A weir is a structure constructed across a channel which raises the upstream water level and may be used to estimate flow rates through the given section of the channel or stream (Singh, 2009). Weirs are commonly used as measuring devices in flumes and channels. Their use dates from the backbone of the national hydrometric system, which provided accurate discharge information to facilitate development planning, flood forecasting, planning, development of flood alleviation schemes and water resources regulation (Mays, 2010).

Weirs can be used to provide information on flow rates, but those not specifically designed for this purpose are likely to give only approximate data (Clemens, 2012). Flow gauging weirs permit engineers and water managers to calculate the discharge in a river or canal reach, monitor it over time, and if real time monitoring is available, to issue flood warnings in order to adjust the flood control structures in response to changing conditions. In their

operational use, weirs have widely been used to abstract water from the rivers for irrigation rather than for flow estimation.

2.5.2 Weir classification

Weirs are classified depending on the existence of the ventilation below the nappe as either free fall or submerged weirs. The discharge equation which is the result of the depth-flow relationship associated with free flow conditions is given as:

$$Q = Cbh^{3/2} \tag{2.3}$$

Where,

Q = flow rate (m^3/s)

C = coefficient of discharge

b = length of the weir crest (m)

h = water depth above the weir crest (m)

Weirs are further classified according to common shapes and width of the weir crest. The classifications include; rectangular, triangular (V-Notch) and trapezoidal, sharp and narrow crested weirs, broad crested weirs and practical profile weirs according to width of the weir crest. Although a universal equation that can accommodate all factors that control flow or that applies to all types of systems (Bansal, 2010) is not available, a general equation applicable to different weir types as given in Equation 2.4 can be applied. This equation is given by the relation:

$$Q = C_e L_e {h_e}^n \tag{2.4}$$

Where,

n = a power factor depending on the type of weir

When n is equal to 3/2, then Equation 2.4 becomes:

$$Q = C_e L_e {h_e}^{3/2} \tag{2.5}$$

Where,

Q = design discharge (m^3/s)

L_e = effective length of the weir crest (m)

h_e = effective water depth (m)

C_e = coefficient of discharge ($m^{1/2}/s$) given as in equation 2.6.

$$C_e = C_1 \left(h_1/p\right) + C_2 \tag{2.6}$$

However, the establishment of modular flow for weirs is necessary since it makes discharge or flow rates measurements possible by only measuring the flow head. For instance, the free overfall occurs, when the discharge is only a function of the upstream water level. This is expressed as:

$$Q = f(h_u) \tag{2.7}$$

Where,

f = function determined through measurements

h_u = water depth above the crest of weir level (m)

The flow relation given in Equation 2.7 may occur along the channel reach when a critical velocity or (shooting flow) develops and does not allow the propagation of downstream effects in upstream direction (May, 2003). The theoretical discharge for a free overfall can be determined for different weir geometric shapes. For instance, the free overfall with a rectangular shape is given as:

$$Q = \frac{2}{3} \sqrt{2g}\, b \left[\left(h_u + \frac{V^2 a}{2g}\right)^{\frac{3}{2}}\right] \tag{2.8}$$

Where,

Q = discharge (m^3/s.)

g = gravitational acceleration (m/s^2)

h_u = water depth above the crest of weir level (m)

b = length of weir crest (m)

V_a = approach velocity (m/s)

In this case, no allowance has been made for the local losses of energy and therefore, the result needs to be multiplied by an experimental factor, referred to as the discharge coefficient (C_d). For smaller velocities, the effect of velocity head $\left(\frac{V_a^2}{2g}\right)^{3/2}$ is normally neglected.

This reduces Equation 2.8 to:

$$Q = \frac{2}{3} C_d \sqrt{2g}\ b\ h_u^{3/2} \tag{2.9}$$

In this case, the value of $\frac{2}{3} C_d \sqrt{2g} = C$ is sometimes called the overfall coefficient, and the expression is reduced to:

$$Q = C b h_u^{3/2} \tag{2.10}$$

While C_d is a dimensionless value, the value of C always has a dimension, and is generally given in units of $m^{1/2}/s$. In the case of free overfall, the discharge or the value of the overfall coefficient depends on; the ratio of geometrical dimension, shape, side contraction of the weir, height of the crest above the bed level and the velocity of approach of the flow (Ratnayaka *et al.,* 2009).

2.5.3 Calibration of hydraulic structures

Calibration of hydraulic structures is the act of comparing and adjusting a measuring device against a standard. Calibration is performed for purposes of control of water distribution and knowledge of water loss in the main canal and distribution channels (Novak *et al.*, 2007). Accurate measurement of flow through structures such as irrigation canal gates makes it achievable for water managers to match supply and demand hence reducing losses and enabling delivery of optimum amount of water to crops (Wahl, 2004). Most accurate flow measurements are estimated using structures such as flumes and weirs. While remarkable improvements have been made in the use of flumes and weirs, there is also a potential for making use of gates to provide accurate flow measurements. Lack of calibration of the hydraulic structures has contributed to poor irrigation water management. Therefore,

hydraulic calibration of canals is a prerequisite in effective canal management and an important activity in improving the performance of irrigation systems.

2.5.4 Flow through canal gates

Canal gates can operate under orifice and non-orifice flow conditions. Either condition can occur under free or submerged flow regimes. Orifice flow occurs when the upstream depth is higher than the downstream water surface elevation (Omar, 2008). Submerged flow condition which is controlled using a vertical rectangular gate is represented in Figure 2.3.

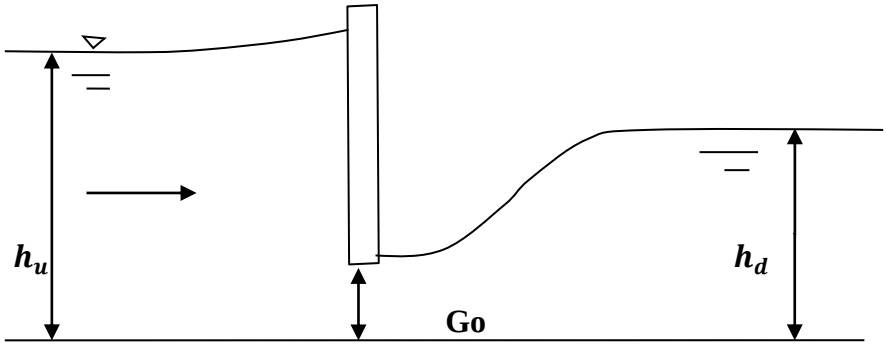

Figure 2.3: Submerged flow section

For non-orifice flow, the free flow equation is given as:

$$Q_f = C_f {h_u}^{n_f} \tag{2.11}$$

Where,

Q_f= free flow discharge

C_f = free flow coefficient

n_f = free flow exponent (for a rectangular structure, a theoretical value of 1.5 is used)

In this case, the downstream water surface elevation is less than C_cG_o where C_c is the contraction coefficient and G_o is the vertical gate opening, referenced from the bottom of the gate opening. Submerged flow discharge equation for a rectangular gate having an opening G_o and a width G_w which is given as:

$$Q_s = C_d\ G_o\ G_w\sqrt{2g\ (h_u - h_d)} \quad (2.12)$$

Where,

$C_d\ G_w$ is the area, A, of the orifice

2.6 Review of canal irrigation models

There has been a rapid increase of interest in flow modelling of irrigation canals since 1987 (Mutua and Malano, 2001). Since then, a number of computer based programmes have been developed. Most of the available unsteady flow simulation models for irrigation canals are fairly similar in accuracy. Although these models share a common general purpose, they differ in many specific aspects from the user's needs. Since this study was not to compare the performance of models, a very brief analysis of some of the commonly used canal flow models in irrigation was presented. However, a well conducted modelling study requires detailed knowledge of the system being modelled and the strengths and weaknesses of the model under consideration. The factors to consider when modelling are; model's complexity and data requirements, transferability of the model to other sites and conditions, in addition, the model's potential to predict specific effects of specific changes and implicit uncertainties in the model predictions was of great importance (Singh, 1996).

A model has to contain parameters that are sensitive to the reach changes taking place such as discharge, Manning's roughness and water depth. Some of the commonly used canal flow models in irrigation include; MODIS and DUFLOW (developed by Delft University of Technology), CANALMAN (developed by Utah State University), CARIMA (Holly and Parrish, 1991), USM (Rodgers and Merkley, 1993), SIC (Cemagref, France), PROFILE (developed by Delft Hydraulic in 1991), FLOP, Mike II (developed by Danish Hydraulic Institute in 1995), DORC (developed by HR Wallingford in 1992), SOBEK (developed by Delft Hydraulic in 1994), MASSCOTE (FAO, 2007), HEC-RAS (developed by the Hydrologic Engineering Center of the United States Army Corps of Engineers) and ODIRMO (developed by Delft University of Technology in1985).

Application of each model is dependent on specific assumptions which differ from one model to another. Some of the models require very huge data inputs which may limit their

application in cases where data is limited. The selection and application of a particular model therefore depends on the data requirements, knowledge by the user and the intended simulation purpose. This study reviewed the following commonly used models with a view to selecting the appropriate model for this study. These models were; USM, DUFLOW, CANALMAN, SIC, SOBEK, MASSCOTE and HEC-RAS.

2.6.1 USM model

The Unsteady Model (USM) which was developed by US Bureau of reclamation in 1993 is a fairly rigorous hydraulic-simulation model that incorporates accurate numerical solutions of the governing equations for a limited range of flow conditions (Khan *et al.*, 2008). The USM can accommodate various cross-sectional channel shapes and several automatic-gate-control algorithms either in metric or English units. The model has been used extensively for several years in the design and analysis of reclamation canals (Singh, 2003). The USM is commonly used for analyzing relatively rapid flow changes during a short time interval. However, its topology is limited to linear series of up to 40 canal pools separated by structures or boundary conditions. The model does not simulate advance on a dry bed, canal dewatering, hydraulic jumps, bore waves, supercritical flow or negative flow through structures. The maximum time span for a single simulation is 24 only hours (Tariq, 2010).

2.6.2 DUFLOW Model

The Dutch flow (DUFLOW) model was designed for simple networks of channels with simple structures. In this model, the water levels and flow rates are determined by solving the Saint Venant equations of continuity and momentum with Preissmann scheme (Aldrighetti, 2007). However, this programme is limited in handling some of the most sophisticated modelling needs such as dry bed condition and automatic gates, some of which this study dealt with.

2.6.3 CANALMAN model

The Canal management (CANALMAN) developed by Utah State University, USA performs hydraulic simulations of unsteady flow in branch canals networks only. It implicitly solves integrated form of the Saint Venant equations of continuity and motion for 1-D unsteady open-channel flow only. However, the CANALMAN is limited in customizing for specific modelling conditions (Huang and Fipps, 2009). This made it not to be selected for use in this study.

2.6.4 SIC model

The Simulation of Irrigation Canal (SIC) model developed in France by Cemagref, in early 1970's is a mathematical model, which can simulate the hydraulic behavior of irrigation canals under steady and unsteady flow conditions. The steady and unsteady flow computations can be performed on any type of hydraulic networks (linear, looped or branched). Although Saint Venant equations have no direct analytical solutions in real geometry, they are normally solved numerically by discretizing the equations. The SIC model can be considered a useful decision support tool for large canals to evaluate performance for better management and operation (Hassain *et al.*, 2013). This model though, has some limitation in handling simulation of canals with branches of networks and also in finer time steps.

2.6.5 MASSCOTE

The Mapping System and Services for Canal Operation Techniques (MASSCOTE) was developed by the Land and Water Division (NRLW) of FAO on the basis of its experience in modernizing irrigation management in Asia (Renault *et al.*, 2007). This model approach consists of eleven steps which are grouped into two main parts. It integrates tools such as the rapid appraisal procedure (RAP) and benchmarking to enable a complete sequence of diagnosis of external and internal performance indicators and the design of practical solutions for improved management and operation of the system. The modernization process is however not a one shot process, as it is estimated to take a maximum of 30 years and may thus require more fundamental restructuring and mobilization of resources. The model therefore was not a preferred mechanism to attain a solution for Mwea Irrigation Scheme due to uncertainty of input data and the extensive model structure.

2.6.6 SOBEK model

The SOBEK model is a highly sophisticated software package capable of solving equations that describe unsteady water flow, salt intrusion, sediment transport, morphology and water quality. It was developed by Delft Hydraulic in 1994 and can be used as a simulation model to solve problems in river management, flood protection, design of canals, irrigation systems, water quality, navigation and dredging (JI *et al.*, 2003). The SOBEK model consists of very few nodes especially for the available open source or trial versions hence, could not be selected for this study. More so, reliable licenses for these models are very expensive making the choice of other models such as the HEC-RAS preferable.

2.6.7 HEC-RAS model

The Hydrologic Engineering Center's (HEC) River Analysis System (RAS) model was developed by the Hydrologic Engineering Center of the United States Army Corps of Engineers. It is an open source software which can be obtained from the HEC web site: www.hec.uasce.army.mil along with its user manuals. The HEC-RAS model allows one to perform one dimensional (1-D) steady and unsteady flow river hydraulics calculations. It is one of the most commonly used models to calculate water-surface profiles and energy grade lines in 1-D, steady-state, gradually-varied flow analysis. The HEC-RAS model is compatible with and supersedes HEC-2 model (Bookman, 1999). However, in the 1-D, steady-state, gradually-varied flow analysis, the following assumptions are made:

i. Dominant velocity is in the flow direction
ii. Hydraulic characteristics of flow remain constant for the time interval under consideration
iii. Streamlines are practically parallel and, therefore, hydrostatic pressure distribution prevails over channel section (Chow, 1959)
iv. Channel slope is less than 0.1%

The model employs a form of the empirical Manning's equation to provide the relationship between the rate of discharge, hydraulic resistance, channel geometry and rate of friction loss. In case of changes in canal prism, energy losses are evaluated using contraction or expansion coefficients multiplied by the change in velocity head.

The fundamental hydraulic equations that govern 1-D, steady-state and gradually-varied flow analysis comprise the continuity, energy and flow resistance equations. In this case, the continuity equation describes discharge as constant and continuous over a specified period of time. This equation is given as:

$$Q = v_1 A_1 = v_2 A_2 \tag{2.13}$$

Where,

Q = discharge (m^3/s)

v_1 = average velocity at the downstream (m/s)

v_2 = average velocity at the upstream (m/s)

A_1 = cross-sectional area to the direction of flow at downstream cross-section (m^2)

A_2 = cross-sectional area to the direction of flow at the upstream cross-section (m^2)

The energy equation is used to calculate the total head of water as the summation of the bed elevation, average flow depth and the velocity head at a given cross-section. This equation illustrates the brief principle of water surface study in HEC-RAS model.

$$H = Z + y + \frac{\alpha v^2}{2g} \tag{2.14}$$

Where,

H = total head of water (m)

α = kinetic energy correlation coefficient

Z = bed elevation at a cross-section (m)

y = flow depth at a cross-section (m)

g = acceleration of gravity (m^2/s)

$\bar{v}$ = average velocity (m/s)

When two channel sections, A and B are taken into consideration, Equation 2.14 becomes:

$$Z_A + y_A + \frac{\alpha v^2}{2g} = Z_A + y_A + \frac{\alpha v^2}{2g} + \ H_L \tag{2.15}$$

In open channels, the energy equation according to USACE (2001) becomes:

$$(\partial A/\partial t)\,\Delta t \ = \ -V_m \ (\partial A/\partial L) - \ VA_m \ (\partial A/\partial L) \tag{2.16}$$

Where,

m = subscriptions for the mean values of V and A

L = channel length (m)

t = incremental time to be calculated

Energy loss between two cross-sections as illustrated in Figure 2.2 which comprises friction losses and contraction or expansion losses is given by Equation 2.17 as:

$$h_e = LS_f + \mathrm{C}\left[\frac{\alpha_2 v_2^2}{2\mathrm{g}} + \frac{\alpha_1 v_1^2}{2\mathrm{g}}\right] \tag{2.17}$$

Where,

h_e = energy head loss

L = discharge weighted reach length

S_f = representative fraction slope between two stations

C = expansion or Contraction loss coefficient

α_1, α_2 = velocity weighting coefficients

g = gravitational acceleration

v_1, v_2 = average velocities

In canal simulation, channel roughness is one of the sensitive parameters in the development of hydraulic models (Timbadiya *et al.*, 2011). Flow resistance equations used for friction losses estimation are computed with a friction slope from Manning's equation as presented in Equation 2.18.

$$Q = KS_f^{1/2} \tag{2.18}$$

Where,

Q = discharge (m^3/s)

K = channel conveyance (m)

S_f = friction slope (m/m)

Conveyance at a cross-section is obtained by Equation 2.19:

$$K = \frac{\Phi}{n} AR^{2/3} = \frac{\Phi}{n} A\left(\frac{A}{P}\right)^{2/3} \tag{2.19}$$

Where,

A = cross-sectional area normal to the direction of flow (m^2)

Φ = unit conversion (SI=1.000)

K = channel conveyance (m)

n = roughness coefficient

P = wetted perimeter (m)

R = hydraulic radius (m)

The cross-sectional area and wetted perimeter are a function of channel geometry. If the cross-section is trapezoidal, then the equations used are given as:

$$A = y\,(b + \text{ƶ}y) \tag{2.20}$$

$$P = b + 2y\left(\sqrt{\text{ƶ}^2 + 1}\right) \tag{2.21}$$

Where,

A = cross-sectional area normal to the direction of flow (m^2)

P = wetted perimeter (m)

y = flow depth at a cross-section (m)

b = bottom channel width (m)

ƶ = side slope of the channel

2.7 Modelling challenges of irrigation canals

There are a number of problems that are frequently encountered in modelling of irrigation canals. Some of these modelling problems include; zero-depth condition or dry-bed flow, mixed-regime flow and gate submergence (Ritter, 1991). In order to solve some of these challenges, detailed field data required as input for the selected irrigation model were collected. These field data are required for the calibration and validation of the simulation models.

2.7.1 Zero-depth condition

The filling and emptying of canals occur regularly in many irrigation systems. During the filling of a dry canal, water flows downstream over the canal bed. However, near the advancing front, the assumption of one-dimensional flow in the Saint Venant equations is violated, and a special boundary condition must be formulated to approximate the flow conditions (Hassain, 2012). An alternative approach that obviates the need for dynamic grid management is to suppress the inertial terms in the Saint Venant equations when dry-bed conditions appear imminent. Such techniques, borrowed from two-dimensional flow modelling on tidal flats, rely on a non-inertial film of water to maintain hydraulic connectivity (Mishra and Singh, 2003). This problem is not fully overcome by use of many models. However, HEC-RAS model captures coherent field data which reasonably addresses this challenge.

2.7.2 Mixed- flow regime

Within a canal reach, the transition between supercritical and sub-critical flow is manifested by a discontinuity in the water surface, and also in the solution to the governing hydraulic equations (Subramanya, 2009). This discontinuity is called a hydraulic jump, and is characterized by large-scale localized turbulence and a consequent loss of energy. A hydraulic jump in itself is simply another kind of boundary condition, similar to an inline gate or pump (Ritter, 1991). Thus, when the jump location is known, to be stationary due to the existence of a stabilizing structure, an unsteady model could easily include the necessary programme steps to successfully handle the governing hydraulics. In HEC-RAS, mixed flow regime is the best. It properly combines both sub and supercritical profiles that are run and uses the momentum equation through hydraulic jumps. If you are running either super or subcritical only, there will be some errors around flow regime transition areas, or anywhere there is not a valid solution for the selected regime.

2.7.3 Gate submergence

The problems associated with the modelling of complete operational range of a gated structure include; changes in flow regime and form of governing equations. These flow regime changes introduce numerical instability during simulation. One of the main challenges in modelling unsteady flow regimes is the data required for calibration for a given structure for specific conditions. In most cases, the required data may not be available. For these reasons, many unsteady-flow models incorporate simplifying assumption about transitions between flow regimes across a gated structure, and often limit the range of operational possibilities. These limitations are significant in some modelling applications and less significant in others (Munir, 2011).

2.8 Application of HEC-RAS in previous case studies

Hicks and Peacock (2005) used the HEC-RAS model to perform an unsteady analysis on a flood event on Peace River in Canada. The results of their study showed that the HEC-RAS model could be applied to obtain comparable results to those obtained through use of more sophisticated hydraulic models such as the Stream flow Synthesis and Reservoir Regulation (SSARR) and River1-D, used for the same analysis.

In Tasmania, Sargison and Barton, (2008) used the HEC-RAS model to determine the maximum pipe and culvert capacity. The model was used to find out if any increased volume

of water carried into the network could be safely discharged out of the network to the adjoining natural water courses in the event that the irrigation activities were suddenly stopped. The authors found out that the system was underutilized in its state at the time of the study. The authors pointed out that in most cases the culverts were capable of running full, which greatly increased the possible flow rates allowable in the system.

Wahl and Lentz, (2011) applied the HEC-RAS model to quantify the effects of canal hydrodynamics. In their study, empirical equations for estimating peak breach outflow as a function of canal cross-section, reach properties and breach time parameters were developed. These produced a tool for building appraisal-level estimates of breach initiation time, breach development time, peak breach outflow and hydrograph shape.

In Iran, Maghsoud *et al.* (2013) investigated hydraulic and structural variations that resulted from sectional changes of soil to concrete canals. According to their study of hydraulic regime of water transport canals, other components of flow could be obtained if the cross-section and velocity of flow were known and it was possible to analyze water surface profiles. This study demonstrated that, in soil and concrete canals, roughness coefficients are one of the predominant parameters on the water surface profile that led to hydraulic drop of the flow.

The HEC-RAS model was found to offer solutions to several design problems, regarding both the development of hydraulic modelling capabilities and integration of GIS with hydraulic models. New and improved analysis capabilities have been included into the HEC-RAS model. Some of the improved capabilities of the model include; channel modification analysis, mixed-flow, hydraulic structures (weirs, gates, etc.), bridge analysis, sediment transport modelling, and modelling of changes in Manning's roughness coefficient (Yang *et al.*, 2006).

The HEC-RAS model can also model subcritical and supercritical flows. In addition, it can model either an entire network of rivers or a single river, and is one of the few models that can run unsteady flow analyses. Use of the HEC-RAS model reveals gaps in knowledge regarding the best ways to determine open channel capacity in irrigation canals. Most of these gaps relate to the inability to fully quantify all flow components, their interactions with structures such as gates, weirs, drops and spillways. Many studies have been carried out on

operations of irrigation infrastructure worldwide. However, many of these studies have not fully linked the impact of safe and optimal canal use to operations and maintenance of irrigation schemes. In this study, flow and optimal canal capacity for sustainability of Mwea Irrigation Scheme was evaluated.

The HEC-RAS model was selected in this study because it has already been applied successfully for canal capacity determination and flood capacity improvement worldwide. Further, the HEC-RAS model is a widely accepted hydraulic modelling tool for open channel flow (OCF). It has continued to be a leading software preferred by hydraulic engineers since its release. It offers a simpler modelling approach and provides accurate results comparable to those of other modelling software (Kragh, 2011). Its capabilities in handling unsteady flow conditions give it a great advantage over other models (Hicks and Peacock, 2005).

2.9 Model assessment criteria

Both statistical and graphical model evaluation techniques are normally used to assess the performance of simulation models. The quantitative statistics are divided into three major categories that include; standard regression, dimensionless, and error index. Standard regression statistics determines the strength of the linear relationship between simulated and measured data. Dimensionless techniques provide a relative model evaluation assessment, and error indices to quantify the deviation in the units of the data of interest (Moriasi *et al.*, 2007). Several graphical techniques provide a visual comparison of simulated and measured constituent data. They also present a first overview of model performance (ASCE, 1993) and are thus essential for model evaluation (Legates and McCabe, 1999). Based on recommendations by ASCE (1993), both graphical techniques and quantitative statistics can be applied to assess the model performance. These criteria were selected to assess the HEC-RAS model performance in this study.

2.9.1 Standard regression

The Pearson's correlation coefficient (r) and coefficient of gain (R^2) describe the degree of collinearity between simulated and measured data. The correlation coefficient, which ranges from −1 to 1, is an index of the degree of linear relationship between observed and simulated data. If r = 0, this indicates that no linear relationship exists. If r = 1 or −1, a perfect positive or negative linear relationship exists. Similarly, R^2 describes the proportion of the variance in measured data explained by the model. In regression, the R^2 coefficient of gain is a statistical

measure of how well the regression line approximates the real data points. R^2 values closer to 1.0 indicate that the regression line perfectly fits the data.

R^2 ranges from 0 to 1, with higher values indicating less error variance, and typically values greater than 0.5 are considered acceptable (Santhi *et al.,* 2001). Although r and R^2 have been widely used for evaluation of model performance, these statistics are oversensitive to high extreme values (outliers) and insensitive to additive and proportional differences between model predictions and measured data (Moriasi *et al*., 2007).

2.9.2 Graphical techniques

Graphical techniques provide a visual comparison of simulated and measured constituent data and a first overview of model performance (ASCE, 1993; Moriasi *et al.,* 2007). According to Legates and McCabe (1999), graphical techniques are essential for appropriate model evaluation. The hydrographs and percent exceedance probability curves are among the commonly used graphical techniques. Other graphical techniques, such as bar graphs and box plots, can also be used to examine seasonal variations and data distributions over a period of time.

CHAPTER THREE
METHODOLOGY

3.1 Description of the study area

Mwea Irrigation Scheme (MIS) is located in Kirinyaga South Sub-County, Kirinyaga County approximately 100 Kilometres North East of Nairobi. It lies on the Southern outskirts of Mt. Kenya and it covers a gazetted area of 30,350 acres. It is located between 1,100 m and 1,200 m above mean sea level (a.m.s.l.). The scheme stretches between latitudes 0° 37'S and 0° 45'S and between longitudes 37° 14'E and 37° 26'E as shown in Figure 3.1.

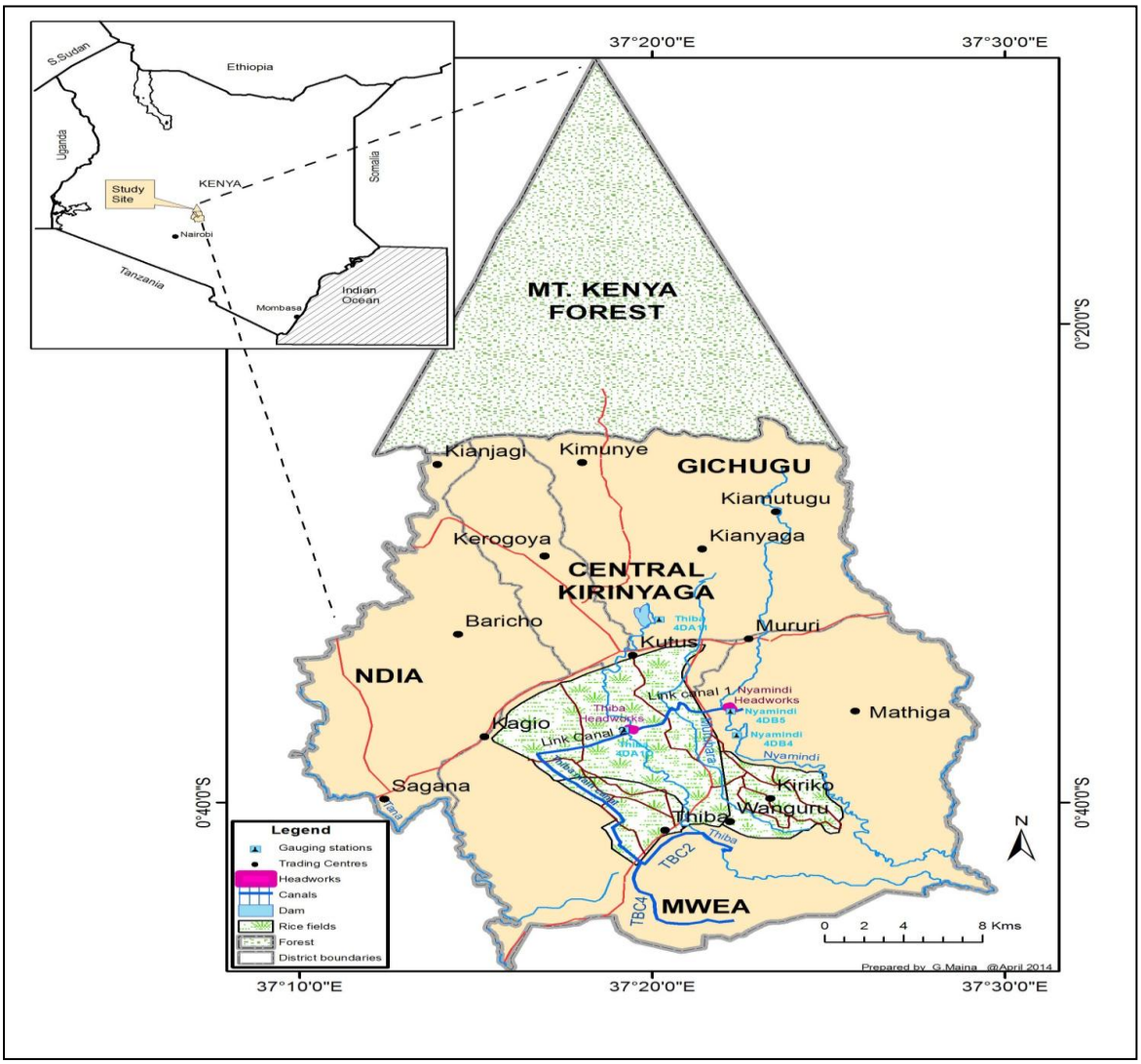

Figure 3.1: Map of Kenya showing Mwea irrigation Scheme

Administratively, MIS was formerly in Mwea Division of the larger Kirinyaga District, but after countrywide review of boundaries, it now falls in both Mwea East and West Divisions of Kirinyaga South sub-county respectively. Mwea area covers several locations and sub-locations. There are currently over 52 villages with approximately 3270 households within the main scheme (MIS) where most of the farmers reside (Koei, 2010). MIS is an open gravity irrigation system where paddy mainly Basmati, ITA, IR and BW varieties are grown.

There are three headworks that divert the water required for the Scheme. The water taken from the Nyamindi headworks flows into the Nyamindi headrace and is then divided into the Nyamindi main canal and the Link Canal I. Nyamindi main canal conveys irrigation water to the Nyamindi system. Link canal I conveys water from the Nyamindi River to the Thiba River. The Thiba headworks takes water from the Thiba River whose flow is combined with water from Link Canal I into Link canal II. The Rubble weir intake located downstream of Thiba headworks conveys 80% of water to Tebere Section while 20% is conveyed and used for domestic purposes at MIS.

The present study focused on Link Canal II reach which is approximately 3.2 km long while Thiba Main Canal, approximately 9.42 km. These structures are shown in Figures 3.2, 3.3, 3.4 and also in Appendix 1.

Figure 3.2: Upstream view of gates at Thiba off-take in MIS

The Link canal II which is shown in Figure 3.3 has a maximum design capacity of 11.12 m^3/s and the channel beds consist mainly of silt soil and scattered small cobles. It has an average bed slope of 0.00030 m/m. The second reach, Thiba Main canal shown in Figure 3.4 is a stable man made channel with a 0.00040 m/m gradient that is controlled by a series of drop structures. The concrete lined canal was designed for a maximum flow capacity of about 6.5 m^3/s.

Figure 3.3: A section of Link canal II

Figure 3.4: A section of lined trapezoidal Thiba Main Canal

3.1.1 Climate

The Scheme area is influenced by seasonal monsoons, with two distinct rainy seasons. The long and short rains occur from April to May and October to November respectively as presented in Figure 3.5.

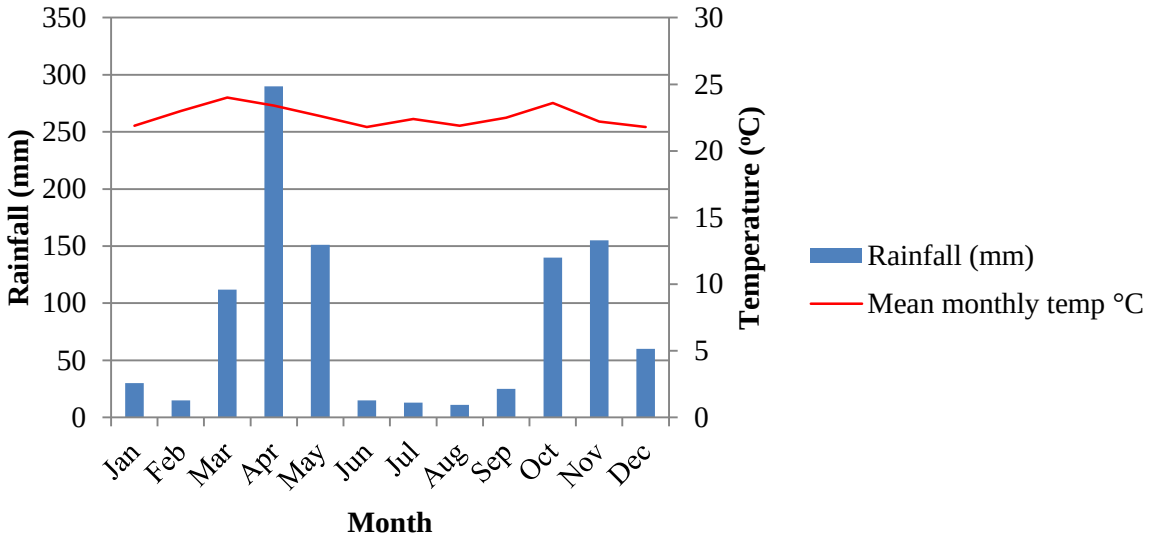

Figure 3.5: Mean monthly rainfall and temperature

The scheme receives an average annual rainfall of 940 mm, most of which is received during the long rains. The mean monthly temperature in the scheme area is 22.2ºC with a minimum and maximum of 21.8ºC and 24.0ºC in January and March respectively as presented in Table 3.1. Generally, the temperatures during the rainy season are higher than those during the dry season (Koei, 2008). The mean monthly evaporation is about 5.8 mm/day, with maximum and minimum values of 7.6 mm and 4.2 mm in March and July respectively (Gibb, 2010).

Table 3.1: Mean monthly rainfall and temperature for MIS (1978-2014)

Month	Jan	Feb	Mar	Apr	May	Jun	Jul	Aug	Sep	Oct	Nov	Dec	Ave.	Max	Min
Rainfall (mm)	30	15	112	290	151	15	13	11	25	140	155	60	84.7	290	11
Mean monthly temp °C	21.9	23.0	24.0	23.4	22.6	21.8	22.4	21.9	22.5	23.6	22.2	21.8	22.2	24.0	21.8

The cropping pattern in the MIS Scheme is mainly single rice cropping system as presented in Figure 3.6. Wetland paddy of Groups I and II is planted from August to January as the short rain (SR) crop. Wetland paddy of Group III is planted in January and harvested in April. This grouping has been made in order to avoid competition of the limited available irrigation water.

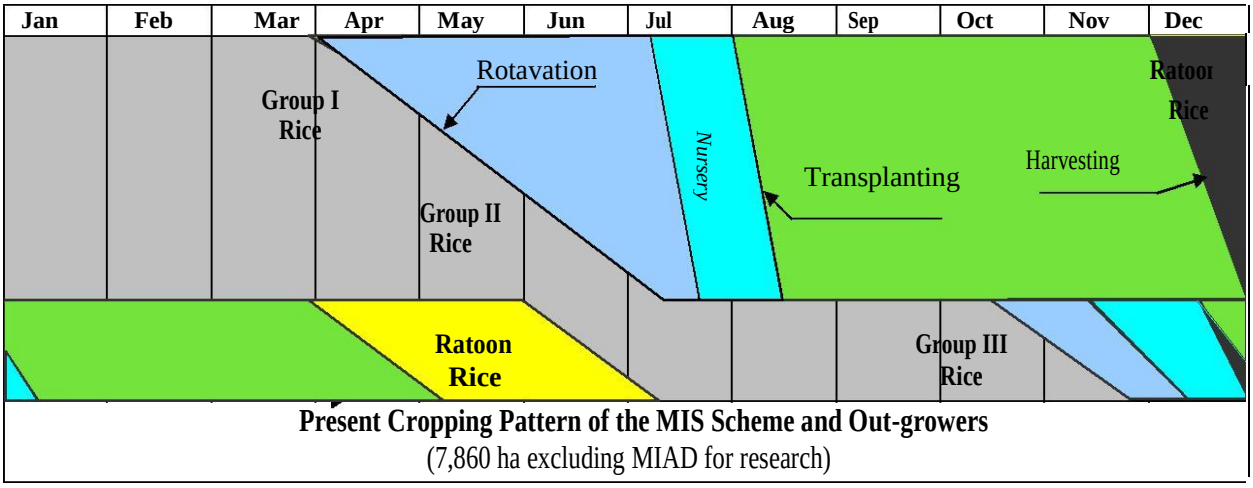

Source: SAPROF (2009)

Figure 3.6 Present Cropping Pattern of the MIS Scheme and out-growers

3.1.2 Vegetation

The original vegetation of the study area is said to have been moist montane forest, scrubland, and cultivated savannah. The upper part of the study area was covered by the Mount Kenya Forest (Gibb, 2010). However, due to the population pressure, some parts of the area have been cleared and replaced with farm crops and eucalyptus forests. The dark-green black wattle trees, scattered eucalyptus trees, cypress and pine trees grow on the hill tops, valley bottoms and along farm boundaries. The swampy areas are dominated with papyrus vegetation. Much of the land in the catchments is under farm crops such as tea, maize, rice, bananas, and horticultural crops.

3.1.3 Rivers

There are four major rivers in and around Mwea Irrigation Scheme. These rivers are; Tana, Nyamindi, Thiba and Ruamuthambi. There are small streams joining to the four rivers as shown in Figure 3.7. These streams are; Murubara, Kituthe, Kiwe, Nyakungu and Kiruara. The parameters of the main river and gauging stations in and around the study area are given in Table 3.2.

Table 3.2: Rivers within the catchment area of Mwea Irrigation Scheme

River	Gauging stations	Catchment area (km^2)	River Length (km)	Mean width of basin (km)	Approximate annual river flow (m^3/s)
Nyamindi	4DB05	284.5	56.9	5.0	6.5
Thiba	4DA10	353.5	47.5	7.4	11.0
Ruamuthambi	4BCO5	86.0	25.3	3.4	2.0
Tana	4BC04	157.5	37.5	4.2	12.5

Source: SAPROF (2009)

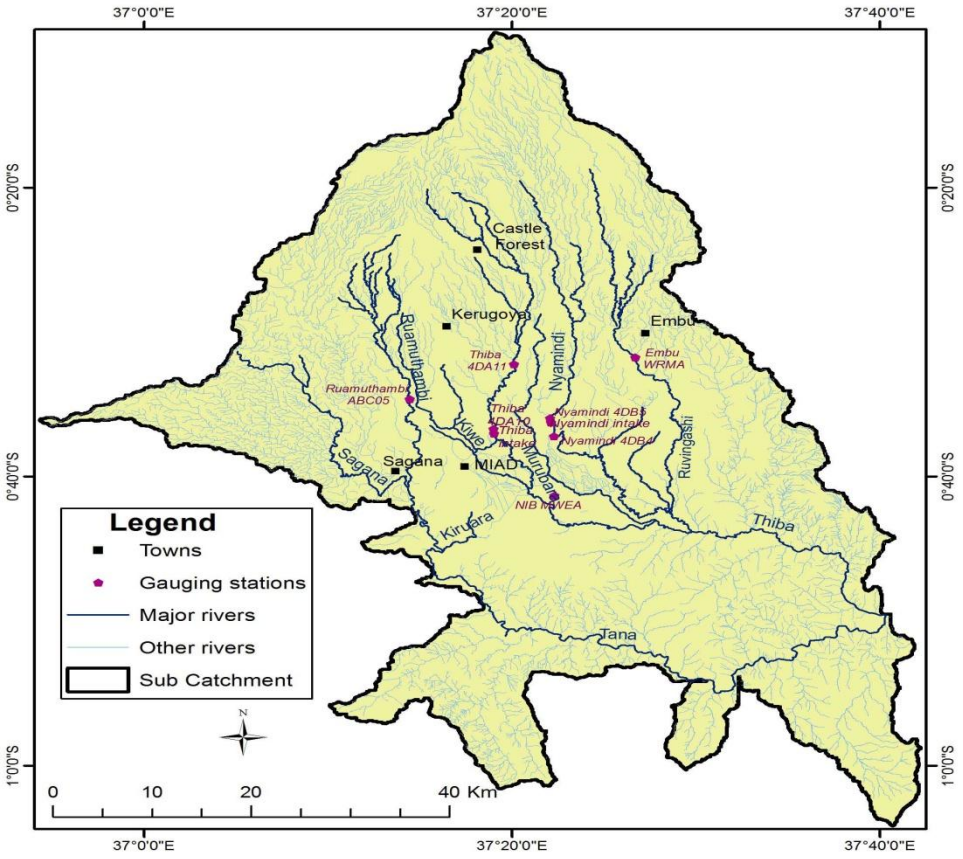

Figure 3.7: Rivers in and around Mwea Irrigation Scheme

3.1.4 Topography and soils

The area consists of low rolling hills separated by wide flat valleys that have been developed for intensive agriculture. The scheme area generally slopes southward. The western edge of the study area slopes towards Tana River flowing down southward. Soils in the study area consist mainly of Pellic Vertisols and Verto-eutric Nitosols that are both suitable for irrigation farming (Koei, 1996). The black cotton soils are found on the northern high altitude edge of the scheme area while red soils on the eastern side of the scheme are mainly coarse-textured with low plasticity and shrinkage rate.

3.2 Evaluation of hydraulic and structural variations on Thiba main canal reach potential capacity

3.2.1 Data collection

Data was collected in two stages during the research period. Preliminary data which included survey of the canal cross-sections and flow velocity was carried out in the month of September, 2014. This was during transplanting stage as per the crop calendar. Observation of the canal reaches was done to obtain Manning's roughness values that were for the study. During the second stage of data collection, continuous observation and water flow velocity measurements were done with confirmation of geometric dimensions such as lengths, widths, bed levels, drops and top bank lining for a period of three months from January to March, 2015. Water depths were also measured at each cross-section. The Canal alignment profiles plots in River CAD were used in the development of the model.

3.2.2 HEC-RAS model input parameters

The HEC-RAS version 4.1.0 model was used in this study. The model is dependent on a set of data which include canal geometry, channel roughness, energy loss coefficient for hydraulic resistance and the expansion or contraction of flow, discharge and conditions for the flow boundaries of the canal (i.e. top of lining). The model has both conceptual and physical parameters which were estimated through calibration and direct measurement in the field respectively. Table 3.3 presents comprehensive details of parameters required in the HEC-RAS model that were taken into consideration in this study.

Table 3.3: HEC-RAS input parameters

	Physical variables/ Parameters		**Means of determination**
	Symbol/unit	**Description**	
1.	*y (m)*	Water depth	Tape measure and navigation rod
2.	*L (m)*	Reach length	Tape measure
3.	*V*(m/s)	Average flow velocity	Flow current meter
4.	*R*(m)	Hydraulic radius	Computed from effective depth and effective width
5.	*S*(m/m)	Bed slope	Computed from elevations
6.	*Q(m^3/s)*	Discharge	Computed from velocity and area using mean section m
7.	Z (m/m)	Side slope	Computed from wetted perimeter, width and water dep

	Conceptual Parameter		
	Symbol	**Description**	**Means of determination**
8.	*n*	Manning's coefficient	Calibration
9.		Contraction and expansion coefficient	Calibration

Tools and equipment that were used in data collection are presented in Table 3.4. The equipment was used during preliminary and detailed data collection stages. In order to measure the flow velocities, the SEBA Universal F2822 current meter was used together with a stop watch and a measuring tape.

Table 3.4: Field equipment used

	Equipment	**Purpose**
1.	Auto Dumpy level (Topcon machine X26324)	Taking levels to determine the slope
2.	30m tape measure	Determining width, depth of canal, distance between cross-section
3.	Tape line	Measuring distance with accuracy
4.	20mm Navigation rod	Attaching current meter and for depth measurement
5.	Stop watch	Determination of time interval
6	Hammer	Pegging
7	Current meter (SEBA Universal F2822)	Measuring flow velocity

3.2.3 Model schematization of Thiba system

In order to run the HEC-RAS model, a schematization of Thiba main canal as given in Figure 3.8 was done with a view to establishing water flow balance in the system. The layout was done to show all the canals, flow directions and control structures. It involved reduction of the system into a layout drawing indicating all branch canals that withdraw water from the main infrastructure. It showed all discharge flow directions as either into or out of the system. Structures in the channel were captured at this stage and a summary of their effect registered. The HEC-RAS model was used to model each reach independently due to the type of canal and the slope differences between the two canals. A detailed system is presented in Appendix 2.

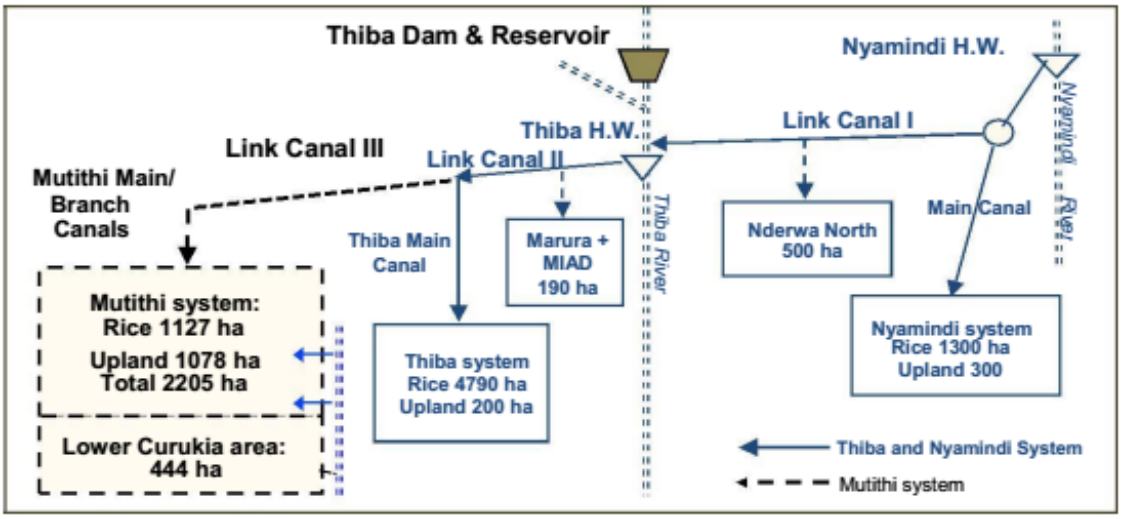

Figure 3.8: Schematic layout of canals and structures

3.2.4 Geometric data input into the HEC-RAS model

The data consisted of a contour map of the area canals in AutoCAD format that was created from actual survey of the canals using an Auto Dumpy level (Topcon machine X26324 model ATB4) and Mobile Mapper 10. The contour maps covered two main canals (Link canal II and Thiba Main Canal). To reduce the processing time of the contour maps, the file was opened in AutoCAD and data relevant to only the reach under study were copied and pasted into a new file. These data comprised the contour lines, canal centerlines and bank lines. The newly created file was then opened in Civil-3D to create a surface 3D representation of the ground and canal surface from which the canal cross-sections were extracted.

The HEC-RAS model has a graphical user interface through which such functions as file management, data entry and editing, river analyses, tabulation and graphical displays of input and output data, reporting and on-line help are performed. At the top of the HEC-RAS main window is a menu bar (Figure 3.9) with the file; edit, view, options, GIS Tools and the Help options tabs.

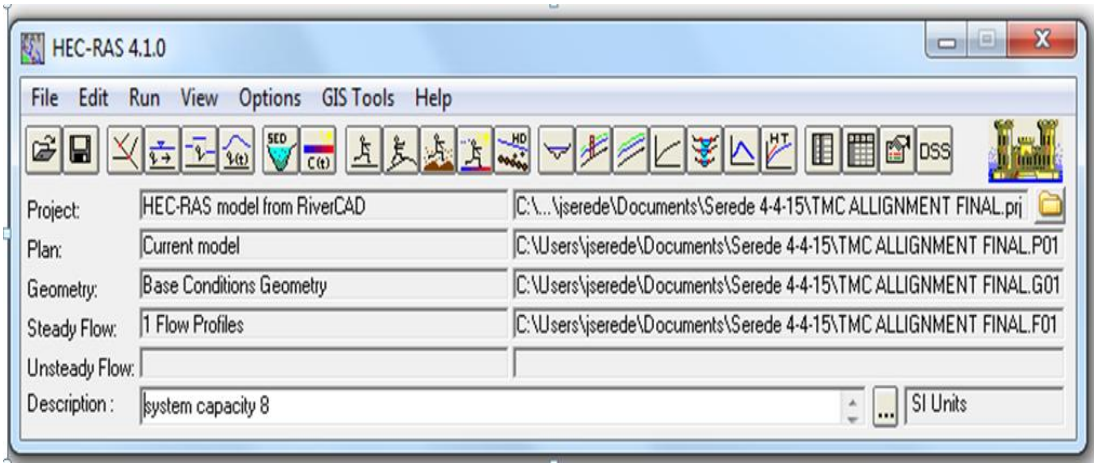

Figure 3.9: HEC-RAS main window

From a "file tab" as given in Figure 3.9, *.geo* format files were created for both canal reaches that could be read as a GIS file by HEC-RAS model. The files were exported into the HEC-RAS model from the Civil-3D output tab. This was to make sure that all the data is uploaded. Care was taken against jagged alignments for increased accuracy. The hydraulic resistance was reflected in the selection of Manning's 'n' values as presented in Table 3.5. Details for each specific cross-section were selected from the Chow's Table as given in Appendix 3 Table 1A. More than one 'n' value was assigned to each cross-section.

Table 3.5: Manning's 'n' values used in the model

Reach	Chainage	Manning 'n' Values used		
		LOB	Channel	ROB
Link II Canal	0+000 to1+740	0.023	0.023	0.023
Thiba Main Canal	0+000 to 0+380	0.020	0.020	0.020
	0+380 to 7+177	0.016	0.016	0.016

Multiple Manning's 'n' values were used for the left over bank (LOB), main channel and the right over bank (ROB). These values were entered in the cross-section data editor as presented in Figures 3.10 and 3.11 for Link Canal II and TMC respectively. The values were adjusted during the calibration process to reflect the real canal conditions.

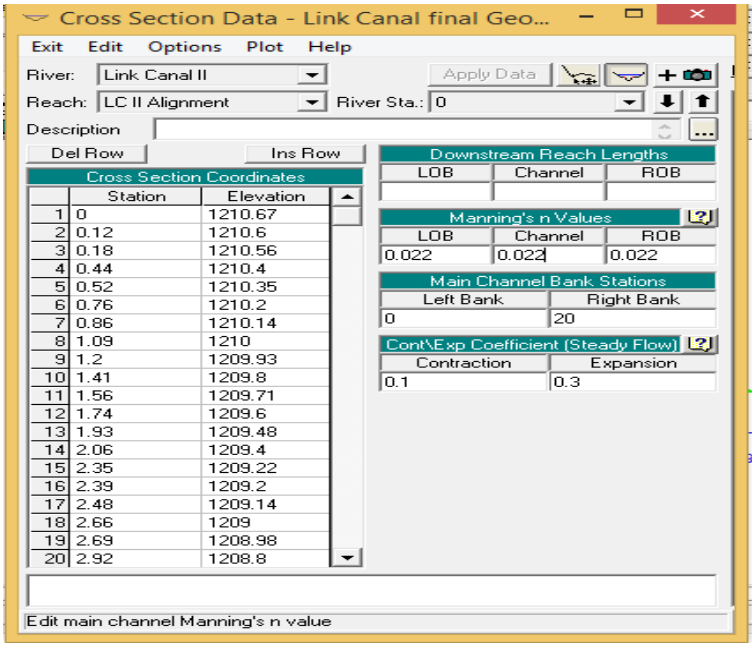

Figure 3.10: Cross-section data editor for LCII

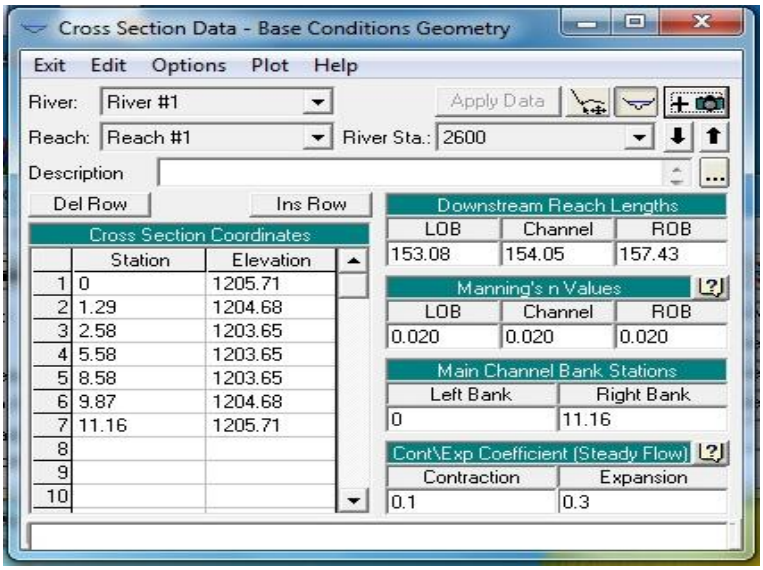

Figure 3.11: Cross-section data editor for TMC

Figures 3.12 and 3.13 illustrate typical cross-section plot showing the left and right canal banks, the inverts, top of lining and bank points on LCII and TMC developed from the model. In both Figures, it is easy to identify the ground bank station, nature of the canal and the hydraulic resistance values used at different points of the Channel and the geo-referenced canal elevations.

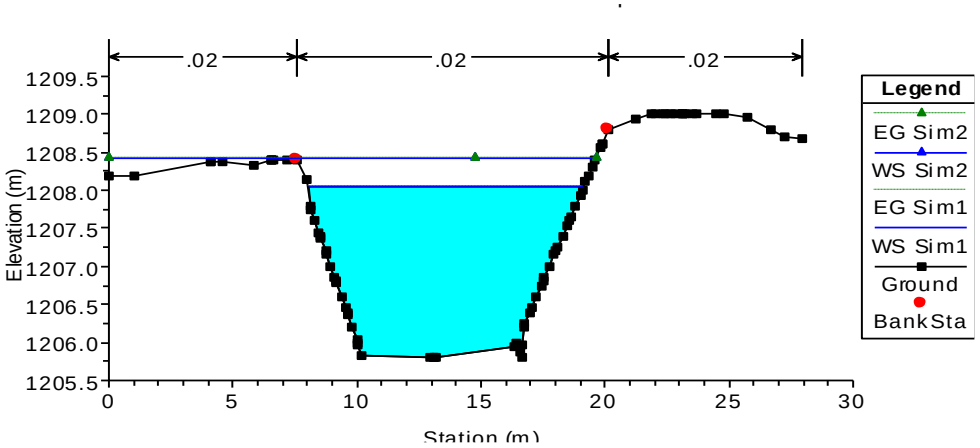

Figure 3.12: A cross-section showing canal banks and top of lining on LCII

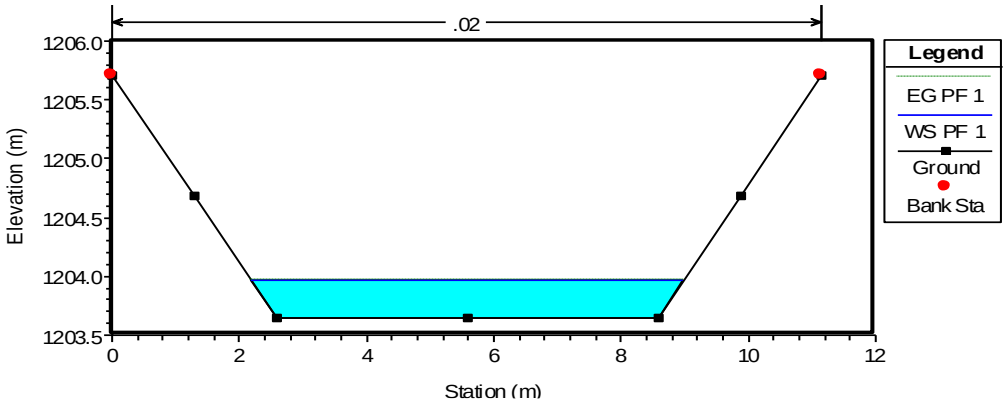

Figure 3.13: A cross-section showing canal banks and top of lining on TMC

3.2.5 Canal cross-sections

The geometric data consisted of cross-sectional geometry collected at periodic stations along the study reach. Six cross-sections were uniformly distributed at about 350 m intervals along the Link II Canal. Forty eight sections on the Thiba Main Canal were separated at an interval of 250 m as given in Table A4 in Appendix 5. The sections were surveyed from the top of the left bank to the top of right bank. The cross-sectional data was collected using a Dumpy level (Topcon machine X26324 model ATB4). The elevations obtained were based on an assumed, local datum of 1200 a.m.s.l. Illustration of cross-section plots for the Link II Canal and Thiba Main Canal are shown in Figures 3.12 and 3.13 respectively. These sections were oriented from left to right in the downstream direction. A positive Cartesian direction was adopted in setting of the start station at the selected cross-section. Cross-sections were developed for both the two canal reaches. Detailed data on elevations used for TMC's as built levels are presented in Appendix 5.

3.2.6 Channel cross-section interval

The required distribution of cross-sections differ from station to station and depends on site specific features such as longitudinal uniformity of cross-sectional shape, channel linearity, degree of channel meander, longitudinal slope and uniformity of slope throughout the study reach. In this study, cross-section spacing on both canals were determined using Equation 3.1.

$$D_X = 0.15\frac{D}{S} \tag{3.1}$$

Where,

D_X = cross-section spacing (m)

D = bankful depth (m)

S = bed slope (m/m)

Additional cross-sections were generated by interpolation to aid in model calibration. This was necessitated by factors such as extents of backwater effects due to check structures and changes in canal geometry, drop structures, slope, or changes in canal roughness. At drop structures and falls, cross-sections were located both on the upstream and downstream to accurately define the slope. All elevations were entered in absolute values in the geometry file. Table 3.6 presents a summary of the details collected during survey on cross-section location, canal stations and the bed slope applied in HEC-RAS model.

Table 3.6: Summary of canal cross-sections surveyed

Reach	Chainage	Location Northing	Easting	Canal station No.	Elevation (m amsl)	Bed slope (m/m)
Link	0+000	0º37'32.6"S	37º17'55.8"E	1	1212.005	0.00029
II	0+380	0º37'44.4"S	37º18'8.3"E	2	1209.490	0.00030
Canal	0+640	0º38'3.6"S	37º18'4.8"E	3	1208.885	"
	0+900	0º38'5.7"S	37º18'43.3"E	4	1208.100	"
	1+490	0º38'11.1"S	37º18'33.3"E	5	1208.920	"
	1+740	0º38'12.3"S	37º18'20.5"E	6	1208.850	"
Thiba	0+000	0º38'19.2"S	37º18'5.5"E	7	1207.845	0.00030
Main	0+480	0º38'28.7"S	37º17'56"E	8	1207.015	0.00030
Canal	0+600	0º38'32.6"S	37º17'54.8"E	9	1206.600	0.00050
	1+157	0º38'45.1"S	37º18'3.1"E	10	1203.350	"
	1+520	0º38'55.9"S	37º18'7.3"E	11	1201.545	"
	2+660	0º39'25.5"S	37º18'23.8"E	12	1196.730	0.00063
	3+240	0º39'39.4"S	37º18'33.2"E	13	1191.880	"
	4+040	0º39'54.7"S	37º18'54.3"E	14	1187.035	0.00049
	4+720	0º40'27.2"S	37º18'55.9"E	15	1185.590	"
	6+040	0º40'46.2"S	37º19'10.2"E	16	1177.025	0.00033
	7+177	0º41'15.2"S	37º19'32"E	17	1173.190	"
	7+720	0º41'32.6"S	37º19'37.5"E	18	1168.505	0.00025
	8+800	0º42'5.3"S	37º19'48.2"E	19	1165.950	0.00020
	9+340	0º42'22.1"S	37º19'53.3"E	20	1164.570	0.00020

3.2.7 Steady flow data

There were minimal operational gauges fixed in the reach. Therefore, current metering method was applied to determine flow velocities at the cross-section locations indicated in Table 3.6. A calibrated SEBA Universal F2822 model current meter was used to measure flow velocity. This device had a timer and counters mounted on a graduated 20 mm shaft. The SEBA signal counter Z-6 was used for recording the number of revolutions made. Time measurements were taken using a stop watch to help in calculation of the number of revolutions per second. The canal width was measured using a 30 m measuring tape at the selected cross-sections and divided into a number of segments at a spacing of 0.5 m using a marker pen. For ease of carrying out the measurements, motorable bridges along the canals were utilized. To cope with the vertical distribution of velocity, measurements were made at 0.6 times the flow depth (0.6d) (Gordon *et al.*, 2004) since the depth of these canals were greater than 0.5m. Calculation of discharge Q, was based on Equations 3.2 and 3.3 using the mean section method.

$$V = 0.0194 + 0.2619 * n \quad (3.2)$$

Where,

V = canal velocity (m/sec)

n = number of propeller rotation per second

$$Q = \sum_i^n q_i = \sum_{i=1}^n Va = \sum_{i=1}^n V \frac{(V_{i-1} + V_i)}{2} \frac{(d_{i-1} + d_i)}{2} (b_i + b_{i+1}) \quad (3.3)$$

Where,

b_i = horizontal distance of measuring point i from the bank of canal
n = number of segments
d_i = depth
V_i = average velocity

3.3 Application of HEC-RAS Model

3.3.1 Model operation

With the geometry and *flow files* established, the HEC-RAS model was executed. This was achieved by selecting *Simulate/Steady Flow Analysis* from the project window. Before running the model, a simulation model plan was created and saved. The plan specified the geometry and flow files to be used in the simulation. This was done by selecting the "File" from the menu bar and then the "New Plan" tab and a plan title was provided as presented in Figure 3.14.

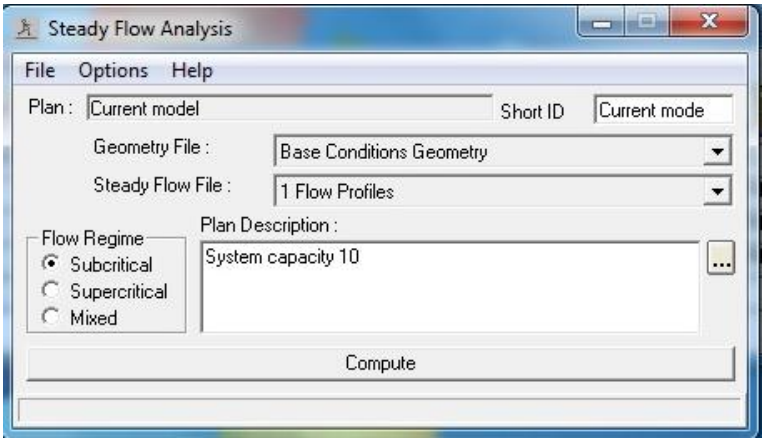

Figure 3.14: Steady flow analysis window

To execute the model, the "flow regime radio button" was set to subcritical status. To this point all of the HEC-RAS model windows were simply graphical user interfaces used to input data for the model. The computations were performed and results obtained as model outputs in form of graphs and tables. Several runs were done and results for the best four recorded.

3.3.2 Model calibration

During calibration, the Manning's coefficient "n", discharge calibration factors and coefficients were changed iteratively until the differences between simulated and observed values of water levels were within the allowable criteria range. A summary of the procedure followed is given in the conceptual framework presented in Figure 3.15. The calibration procedure gave the actual Manning's of the canal which was further optimized.

Once the steady flow simulation was performed, the program outputs a profile plot including the water elevation that represented the actual water surface profile depth. The modelled energy gradeline was to align parallel to the actual water surface profile. Achievement of this suggested that the canal channel was adequately defined and that the roughness coefficient was appropriately assigned. Four runs were thus carried out for both LCII and TMC.

Figure 3.15: Conceptual framework for HEC-RAS Model calibration

3.3.3 Sensitivity analysis

The reliability of the modelling results depends on the capability to accurately estimate these model parameters. All parameters selected were confirmed to be within accepted ranges for the conditions that were modelled. A sensitivity analysis was performed on the model to determine the impact of varying discharge, boundary conditions and the Manning's 'n' values within the range of values for a given material. For instance, the Manning's value chosen for the concrete lined sections was compared with the recommended values for comparable material in the HEC-RAS Hydraulic Reference Manual, Version 4.1 (USACE, 2013). In addition, the sensitivity analysis was done to determine the impact of varying the Manning's value within the range of values for a given material as presented in Table A1 in Appendix 3.

3.3.4 Model validation and optimization

The accuracy of calibrated parameters was tested using the differences between second set of observed data and the new simulated values which validated the model. The suitability of the model was evaluated based on the differences between observed and simulated values by checking the coefficient of gain (R^2) for the observed and simulated values. The expansion and contraction coefficients used in analyzing flow test data were 0.3 and 0.1 respectively (Giovannettone, 2008). Inbuilt automatic algorithm within the HEC-RAS model was used for automatic flow optimization through the steady state flow window. The result was checked against values obtained during the calibration process.

3.4 Formulation of operational and maintenance procedures using HEC-RAS as a decision support tool

This analysis was aimed at generating procedures that were to ensure improved water management and sustainability of the infrastructure. This was achieved by comparing the amount of water used at flooding and irrigation stages versus the reach capacity potential. Recommendations were proposed which would enable the water guards, operators, scheme managers and the water users to efficiently convey water through the canals at the required capacity. Further, necessary recommendations were made on feasible options to convey water to Mutithi expansion area located south west border of the existing MIS.

3.4.1 Canal operation and maintenance

Analysis of the calibration results was carried out after adequately aligning modelled energy grade line to the actual water surface profile. The roughness coefficients at various sections were used to recommend the best canal maintenance practices. Comparison of the canal capacity potential against canal geometry was used to check for overtopping of the banks against the 0.55m freeboard, bank repair and slope shaping.

To check for the hydraulic parameters, the model offers an option for tabular output display through the view cross-section table option. Errors and notes resulting from the steady flow computations were shown and assisted in decision making. Recommendations were made on flow capacity that could be operated in a specific canal size and the precautionary measures to be undertaken to avert canal breach.

CHAPTER FOUR

RESULTS AND DISCUSSION

This Chapter presents results and discussions based on the model application that was applied in the Mwea Irrigation Scheme on two canal reaches. These reaches are; Link canal II and the Thiba Main Canal, 3.2 km and 9.42 km respectively. The results and discussions are used to make inferences from the study.

4.1 Data collection results

Table 4.1 presents a summary of data collected during the fieldwork. These were used during model simulation, calibration and validation.

Table 4.1: Summary of data collected during fieldwork

Reach	Chainage	Flow (m^3/s)	Water depth (m)	Mean Bed slope (m/m)	Manning's coefficient			Optimized value
					Min	Normal	Max	
Link II Canal	1+740	5.80	1.85					
	1+490	6.00	2.06					
	0+900	6.50	2.03					
	0+640	6.50	2.00	0.00030	0.022	0.027	0.033	0.023
	1+380	6.50	1.50					
	1+000	6.50	1.00					
Thiba Main Canal	2+600	0.80	0.32					
	2+500	0.80	0.35					
	2+400	0.90	0.20	0.00258	0.013	0.015	0.016	0.016
	2+300	1.20	0.28					
	2+200	1.20	0.35					
	2+100	1.20	0.35					
	2+000	1.20	0.35					
	1+900	1.20	0.20					
	1+800	1.20	0.28	0.000635	0.013	0.015	0.016	0.016
	1+700	1.20	0.20					
	1+600	1.20	0.20					
	1+500	1.31	0.35					
	1+400	1.63	0.20					
	1+300	1.63	0.22					
	1+200	1.63	0.22					
	1+100	1.83	0.22					
	1+000	1.83	0.20					
	0+900	1.90	0.45					
	0+800	2.00	0.50					
	0+700	2.00	0.50					
	0+600	2.00	0.48	0.00050				
	0+500	2.00	0.70					

0+400	3.30	0.40				
0+300	3.30	0.40	0.00030			
0+250	3.50	0.85				
0+000	3.50	1.00		0.020	0.020	0.020

From Table 4.1, the results show average bed slope values of 0.00030 and 0.003895 m/m that were used in simulation of the LCII and TMC respectively. However, for increased accuracy specific slope values of 0.00258, 0.00030, 0.00050 and 0.000635 m/m were used for different cross-sections. According to May *et al*. (2000), in their study on Florida canal in Colorado average slope of 0.00078 m/m was used in simulation. However, in their modelling results, it was realized that a 1.2% and up to 20.8% validation error occurred on very low and very steep study reaches respectively.

Table 4.2 presents Manning's 'n' values for excavated and lined channels as extracted from the Chow's Table (Chow, 1959).

Table 4.2: Manning's values used in analysis of earth and lined canals

Type of Channel and description	Minimum	Normal	Maximum
1. Excavated or dredged channels			
a. Earth, straight, and uniform			
1. clean, recently completed	0.016	0.018	0.020
2. clean, after weathering	0.018	0.022	0.025
3. gravel, uniform section, clean	0.022	0.025	0.030
4. with short grass, few weeds	0.022	0.027	0.033
b. Rock cuts			
1. smooth and uniform	0.025	0.035	0.040
2. jagged and irregular	0.035	0.040	0.050
2. Lined or constructed channels			
a. Cement			
1. neat surface	0.010	0.011	0.013
2. mortar	0.011	0.013	0.015
b. Concrete			
1. trowel finish	0.011	0.013	0.015
2. float finish	0.013	0.015	0.016
3.finished, with gravel on bottom	0.015	0.017	0.020
4. unfinished	0.014	0.017	0.020
c. Asphalt			
1. smooth	0.013	0.013	
2. rough	0.016	0.016	

Source: Chow (1959)

From Table 4.2, it is observed that Manning's 'n' values for LCII range from 0.022 to 0.033, with 0.022 identified as 'minimum' and 0.033 as 'maximum'. These values represented excavated or dredged channel type with short grass and few weeds as it was the conditions of LCII during the time of data collection.

On the other hand the 'n' values for TMC range from 0.013 to 0.016. The value of 0.013 was identified as 'minimum' and 0.016 as 'maximum.' These values represented a concrete lined channel type with a float finish as it was the case for TMC. These values were selected from the Chow's Tables after field inspection along the canals during data collection period as a form of ground truthing.

4.2 Cross-sections

The modelling results vary depending on the number of cross-sections. Typically, it is suggested that cross-sections to be spaced in the order of 90 m to 150 m apart (May *et al.*, 2000). In this study, Equation 3.1 (Simpson's equation) was used to determine the cross section spacing. If they are spaced too far apart, the computational algorithm may become unstable and have difficulties balancing the energy between these sections. Cross-section cut lines were drawn covering the extent of the channels in a straight line perpendicular to the flow of the canal. Table 4.3 presents the number of cross-sections obtained in each reach.

Table 4.3: Number of cross-sections per reach

Reach	Distance modeled (km)	Number of cross-sections developed	Number of cross-sections interpolated
LCII	1.74	7	4
TMC	7.17	48	0

In case of modelling errors, a common remedy is to insert additional cross-sections. In practice the additional sections are frequently interpolated from the immediate upstream and downstream sections, thus alleviating the need for further fieldwork. The more the number of cross-sections used, the more accurate the canal definition becomes. TMC had more cross-sections used due to the high number of canal drop structures and its length as compared to LCII as given in Figure 4.1.

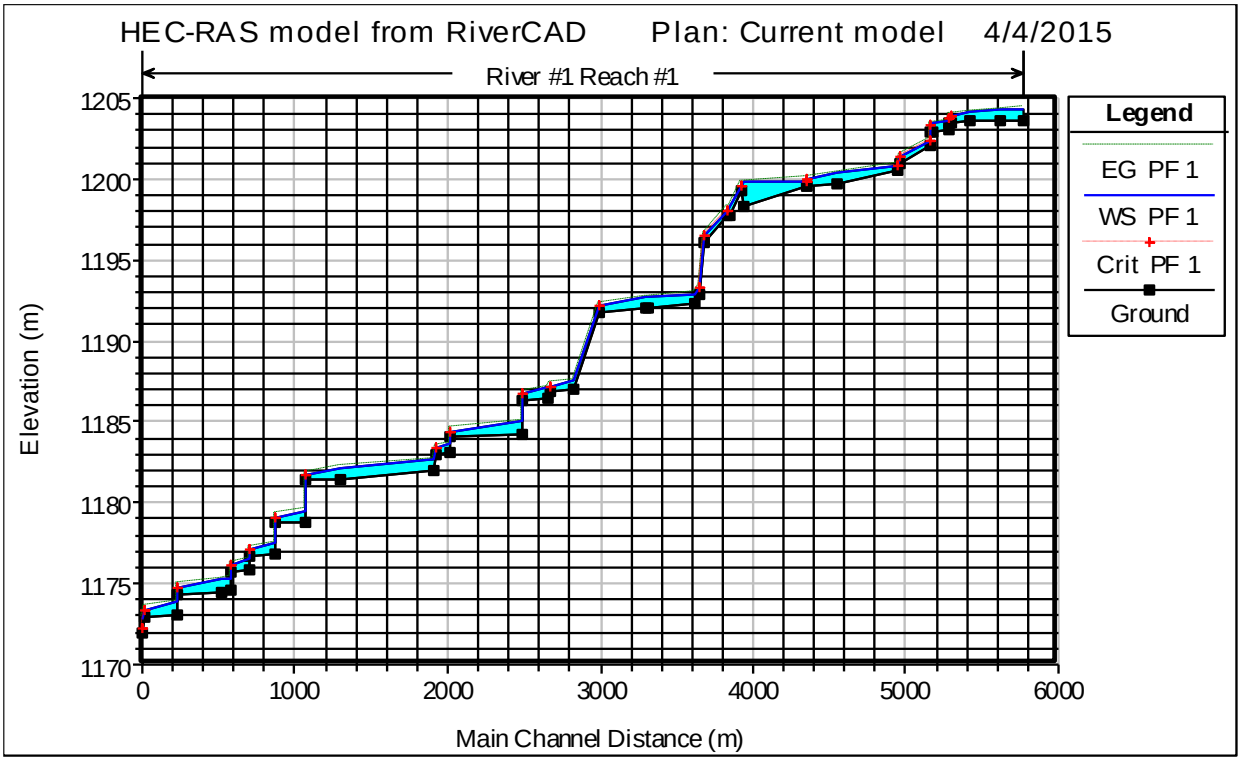

Figure 4.1: Profile for Thiba Main Canal

From Figure 4.1, it is evident that the model was able to capture all the drop structures. From the profile plot, the energy grade line, canal bed elevation, slope, critical depth and the water surface plot for the canal including the analysis date for record monitoring were depicted.

4.3 Steady flow

Estimated discharges were entered in the model through the steady flow data editor. It allowed for multiple flow profiles to be used in simulations. The HEC-RAS model has capabilities for the user to select the flow profile to be used in the modelling process. Figure 4.2 presents a steady flow data window for LCII that was used to enter and edit flow profiles in the model.

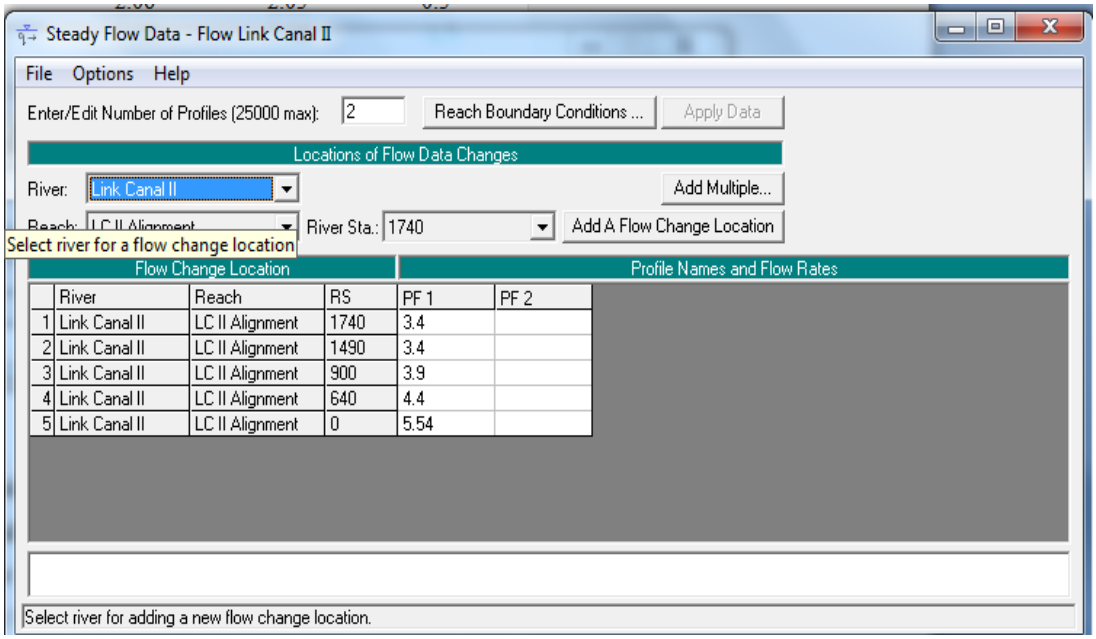

Figure 4.2: Steady flow data window for LCII

From Figure 4.2, flow profile 1 (PF1) indicates discharge calculated using the mean section method and entered into the model. The flow reduced gradually from 5.54 m^3/s to 3.4 m^3/s indicating that some flow was released through the off take structures along the canal. From the several functionalities indicated on the window, it was possible to save and add more data to the model for comparison of different flow regimes.

4.4 Model parameters

4.4.1 Manning's roughness coefficient

The Manning's roughness coefficients for the Thiba main canal reach could not be measured explicitly and was determined through calibration. In this application, roughness coefficients did not vary horizontally across individual cross-sections but were allowed to vary over different reaches specified along the length of the canal reach. The reach was divided into two different calibration reaches in which Manning's roughness was different as presented in Table 4.4.

Table 4.4: Calibrated Manning's 'n' values

Calibration Reach	Chainage	Calibrated Manning 'n' Value
Link II Canal	0+000 to1+740	0.023
Thiba Main Canal	0+000	0.020
	0+380 to 7+177	0.016

From Table 4.4, the obtained values ranged from 0.022 – 0.033 for LCII while 0.013 – 0.016 for TMC. These values were consistent with those observed by DeVries *et al.* (2004) while conducting hydraulics of the East Branch of California Aqueduct.

4.4.2 Contraction and expansion coefficients

Contraction and expansion coefficients were set to standard values of 0.1 and 0.3 respectively based on recommendations from HEC-RAS manuals (USACE, 2001). Due to the fact that there are no significant contraction and expansion losses at motorable bridges or check structures in the entire reach, it would be expected that adjusting these coefficients would have little impact on model performance. This was consistent with Giovannettone (2008) findings in the study in St. Clair River in Michigan, where no significant contraction and expansion losses at bridges and other larger obstructions were experienced.

4.4.3 Flow roughness factor

Flow roughness factors were not used in this model since they are features that are useful in calibration of unsteady flow model. This option allows the user to adjust the roughness coefficients with changes in flow. However, calibration and validation results from section 4.7 show that the model did not have difficulty simulating water levels for high and low flow extremes. Also, previous work has shown that calibrated n-values are not affected by flow. These findings further agree with those found by Giovannettone (2008) in the study carried out in Michigan.

4.5 Model operation and simulation

The results of the simulated and measured water depths for LCII and TMC for Manning's (n) value of 0.023 and 0.016 are presented in Tables 4.5 and 4.7.

Table 4.5: Simulated and measured water depth for LCII when n = 0.023

Canal	Chainage (m)	Canal station	Measured Flow (m^3s^{-1})	Water depth		Percentage Error (%)
				Measured (m)	Simulated(m) n = 0.023	
LCII	1+740	0	4.1	1.85	1.85	0.0
	1+490	1	4.3	2.06	2.05	-0.5
	1+293	2	3.4	2.05	2.08	1.5
	1+096*	3	3.6	2.03	2.09	3.0
	0+900	4	3.9	2.03	2.12	4.4
	0+770*	5	4.2	2.02	2.07	2.5
	0+640	6	4.4	2.00	2.02	1.0
	0+510*	7	4.5	1.80	1.78	-1.1
	0+380	8	4.5	1.50	1.49	-0.7
	0+190*	9	4.5	1.20	1.12	-6.7
	0+000	10	5.5	1.00	1.00	0.0

*Interpolated cross-sections

From Table 4.5, at n=0.023, the modelled values fitted well to the measured values. This was evident from the percentage errors from chainage 0+380 to 1+740. The higher value of 6.7% at chainage 0+190 was as a result of interpolation of the existing cross-section. An increase in flow at chainage 1+490 followed by a subsequent drop at chainage 1+740 was suspected to be as a result of either data flow measurement errors, wider canal or cross section spacing.

Table 4.6 presents a summary of simulated results that were obtained after the set up and data entry into the model for LCII. The simulation process was carried out at selected boundary conditions where the ‘n’ value was set at 0.025 and the water surface (Ws) at 0.45 m. Three simulation scenarios; Sim 1, Sim 2 and Sim 3 were carried out with a constant Ws set at 1 while the ‘n’ values were set at 0.023, 0.025 and 0.027 respectively. In order to capture the variation of the simulations, the values obtained were plotted along the canal chainage (different stations) as presented in Figure 4.3.

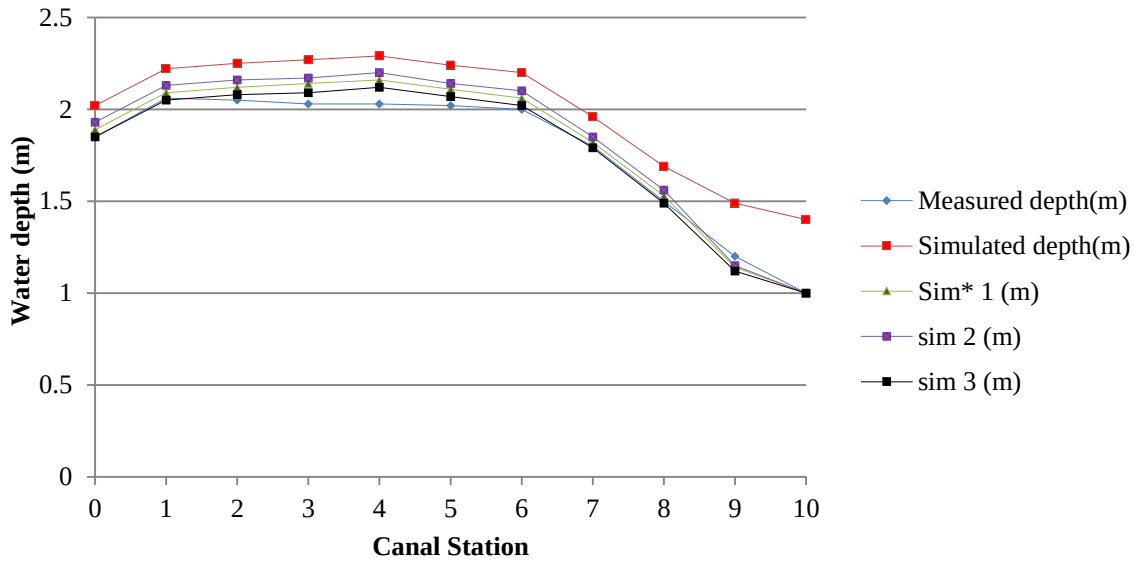

Figure 4.3: Simulated and measured water depth along the canal stations for LCII

Table 4.6: Summary of simulation results for LCII

Boundary conditions			n = 0.025 Ws = 0.45	n = 0.025 Ws = 1	n = 0.027 Ws = 1	n = 0.023 W_S = 1
Chainage (m)	**Canal station**	**Measured depth (m)**	**Simulated depth (m)**	**Sim* 1 (m)**	**Sim 2 (m)**	**Sim 3 (m)**
1+740	0	1.85	2.02	1.89	1.93	1.85
1+490	1	2.06	2.22	2.09	2.13	2.05
1+293	2	2.05	2.25	2.12	2.16	2.08
1+096	3	2.03	2.27	2.14	2.17	2.09
0+900	4	2.03	2.29	2.16	2.2	2.12
0+770	5	2.02	2.24	2.11	2.14	2.07
0+640	6	2.00	2.20	2.06	2.10	2.02
0+510	7	1.80	1.96	1.82	1.85	1.79
0+380	8	1.50	1.69	1.53	1.56	1.49
0+190	9	1.20	1.49	1.14	1.15	1.12
0+000	10	1.00	1.40	1.00	1.00	1.00

Sim* - Simulation
Ws - Starting point water level (Initial Boundary Condition)

Table 4.6 presents a summary of simulation results which were further used to develop the graphs in Figure 4.3. From Table 4.6, increase in values of 'n' led to an increase in corresponding water depth. The water depth along the canal was initially low, then increased upstream and as it flowed, it decreased further downstream. These results show that with increase in roughness coefficient, water level profile is no longer uniform and appears as a gradual variable flow, thus the water level profile changed. In the downstream direction, the flow reduces along the canal leading to further increase of energy drop.

Table 4.7 presents results for TMC canal with the 'n' value set at 0.016 for different canal stations. For each flow the corresponding measured and simulated water depths are also presented. From the Table, the modelled values fitted well to the measured values apart from values from chainage 5+160 to 5+800. This was evident from the high percentage errors (48.5%) recorded. However, the percentage errors gradually increased and later decreased as the flow decreased downstream. These margins of errors can be attributed to differences in inherent uncertainties in measurement of velocities such as the pooling effect of canal water at the various drop structures, discharge calculation technique, measuring devices, discharge rating equation and the length of canal being modelled.

Table 4.7: Simulated and measured water depth for TMC when n=0.016

Remark	Chainage (m)	Canal station	Measured Flow (m^3/s)	Water Depth (m)		Percent Error (%)
				Measured	Simulated	
TMC	7+175	000	0.80	0.32	0.32	0.0
	6+028	250	0.80	0.35	0.33	-5.7
	6+018	300	0.90	0.20	0.18	-10.0
	5+800	400	1.20	0.28	0.31	+10.7
	5+443	500	1.20	0.35	0.18	-48.5
	5+326	600	1.20	0.35	0.18	-48.5
	5+160	700	1.20	0.35	0.18	-48.5
	4+960	800	1.20	0.20	0.18	-10.0
	4+720	900	1.20	0.28	0.18	-35.7
	3+978	1000	1.20	0.20	0.18	-10.0
	3+880	1100	1.20	0.20	0.18	-10.0
	3+406	1200	1.31	0.35	0.38	+8.5
	3+220	1300	1.63	0.20	0.22	+10.0
	2+896	1400	1.63	0.22	0.22	0.0
	2+575	1500	1.63	0.22	0.23	+4.5
	2+231	1600	1.83	0.22	0.23	+4.5
	2+053	1700	1.83	0.20	0.24	+20
	1+954	1800	1.90	0.45	0.48	+6.6
	1+530	1900	2.00	0.50	0.51	+2.0

1+329	2000	2.00	0.50	0.51	+2.0
0+858	2100	2.00	0.48	0.49	+2.0
0+613	2200	2.00	0.70	0.73	+4.2
0+491	2300	3.30	0.40	0.39	-2.5
0+480	2400	3.30	0.40	0.39	-2.5
0+155	2500	3.50	0.85	0.86	+1.1
0+000	2600	3.65	1.00	0.98	-2.0

Table 4.8 presents a summary of simulated results that were obtained after the set up and data entry into the model for TMC. The simulation process was carried out at selected boundary conditions where the 'n' value was set at 0.020 and 0.016 while the water surface between 0.98 and 1.00 m. Three simulation scenarios; Sim 1, Sim 2 and Sim 3 were carried out with a constant Ws set at 0.98 while the 'n' values were set at 0.016 and 0.020 respectively. In order to capture the variation of the simulations, the values obtained were plotted along the canal stations as presented in Figure 4.4.

Table 4.8: Summary of simulation results for TMC

		Q=3.4 to 0.8; n=0.016	**Q=3.4, n= 0.020**	**Q=3.4, n= 0.016**	**Q=3.4 to 0.19; n= 0.016**
Chainage	**Measured**	**Simulated**	**Sim 1**	**Sim 2**	**Sim 3**
2600	0.32	0.32	0.721	0.66	0.15
2500	0.35	0.33	0.713	0.65	0.18
2450	0.35	0.34	0.65	0.6	0.20
2400	0.20	0.18	0.355	0.35	0.09
2350	0.20	0.18	0.352	0.35	0.09
2300	0.28	0.31	0.6	0.55	0.17
2250	0.30	0.25	0.47	0.45	0.13
2200	0.35	0.18	0.349	0.35	0.09
2150	0.35	0.18	0.386	0.35	0.09
2100	0.35	0.18	0.35	0.35	0.08
2050	0.35	0.18	0.381	0.35	0.09
2000	0.35	0.36	0.679	0.62	0.20
1950	0.20	0.18	0.35	0.35	0.09
1900	0.20	0.18	0.348	0.35	0.09
1850	1.30	1.31	1.565	1.56	1.17
1800	0.28	0.18	0.349	0.35	0.09
1750	0.20	0.23	0.452	0.41	0.12
1700	0.20	0.18	0.349	0.35	0.09
1650	0.20	0.18	0.349	0.35	0.09
1600	0.20	0.18	0.349	0.35	0.09
1550	0.32	0.32	0.66	0.58	0.32

1500	0.35	0.38	0.678	0.61	0.35
1450	0.41	0.41	0.704	0.63	0.38
1400	0.20	0.22	0.34	0.35	0.19
1350	0.40	0.40	0.64	0.59	0.40
1300	0.22	0.22	0.34	0.35	0.22
1250	0.40	0.43	0.65	0.60	0.41
1200	0.22	0.23	0.34	0.35	0.22
1150	0.50	0.50	0.76	0.69	0.47
1100	0.22	0.23	0.34	0.35	0.22
1050	0.40	0.41	0.60	0.56	0.38
1000	0.20	0.24	0.34	0.35	0.22
950	0.32	0.32	0.57	0.49	0.27
900	0.45	0.48	0.70	0.64	0.46
850	0.25	0.25	0.35	0.35	0.24
800	0.50	0.51	0.72	0.67	0.49
750	0.30	0.28	0.40	0.40	0.28
700	0.50	0.51	0.73	0.67	0.50
650	0.28	0.28	0.39	0.40	0.28
600	0.48	0.49	0.69	0.64	0.47
550	0.30	0.29	0.40	0.40	0.28
500	0.70	0.73	0.80	0.72	0.55
450	0.70	0.71	0.80	0.73	0.55
400	0.40	0.39	0.39	0.40	0.28
350	0.65	0.69	0.77	0.70	0.53
300	0.40	0.39	0.39	0.40	0.29
250	0.85	0.86	0.95	0.84	0.84
0	1.00	0.98	0.98	0.98	0.98

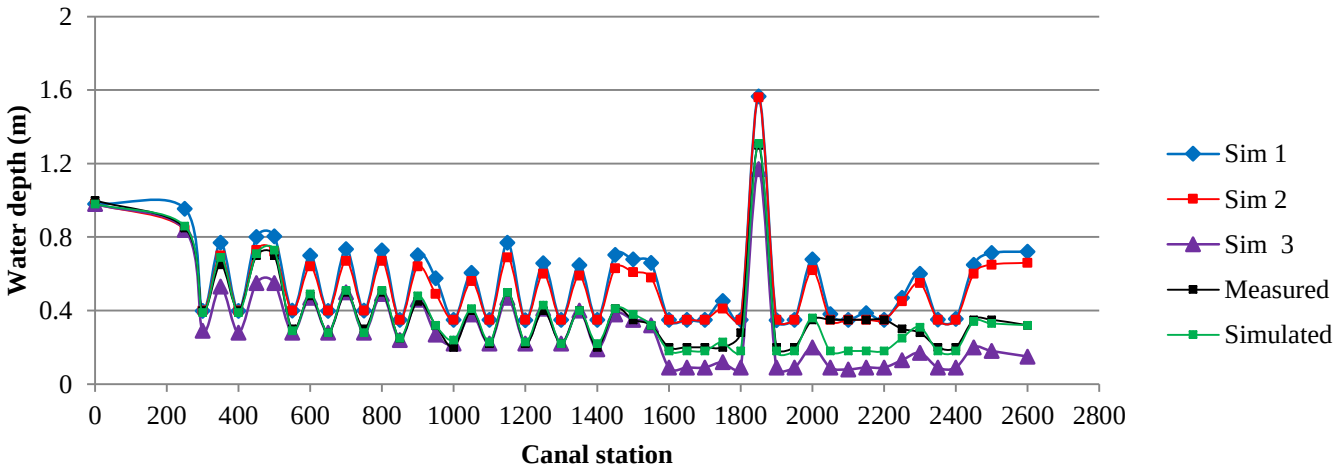

Figure 4.4: Simulated and measured water depth along the canal stations for TMC

Figure 4.4 presents results of measured and simulated flow depths at values of 'n' set as 0.016 and 0.020 along the canal stations. The results show a similar trend in energy drop as the roughness coefficient was changed. From the graphs, it can be seen that this section of the canal had very many drop structures captured in the model for accurate results. At canal station 1850, a very sharp drop was observed which further caused a corresponding energy drop. Due to the numerous drop and check structures in the main canal path for water transport, their effects are sometimes greater than those of roughness coefficient (Bookman, 1999).

4.6 Sensitivity analysis

A sensitivity analysis was performed on the model parameters, mainly the bed roughness coefficients and model geometry to determine how the simulated flows and water levels were affected by controlled changes. Also, boundary conditions were set to an upstream discharge of 5.54 and 3.65m^3/s for LCII and TMC respectively. Downstream canal stage levels of 1m were applied in all reaches to ensure accuracy of the results due to subcritical flow conditions.

4.6.1 Manning's coefficient

Model runs to test sensitivity of Manning's roughness were performed by increasing and decreasing the roughness coefficients in each calibration reach by eight percent in LCII and six percent in TMC. The results show that an increase in roughness coefficients caused an increase in the water levels simulated for both LCII and TMC, while a decrease in roughness coefficients led to a decrease in water levels simulated for both canals. The largest change in simulated water levels in TMC was 0.45 and 0.12 m in LCII. Generally, the changes occurred when the roughness coefficients were adjusted in TMC reach. This was logical considering that TMC changes affected a larger section of the system. The details of the analysis are presented in Tables A5 and A6 in Appendix 8.

4.6.2 Cross-section interpolation

This analysis showed that few cross-sections in the LCII geometry could not be accurately used to run the model. The use of few cross-sections yielded errors and warnings which indicated a need for additional cross-sections at chainage 0+190, 0+510, 0+770 and 1+096. This caused a change in simulated water level. The result suggested that a sufficient number of cross-sections were necessary in the development of the HEC-RAS geometry to accurately

model the canal. Further, it showed that the model was most sensitive in the section along the LCII reach.

4.6.3 Boundary condition adjustment

The boundary conditions of the model were adjusted for two separate cases. In the first simulation, the upstream boundary condition of flow in LCII was adjusted while holding the downstream boundary condition at a known water surface of 0.45 m. This analysis showed that increasing the flow boundary at Chainage of 0+000 to 3.65 m^3/s raised water levels far above the simulated level by 0.40 m. These results are shown in detail in Table 4.6.

In the second run, the stage boundaries at LCII and TMC were adjusted while holding the stage boundary at a known water surface at 1.00 m and 0.98 m respectively. Different values for stage boundaries were used because the canals carried different flows at the downstream ends due to branch canals along the reach. Figures 4.3 and 4.4 shows the trend of increasing roughness coefficient from 0.023 to 0.027 for LCII and decreasing 0.020 to 0.016 for TMC that corresponds to increasing water depth levels for both reaches. The graph shows that under these conditions, the simulated values had a similar trend corresponding to the measured values.

4.7 Model calibration and validation results

The objective of model calibration was to minimize the error between observed and simulated water levels. This was done through the adjustment of Manning's roughness coefficients. Initial roughness coefficients for each calibration are presented in Table 4.9. The calibration was completed using steady water level and flow boundary conditions. The downstream boundary at LCII and TMC was set at 1 m, and the upstream boundary at LCII was set at a discharge of 6.50 m^3/s while 3.65 m^3/s was set for TMC. The scenario represented approximately average conditions in the Thiba system.

Table 4.9: Initial Roughness coefficient and boundary conditions

Canal	Chainage (m)	Max. Discharge (m^3/s)	Known water surface (m)	Roughness coefficient
LCII	0 to 1+740	6.50	1	0.025
TMC	0 to 7+400	3.65	1	0.020

To determine the sensitivity of the model to changes in Manning's roughness coefficient, a range of n-values in a single calibration reach were simulated separately. The HEC-RAS model was executed repeatedly while varying these parameter estimates and the difference between the observed water levels and simulated water levels for both canals presented in Tables 4.10 and 4.11. Plots of simulated versus measured water levels in each calibration reach are shown in Figures 4.5 and 4.6. The Figures show those adjustments of n-values to 0.020 and 0.016 for LCII and TMC respectively. Further, they show that adjustments at certain calibration sections only affect observed water levels at certain canal stations.

Table 4.10: Summary of measured and simulated water depths for LCII

Canal station	Measured depth(m)	Simulated depth (m)
0	1.85	1.85
1	2.06	2.05
2	2.05	2.08
3	2.03	2.09
4	2.03	2.12
5	2.02	2.07
6	2.00	2.02
7	1.80	1.79
8	1.50	1.49
9	1.20	1.12
10	1.00	1.00

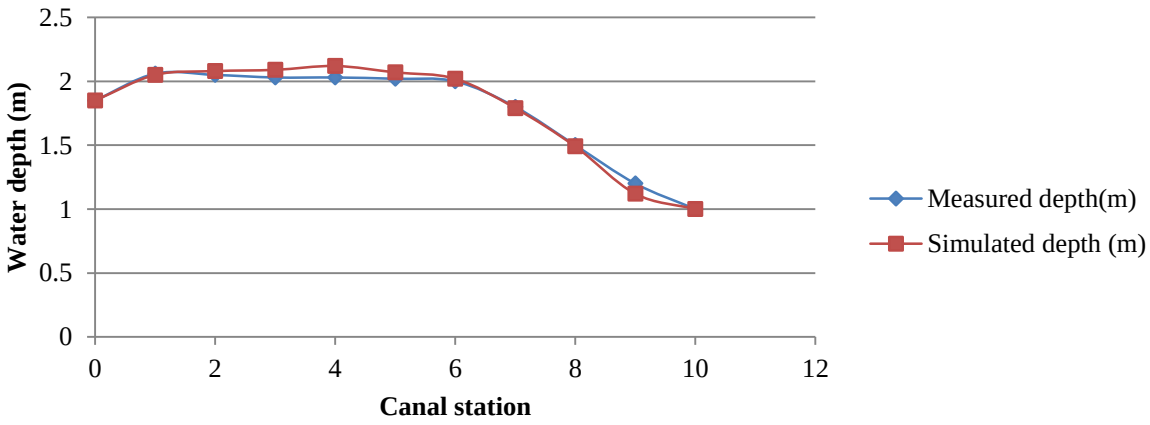

Figure 4.5: Model behaviour with roughness coefficient of 0.020 in LCII

Table 4.11: Summary of measured and simulated water depths for TMC

Chainage	Measured	Simulated n = 0.016
2600	0.32	0.32
2500	0.35	0.33
2450	0.35	0.34
2400	0.20	0.18
2350	0.20	0.18
2300	0.28	0.31
2250	0.30	0.25
2200	0.35	0.18
2150	0.35	0.18
2100	0.35	0.18
2050	0.35	0.18
2000	0.35	0.36
1950	0.20	0.18
1900	0.20	0.18
1850	1.30	1.31
1800	0.28	0.18
1750	0.20	0.23
1700	0.20	0.18
1650	0.20	0.18
1600	0.20	0.18
1550	0.32	0.32
1500	0.35	0.38
1450	0.41	0.41
1400	0.20	0.22
1350	0.40	0.40
1300	0.22	0.22
1250	0.40	0.43
1200	0.22	0.23
1150	0.50	0.50
1100	0.22	0.23
1050	0.40	0.41
1000	0.20	0.24
950	0.32	0.32
900	0.45	0.48
850	0.25	0.25
800	0.50	0.51
750	0.30	0.28
700	0.50	0.51
650	0.28	0.28
600	0.48	0.49
550	0.30	0.29
500	0.70	0.73
450	0.70	0.71
400	0.40	0.39

350	0.65	0.69
300	0.40	0.39
250	0.85	0.86
0	1.00	0.98

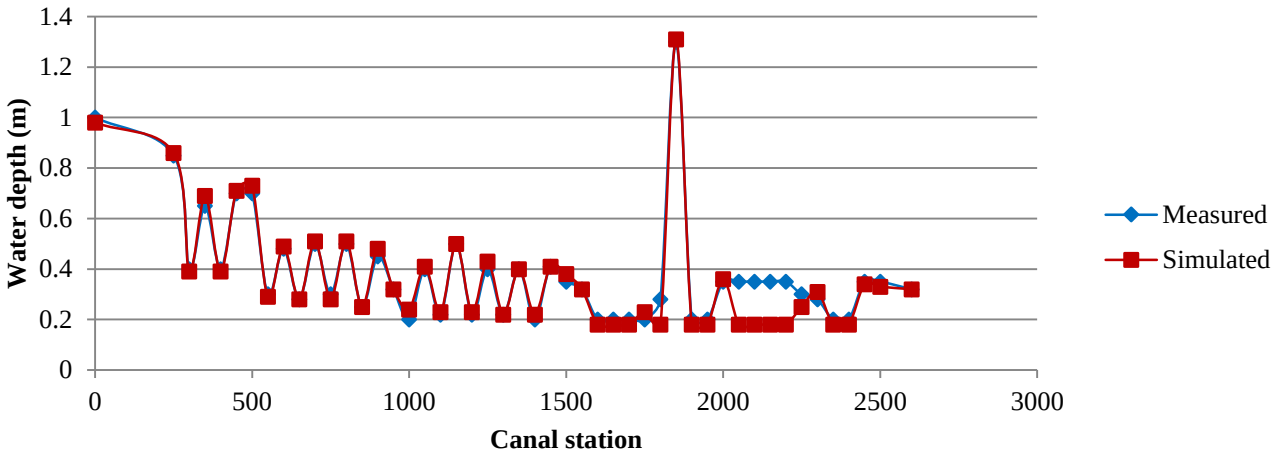

Figure 4.6: Model behaviour with roughness coefficient of 0.016 in TMC

4.8 Model operation and maintenance procedures

On canal capacity estimation, it was evident that both the two canal reaches could no longer carry the design discharge capacity as per Tables 4.12 and 4.13 respectively. LCII presented a drop of 10.97% while TMC by 11.61%. For earth canals, in this case LCII, lose their maximum capacity potential over time, which causes a reduction in water discharge. Further deformation of the bottom slope in earth canals due to improper dredging and sedimentation, changes the canal hydraulic regime and in some cases, reduce canal capacity.

4.8.1 Canal capacities

The estimated canal capacities for the Link Canal II and the Thiba main canal are summarized in Tables 4.12 and 4.13.

Table 4.12: Link Canal II summary of estimated maximum capacities

Reach	Chainage (m)	Maximum design flows (m^3/s)	Estimated maximum flows (m^3/s)	Percentage change (%)
LC II	**0+000 to 1+740**	**11.12**	**9.9**	**10.97**

Table 4.13: Thiba Main Canal summary of estimated maximum capacities

Reach	Chainage (m)	Maximum design flows (m^3/s)	Estimated maximum flows (m^3/s)	Percentage change (%)
TMC	0+000 to 0+497	10.20	9.2	9.8
	0+497 to 1+530	6.40	5.8	9.4
	1+530 to 3+406	6.20	5.5	11.3
	3+406 to 4+065	6.10	5.3	13.1
	4+065 to 4+744	5.90	5.1	13.5
	4+744 to 5+151	5.80	4.9	15.5
	5+151 to 6+018	5.60	4.9	12.5
	6+018 to 7+175	5.10	4.7	7.8
	Average		**5.7**	**11.61**

From tables 4.12 and 4.13, the results indicate a decrease of maximum canal capacity for the two reaches by 10.97% and 11.61% respectively. These results compare fairly well with those obtained by DeVries *et al*., (2004) while carrying out a study in California. Bookman (1999) on the other hand found out that an increase in Manning's 'n' coefficient resulted to 12% and 5% decrease of maximum canal capacity in reach one and two respectively at Beardsley canal for the U.S. Bureau of Reclamation. The author attributed the greater effect in reach one to lack of regulating structures in that section.

From Table 4.12, the reduction of canal capacity in LCII is attributed to absence of regulating structures in the reach, seepage losses and flow within the canal with minimum branching. Table 4.13 presents an average discharge reduction of $5.7 m^3/s$ for Thiba Main Canal. This reduction in canal capacity is attributed to reduction of canal dimensions during past rehabilitation process. Further, the analysis indicates that the effect caused by a slight change in the roughness coefficient to the canal discharge is substantial. This makes the canal roughness a sensitive parameter.

TMC consists of twenty seven hydraulic drop structures in the main canal path for water transport. This is among the main factors generating flow drop and their effects are sometimes greater than those of roughness coefficients. In addition, the walls of the left and

right banks have more roughness coefficients than the center of the earth canal. This issue becomes more severe in modelling of maximum flow rates. This could be the other reason attributed to the 11.61% drop in canal capacity for TMC reach.

4.8.2 Canal bank overflows

It is noted from the results that the integrity of the canal lining in TMC varied from one section to the other. Some sections were in good rehabilitated state while other sections downstream had breaks in the lining. The results show that on LCII, three canal stations 840, 1293 and 1490 were submerged by the design flow rate of 11.12 m^3/s. More details on cross-section profiles for the LCII canal are presented in Figure A5 of Appendix 7. On TMC, two canal stations at 250 and 1850 were submerged by a design discharge of 6.4 m^3/s as presented in Figure A6 of Appendix 7. This might have been caused by erosion of the right hand side (RHS) bank on LCII, while changes in canal dimensions during rehabilitation of TMC could be the main cause of bank overflow. Several remedies including canal lining of the LCII could be the long term solution for the canal to carry its design flow capacity.

4.8.3 Distribution plan to units

The modelling results indicated that the reduction in canal carrying capacities on average were 5.7 m^3/s and 9.9 m^3/s for TMC and LCII respectively. Managers and operators can therefore make feasible decisions on how water can be distributed to various units based on Table 4.14. Due to the reduction of canal carrying capacities, distribution plan values must be recalculated or gate opening time increased to achieve the same discharge per 100 ha as indicated.

Table 4.14: Standard discharge for different water supply to units

Level	Standard discharge ($m^3/s/100$ Ha)	Period
A	0.18	Flooding season (land preparation)
B	0.12	High ET period
C	0.09	Ponding and transplanting period and during deficit in level B

Source: Abdullahi and Tanaka (2009)

4.9 Model evaluation

The model performance results for the LCII canal and Thiba main canal are presented in Figures 4.7 and 4.8 respectively. The results in both cases show that the coefficients of gain (R^2) are 0.9927 and 0.949 for the LCII and Thiba main canal respectively. These results show that the model performed very well. According to Santhi *et al.*, (2001), higher values of R^2 indicate less error variance and typically values greater than 0.50 are considered acceptable.

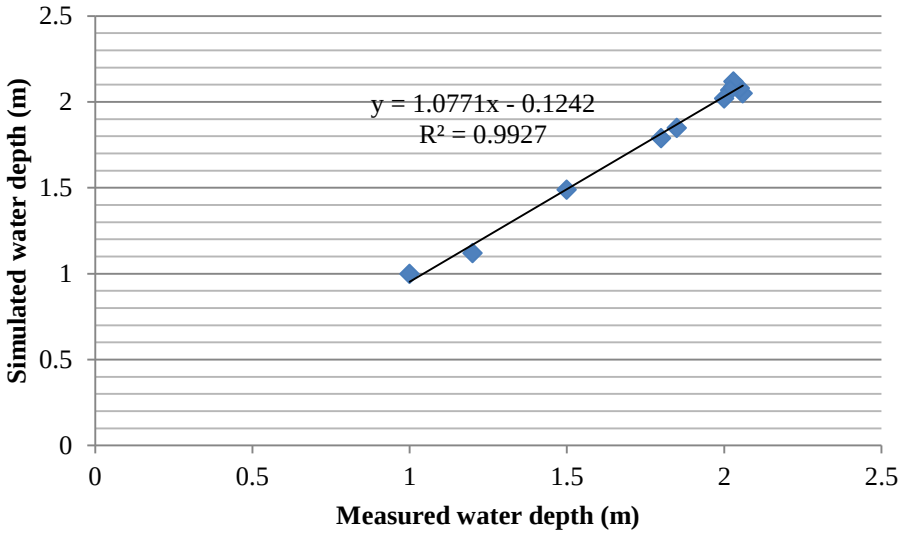

Figure 4.7: Measured vs simulated water depth for LCII

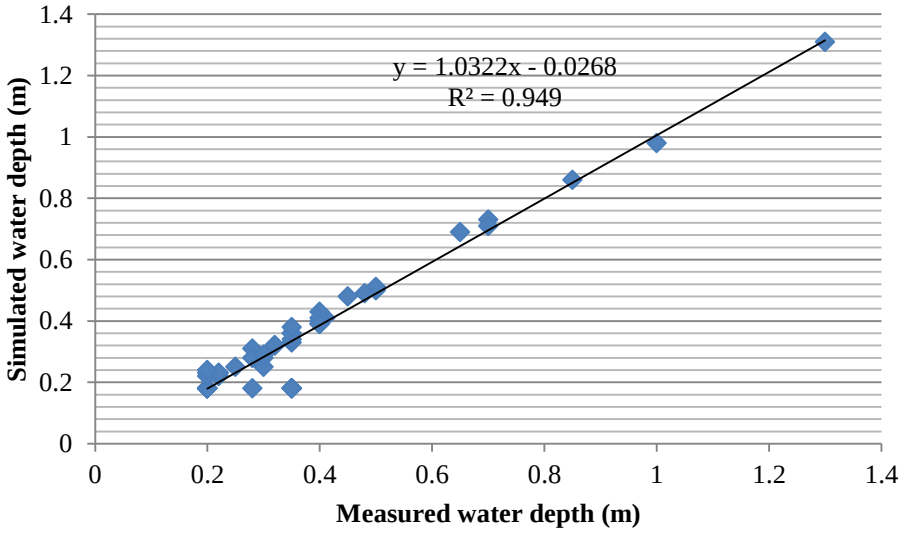

Figure 4.8: Measured vs simulated water depth for Thiba Main Canal

A graphical display was used for visual comparison of the predicted and measured water depth in the two sub-reaches. The results are as presented in Figures 4.7 and 4.8. A plot of coefficient of gain (R^2) revealed that the correlation between simulated and measured water depth was relatively high for both sub-reaches. The R^2 value gave information about the goodness of fit of the model. In this regard, the modeled results for LCII and TMC indicated a near perfect goodness of fit of 0.99 and 0.95 respectively which suggested that the modelled simulations were as good as measured water depths. Visual inspection of the scatter plots of simulated versus measured water depths in Figures 4.7 and 4.8 show an equally good spread around the line of equal values.

CHAPTER FIVE

CONCLUSION AND RECOMMENDATION

5.1 Conclusion

Evaluation of the effect of hydraulic and structural variations on Thiba main canal reach potential capacity and formulation of improved operational and maintenance procedures for the system using HEC-RAS model as a decision support tool were the specific objectives of this research. This was achieved by calibrating the model to maximize the coefficient of roughness as the key parameter. Physical and conceptual parameters were obtained through direct measurement in the field, calibration and derivation using manuals respectively.

Statistical and graphical techniques were used for the HEC-RAS model assessment to establish model performance. The coefficient of gain (R^2) values for LCII and TMC were 0.9927 and 0.949 respectively which verified the close agreement between simulated and observed water levels. On canal capacity estimation, both canal reaches could no longer carry the design discharge capacities as LCII and TMC reflected a drop in flow capacity by 10.97% and 11.61% respectively. The results of the assessment showed that the HEC-RAS model simulated the water depth in the two canals within acceptable ranges. Since most schemes or projects do not maintain canal data like as-built drawings and design data, it was clear that the HEC-RAS model can be used to estimate the canal capacity potential.

On formulation of improved operational and maintenance procedures, the model indicated areas of potential bank overflow at specific discharges in each reach. Dredging of canals due to siltation in LCII was identified as one of the contributing factor to deterioration of the earth canal due to irregular wall shaping and slope changes. Recalculation of water distribution plans and increase of gate opening time for efficient water supply in the system was suggested. In this regard, it can be concluded that the HEC-RAS model provides a useful technique which is essential in canal operation and management.

5.2 Recommendations

Based on the results of the HEC-RAS model, further assessment of the model should be carried on the following:

i. Use of a higher conveyance ratio (Upstream conveyance/downstream conveyance) and testing of the results obtained with other methods of cross section spacing.
ii. Calibration and immediate installation of flow measuring gauges and data loggers directly after the primary off-takes so that the model can be tested using long periods of continuous flow data covering both the long and short rainy seasons in the two canals and also tested in other schemes with similar conditions.
iii. Whether the canals were constructed as per the original designs and the quantities required for further rehabilitation.
iv. Since HEC-RAS model does not account for water losses through seepage and evaporation, other techniques should be used to estimate the water losses. Further research should come up with techniques of combining the HEC-RAS model capabilities in addition to techniques of estimating water losses through seepage and evaporation.

REFERENCES

Abdullahi, M. and Tanaka, S. (1995). Mwea Irrigation Scheme Water management manual. *1*:13.

Africa Rice Center (WARDA). (2007). *Rice trends in Sub Saharan Africa.* (3rd ed.). Contonou.

Aldrighetti, E. (2007). *Computational hydraulic techniques for the saint Venant equations in arbitrarily shaped geometry*. Unpublished doctoral dissertation Department of mathematics, University of Trento.

ASCE. (1993). Criteria for evaluation of watershed models. *Journal of Irrigation Drainage Engineering, 119* (3): 429-442.

Bansal, R. K. (2010). *Textbook of fluid mechanics: (In SI Units).* Bangalore: Laxmi publication Pvt. Ltd.

Bitner, C. J. (2003). *Selection and design of porous low drop grade control structures*. Unpublished master's thesis Department of Civil Engineering, Colorado State University. Fort Collins: Colorado.

Bookman, E. (1999). *Maricopa Water District Beardsley Canal and associated delivery system hydraulic capacity analysis report, 1(1),* 1-12.

Chadwick, A., Morfett, J. and Borthwick, M. (2013). *Hydraulics in Civil and Environmental Engineering.* (5th ed.). London: CRC Press.

Chanson, H. (2004). *The Hydraulics of Open Channel Flows; basic principles, sediment motion, hydraulic modelling, design of hydraulic structures*. Amsterdam: Elsevier Butterworth Heineman publishers.

Chow, V. T. (1959). *Open Channel Flow*. New York, NY: McGraw Hill Publishers.

Clemens, C. B. (2012). *Turbulent open channel flow, sediment erosion and sediment transport.* Karlsruhe: KIT scientific publishers.

Corplan Management Consultants (CMC). (2011). *Monitoring and Evaluation Main Report findings,* (Rep. No.03.). Nairobi: CMC Press.

de Fraiture, C., Wichelns, D., Rockström, J., Kemp-Benedict, E., Eriyagama, N., Gordon, L.J., Hanjra, M.A., Hoogeveen, J., Huber-Lee, A. and Karlberg, L. (2007). *Looking ahead to 2050: scenarios of alternative investment approaches*. In: Molden, D. (Ed.), Comprehensive Assessment of Water Management in Agriculture, Water for Food, Water for Life: A Comprehensive Assessment of Water Management in Agriculture. International Water Management Institute, London.

DeVries, J. J., Tod, I.C. and Jensen M.R. (2004). Study of the Hydraulic Performance of the East Branch, California Aqueduct, J. Amorocho Hydraulics Laboratory, Department of Civil and Environmental Engineering, University of California, Davis.

Food and Agriculture Organization (FAO). (2006). *Overview: Rice in Africa a compendium*. Africa Rice 2008. Africa Rice Center, Bouaké.

Food and Agriculture Organization (FAO). (2007). *Modernizing Irrigation Management-the MASSCOTE approach.* FAO Irrigation and Drainage Paper 63. (Available at: http://www.fao.org/nr/water/docs/masscote/technical/masscote.pdf.)

Food and Agriculture Organization. (FAO). (2011). *The state of the World's land and water resources for food and agriculture. Managing systems at risk*. (Assessment Rep. No.6.). Rome: Publishing Policy and support Branch.

Gautum, D.K. and Kharbaja, R.G. (2006). Flood hazard mapping of Bagmati River in Kathiamandu valley using geo-infirmatics tools. *Journal of hydrology and meteorology, 12* (3):1-9.

Gibb Africa Limited. (2010). *Mwea Irrigation Development Project Design review main report. 1*: 36-37.

Giovannettone, J. (2008). *Preparation of the 1-D St. Clair River HEC-RAS Model in order to study changes in River conveyance and morphology. 1*: 4-43.

GoK. (2013). *Economic recovery strategy second medium term Plans 2012-2017*. Ministry of Devolution and planning, Nairobi: Government printers.

Gordon, N.D., McMahon, T.A., Finlayson, B.L., Gippel, C.J and Nathan, R.J. (2004). *Stream hydrology: an introduction for ecologists.* (2nd ed.). West Sussex, England: John Wiley and Sons Publishers.

Hassain, M. (2012). *Numerical simulation of canals irrigation systems in Pakistan*. Paper presented at engineering congress, 70th annual session proceedings, Pakistan.

Hassain, M., Shakir, A.S. and Khan, N.M. (2013). Steady and Unsteady Simulation of Lower Bari Doab canal using SIC model. *Journal of Engineering and Applied Sciences, 52*(12): 60-72.

Hicks, F. and Peacock, T. (2005). Suitability of HEC-RAS for flood forcasting. *Canadian water resources journal, 30* (2):159-174.

Hill, R. (2007). *How well does your irrigation canal hold water*. Utah State University Extension Electronic Publishing. Logan, Utah.

Holly, F.M. and Parrish, J.B. (1991). *Description and evaluation of program CARIMA*. In: Ritter, W.F. (2nd ed.), 1991: 432-437.http:// www.hec.usace.army.mil/software/ hec-ras/downloads.aspx.

Huang, Y. and Fipps, G. (2009). *Developing a modelling tool for flow profiling in irrigation distribution networks.* In: Ritter, W.F. (2nd ed.), 1991: 432-437.

Islam, A., Raghuwanshi, N. and Singh, R. (2008). Development and Application of Hydraulic Simulation Model for Irrigation Canal Network. *Journal of Irrigation and Drainage Engineering*, *134*(1), 49–59.

JI, Z., Vriend, H. and Hu, C. (2003). *Application of SOBEK in the Yellow River estuary*. Paper presented at International conference on estuaries and coasts, Hanhzhou, China.

John, A. and Fielding, M. (2014). Rice production constraints and new challenges for South Asian smallholders: Insights into *de fatcto* research priorities. *Journal of Agriculture and food security. 3*(18):18-46.

Kay, M. (2007). *Practical hydraulics*. (2nd ed.). New York, USA: Taylor and Francis Publishers.

Keya, O. S. (2013). *More rice Less water*. (3rd ed.). Nairobi, Kenya: East African publishers.

Khan, S., Malano, H. and Davidson, B. (2008). System harmonization: a framework for applied regional irrigation planning. *Irrigation and drainage, 122*(10):1-26.

Khatib, J.M. (2009). *Sustainability of construction materials*. (2nd ed.). Cambridge: Woodhead publishers.

Koei, N. (1996). *Mwea Irrigation Development Project Design main report*. *1* (2):16.

Koei, N. (2008). *Mwea Irrigation Development Project Design main report. 2* (1):28.

Koei, N. (2010). *Mwea Irrigation development Project Development plan main report*. *1* (6):23.

Kragh, E. M. (2011). *Flood capacity improvement of San Jose Creek Channel using HEC-RAS*. San Jose Creek, California.

Legates, D. R. and McCabe, G. J. (1999). Evaluating the use of "goodness-of-fit" measures in hydrologic and hydroclimatic model validation. *Journal of Water Resources, 35* (1):23-24.

Maghsoud, A., Alireza, P. and Majid, R. (2013). Study and simulation of Hydraulic and structural changes of changing of section from soil to concrete. *Middle East Journal of Scientific research. 23*(11):1-24.

May, D.R., Lopez, A. and Brown, L. (2000). *Validation of the hydraulic-open channel flow model HEC-RAS with observed data.* Available from www.hec.usace.army. (Accessed 20 May, 2015).

May, R.W.P. (2003). *Hydraulic design of side weirs*. London: Thomas Telford publishers.

Mays, L.W. (2010). *Ancient water technologies.* New York: Springer publishers.

Merkley, G. and Rogers, D. (1993). Description and Evaluation of Program Canal. *Journal of Irrigation and Drainage Engineering*, *119* (4) : 714-723.

Mishra, S. K. and Singh, V. P. (2003). *Soil Conservation Service Curve Number (SCS-CN) Methodology*. Dordrecht: Springer Netherlands.

Molden, D. (2007). *Water for Food, Water for Life: A Comprehensive Assessment of Water Management in Agriculture.* Earthscan and International Water Management Institute. London and Colombo.

Moriasi, D. N., Arnold, J. G., Van Liew, M. W., Bingner, R. L., Harmel, R. D. and Veith, T. L. (2007). Model evaluation guidelines for systematic quantification of accuracy in watershed simulations. Transactions of the ASABE, *50* (3): 885-900.

Munir, M. A. and Qurreshi, M. E. (2010). Global water crisis and future food security in an era of climate change. *Food Policy*, *35*: 365-377.

Munir, S. (2011). *Role of sediment transport in operation and maintenance of supply and demand based irrigation canals*. (2nd ed.). Hague, Netherlands: CRC press.

Mutua, B.M. and Malano, H.M. (2001). Analysis of manual and centralized supervisory control operations to improve level of service: a case study of Pyramid Hill No. 1 Channel, Victoria, Australia. *Irrigation and drainage Journal*, *1*(3): 1-19.

Nalluri, C., Featherstone, R.E. and Marriott, M. (2009). *Civil Engineering Hydraulics*. (5th ed.). Chichester, West Sussex: John Wiley and Sons publishers.

Novak, P., Guinot, V., Jeffrey, A. and Reeve, D.E. (2010). *Hydraulic ModellingModelling - An Introduction: Principles, Methods and Applications*. CRC Press publishers.

Novak, P., Moffat, A.I.B., Nalluri, C. and Larayanan, R. (2007). *Hydraulic Structures*. (4th Ed.). 2 Park Square, Milton Park Abingdon Oxon OX14 4RN. Taylor and Francis publishers.

Ochieng, G.M., Ojo, I.O. and Otieno, O.A. (2010). Irrigation canal simulation models and its application to large scale Irrigation Schemes in South Africa. *International Journal Sustainable Development*, *1*(4):8-13.

Omar, A. C. (2008). *Transitional flow between orifice and non-orifice regimes at a rectangular canal gate*. Utah State University.

Omwenga, K.G., Mati, B.M. and Home, P.G. (2014). Determination of the effects of the system of Rice Intensification (SRI) on Rice yields and water saving in Mwea Irrigation Scheme, Kenya. *Journal of Water Resources and Protection, 6*: 1-18.

Ratnayaka, D.D., Malcolm, J.B., Johnson, M. and Twort, A.C. (2009). *Twort's water supply*. Oxford: Butterworth-Heinemann.

Renault, D., Facon, T., Wahaj, R. and Food and Agriculture Organization of the United Nations. (2007). *Modernizing irrigation management: The MASSCOTE approach--Mapping System and Services for Canal Operation Techniques*. Rome: Food and Agriculture Organization of the United Nations.

Ritter, W. F. (1991). *Irrigation and drainage* (2nd ed.). New York: National Academy Press.

Rosegrant, M. W., Cai, X. and S. A. Cline. (2002). *World Water and Food to 2025: Dealing with Scarcity.* International Food Policy Research Institute. Washington DC.

Santhi, C., Arnold J. G., Williams, J. R., Dugas, W. A., Srinivasan, R. and Hauck, L. M. (2001). Validation of the SWAT model on a large river basin with point and nonpoint sources. *Journal of American Water Resources Association, 37*: 1169-1188.

SAPROF (2009). Mwea Irrigation Scheme JICA Special Assistance for Project Formulation report Safeguards on ESIA and RAP.

Sargison, J. E. and Barton, A. F. (2008). *Application of the HEC RAS to Hydraulic Modelling of an irrigation Scheme to determine potential for capacity increase*, Proceedings of 9th National Conference on Hydraulics in Water Engineering, 23-26 September, 2008, Darwin, Australia.

Seck, P.A., Diagne, A., Mohanty, S. and Wopereis, M.S. (2012). Crops that feed the world 7: rice. *Journal of Food Security, 4*: 7-24.

Shahrokhnia, M.A., Javan, M. and Keshavarzi, A.R. (2008). Application of HEC-RAS and MIKE-11 models for flow simulations in irrigation canals. *Journal of Agricultural Engineering Research, 9*(1): 49-62.

Sharma, R. K. and Sharma, T. K. (2007). *Irrigation engineering for students of civil engineering*. (3rd ed.). New Delhi S Chand publishers.

Singh, S. (2009). *Experiments in fluid mechanics*. New Delhi: PHI learning publishers.

Singh, V.P. (1996). Kinematic Wave modelling in Water resources. Water hydrology. New York. John Wiley & Sons publishers.

Singh, V.P. (2003). *International conference on water and environment*. New Delhi Allied publishers.

Subramanya, K. (2009). *Flow in open channels*. New Delhi: Tata McGraw-Hill publishers.

Tariq, J.A. (2010). *Improving operational performance and management of canal irrigation system using hydraulic modelling.* Unpublished master's thesis, University of Engineering and Technology, Lahore, Pakistan.

Timbadiya, P. V., Patel, P. L. and Porey, R.D. (2011). Calibration of HEC-RAS model prediction of flood for lower Tapi River, India. *Journal of water resources and protection, 23* (9): 1-11.

Trimmer, C. (2010). *Food Security in Asia: The Role of Larger Rice Reserves to Build Confidence in Trade.* IFPRI Policy Note, June 9. Presented at the Bangladesh Food Security Investment Forum, 26-27 May, 2010, Dhaka.

U.N. (2013). The 2012 Revision, key findings and advance Tables. Department of Economic and Social Affairs, Population Division. *World Population Prospects.* Working Paper No. ESA/P/WP.227: 2-14.

USACE. (2001). HEC-RAS: User's and hydraulic reference manuals.

USACE.(2013). *HEC-RAS 4.1.0 model software.* Retrieved March 3, 2014, from

Wahl, T. L. and Lentz, D. J. (2011). *Physical hydraulic modelling of canal breaches*. Hydraulic Laboratory Report HL-2011-09, U.S. Dept. of the Interior, Bureau of Reclamation, Denver, Colorado, 56.

Wahl, T.L. (2004). *Issues and problems with calibration of Canal Gates*. World water and Environmental resources Congress, Salt Lake City, UT, June 27-July 1, 2004 Environmental and Water Resources Institute of the American Society of Civil Engineers.

Yang, J., Townsend, R. D. and Daneshfar, B. (2006). Applying the HEC-RAS Model and GIS Techniques in River Network Floodplain Delineation. *Canadian Journal of Civil Engineering*, *112* (7): 19-28.

APPENDICES

Appendix 1: Plan of the Thiba headworks

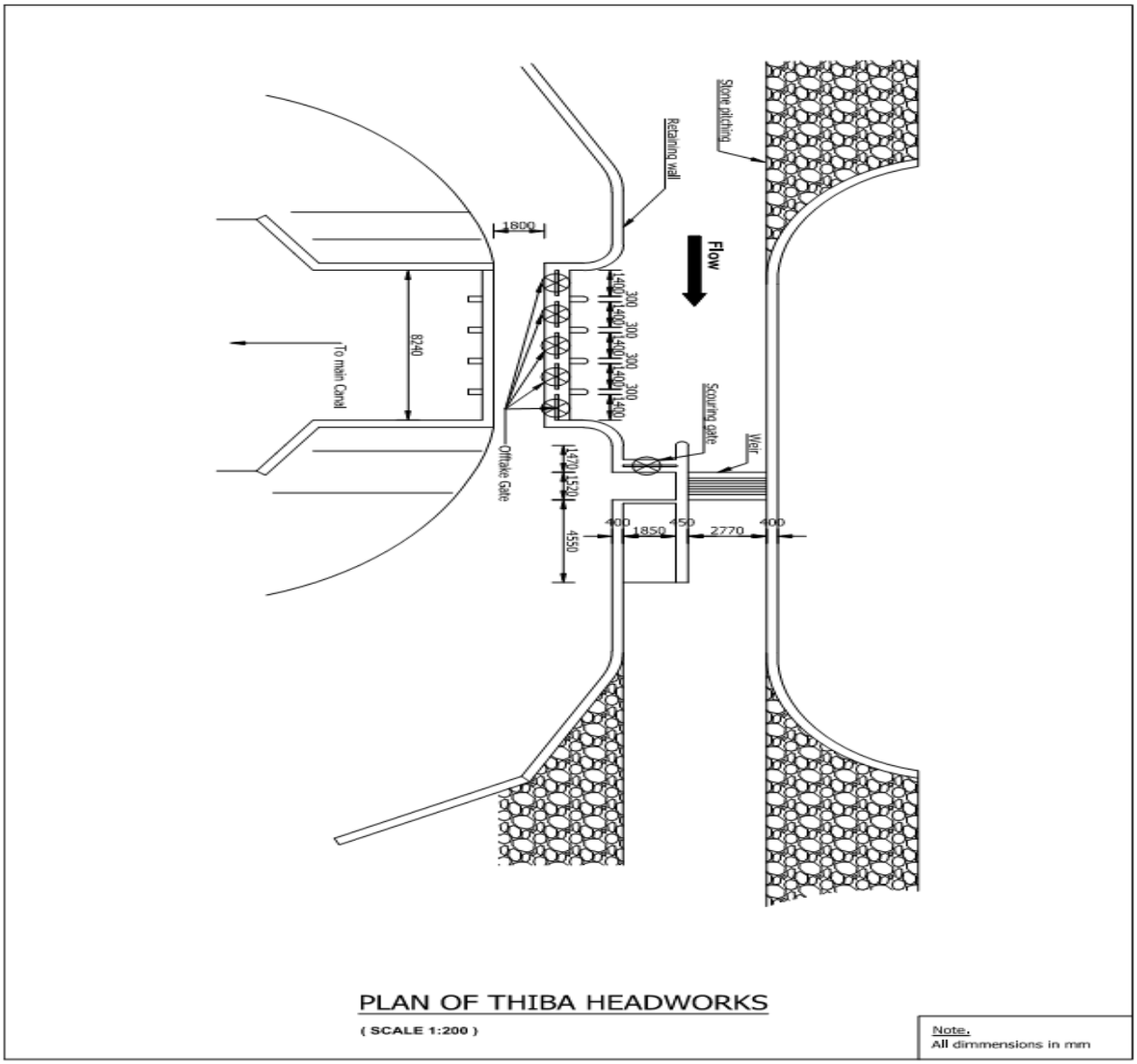

Figure A1: Plan of the Thiba Headworks

Appendix 2: Thiba System Layout

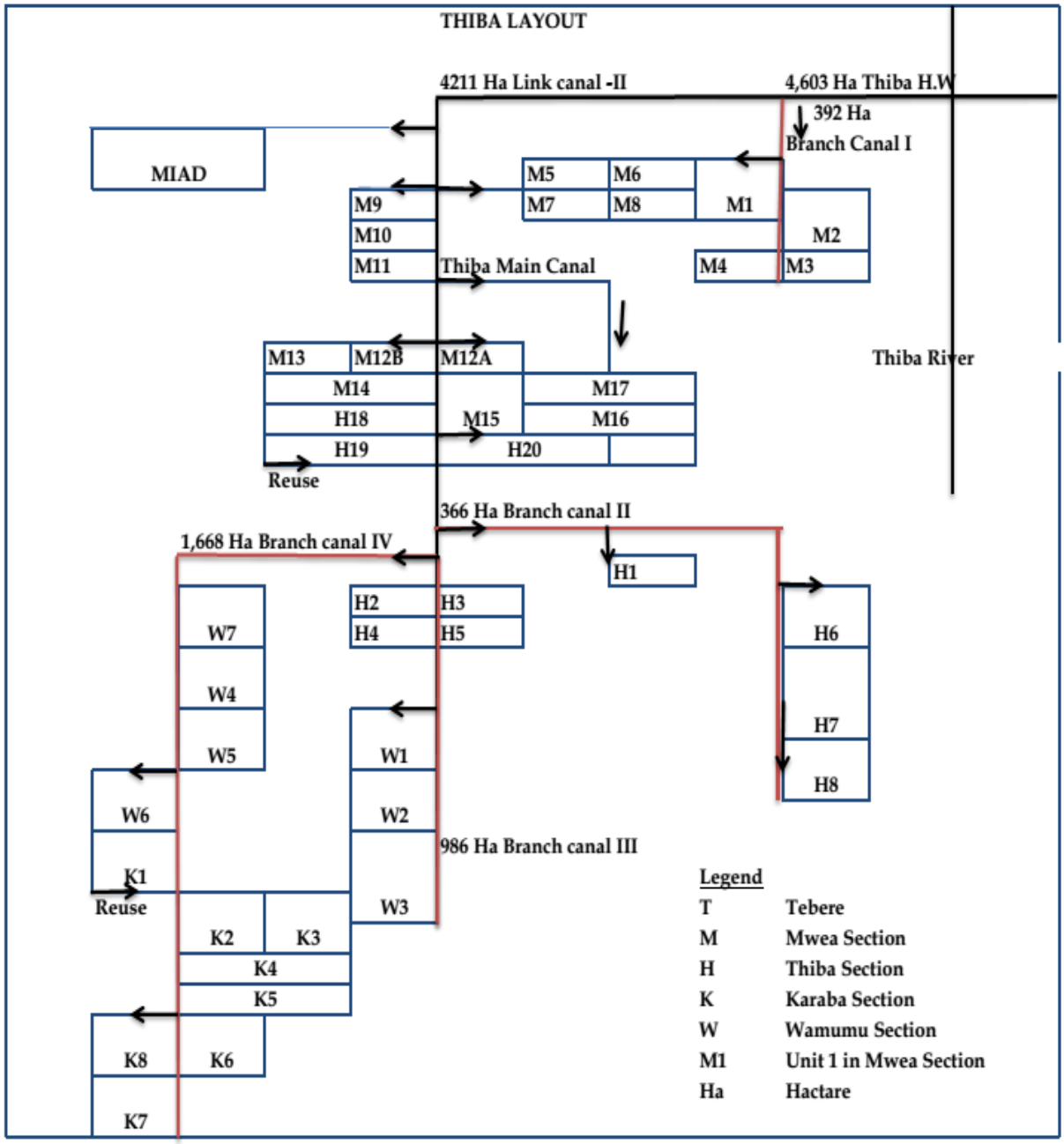

Figure A2: Thiba system layout

Appendix 3: Manning's 'n' Values (Chow's Table)

Table A1: Manning's 'n' values

Type of Channel and description	Minimum	Normal	Maximum
1. Main channels			
a. clean, straight, full stage, no rifts or deep pools	0.025	0.030	0.033
b. same as above, but more stones and weeds	0.030	0.035	0.040
c. clean, winding, some pools and shoals	0.033	0.040	0.045
2. Excavated or dredged channels			
a. Earth, straight, and uniform			
1. clean, recently completed	0.016	0.018	0.020
2. clean, after weathering	0.018	0.022	0.025
3. gravel, uniform section, clean	0.022	0.025	0.030
4. with short grass, few weeds	0.022	0.027	0.033
b. Rock cuts			
1. smooth and uniform	0.025	0.035	0.040
2. jagged and irregular	0.035	0.040	0.050
3. Lined or constructed channels			
a. Cement			
1. neat surface	0.010	0.011	0.013
2. mortar	0.011	0.013	0.015
b. Concrete			
1. trowel finish	0.011	0.013	0.015
2. float finish	0.013	0.015	0.016
3. finished, with gravel on bottom	0.015	0.017	0.020
4. unfinished	0.014	0.017	0.020
c. Asphalt			
1. smooth	0.013	0.013	
2. rough	0.016	0.016	
4. Closed conduit running partly full			
a. Welded steel	0.010	0.012	0.014
b. Concrete culvert	0.010	0.011	0.013

Source: Chow (1959)

Appendix 4: Cross-sections

Table A2: Model Output Details for LCII

Link Canal II Summary Table - HEC-RAS model output at calibration and maximum flow rate profiles n=0.023 WS=1.00															
Reach	**Canal Station**	**Profile**	**Q Total**	**Min Ch Elev**	**W.S. Elev**	**Crit W.S.**	**E.G. Elev**	**E.G. Slope**	**Vel Chnl**	**Flow Area**	**Top Width**	**Froude # Chnl**	**Measured depth**	**Simulated depth**	**Percentage error**
			(m^3/s)	**(m)**	**(m)**	**(m)**	**(m)**	**(m/m)**	**(m/s)**	**(m^2)**	**(m)**		**(m)**	**(m)**	(%)
LC II Alignment	1740	PF 1	4.1	1206.00	1207.85		1207.85	0.000075	0.37	11.12	10.27	0.11	1.85	1.85	0.00
LC II Alignment	1490	PF 1	4.3	1205.79	1207.84		1207.84	0.000022	0.25	17.37	11.73	0.06	2.06	2.05	0.49
LC II Alignment	1293.33*	PF 1	3.4	1205.76	1207.84		1207.84	0.000016	0.21	16.25	11.37	0.06	2.05	2.08	1.46
LC II Alignment	1096.66*	PF 1	3.6	1205.74	1207.83		1207.84	0.000019	0.23	15.6	10.62	0.06	2.03	2.09	2.96
LC II Alignment	900	PF 1	3.9	1205.71	1207.83		1207.83	0.000024	0.25	15.38	10.47	0.07	2.03	2.12	4.43
LC II Alignment	770.*	PF 1	4.2	1205.76	1207.83		1207.83	0.000028	0.27	15.56	10.74	0.07	2.02	2.07	2.48
LC II Alignment	640	PF 1	4.4	1205.8	1207.82		1207.83	0.000025	0.26	16.66	10.74	0.07	2.00	2.02	1.00
LC II Alignment	510.*	PF 1	4.47	1206.03	1207.81		1207.82	0.000148	0.44	10.19	9.56	0.14	1.80	1.78	1.11
LC II Alignment	380	PF 1	4.5	1206.26	1207.75		1207.78	0.000942	0.73	6.19	6.66	0.24	1.50	1.49	0.67
LC II Alignment	190.*	PF 1	4.5	1206.33	1207.45		1207.50	0.002397	1.01	4.43	7.1	0.41	1.20	1.12	6.67
LC II Alignment	0	PF 1	4.5	1206.40	1207.4	1206.78	1207.41	0.000166	0.47	9.75	12.31	0.17	1.00	1.00	0.00
	PF = Profile Flow *Interpolated values														

Table A3: Model Output Details for TMC n=0.016

Reach	Canal Station	Profile	Q Total	Min Ch Elev	W.S. Elev	Crit W.S.	E.G. Elev	E.G. Slope	Vel Chnl	Flow Area	Top Width	Froude # Chnl	Measured Depth	Simulated Depth
			(m^3/s)	(m)	(m)	(m)	(m)	(m/m)	(m/s)	(m^2)	(m)		(m)	(m)
Reach #1	2600	PF 1	0.80	1203.65	1203.97		1203.97	0.000330	0.40	2.02	6.79	0.23	0.32	0.32
Reach #1	2500	PF 1	0.80	1203.60	1203.93		1203.94	0.000183	0.38	2.11	6.85	0.22	0.35	0.33
Reach #1	2450	PF 1	0.90	1203.54	1203.88		1203.89	0.000313	0.50	1.81	5.73	0.28	0.35	0.34
Reach #1	2400	PF 1	1.20	1203.50	1203.68	1203.68	1203.76	0.004685	1.30	0.92	5.40	1.00	0.20	0.18
Reach #1	2350	PF 1	1.20	1203.46	1203.64	1203.64	1203.72	0.004774	1.31	0.92	5.38	1.01	0.20	0.18
Reach #1	2300	PF 1	1.20	1203.02	1203.33		1203.36	0.000725	0.72	1.66	5.69	0.43	0.28	0.31
Reach #1	2250	PF 1	1.20	1202.96	1203.21		1203.25	0.001552	0.91	1.31	5.62	0.60	0.30	0.25
Reach #1	2200	PF 1	1.20	1202.95	1203.13	1203.13	1203.21	0.004701	1.30	0.93	5.44	1.00	0.35	0.18
Reach #1	2150	PF 1	1.20	1202.03	1202.21	1202.21	1202.29	0.004701	1.30	0.93	5.44	1.00	0.35	0.18
Reach #1	2100	PF 1	1.20	1201.01	1201.19	1201.19	1201.27	0.004707	1.30	0.93	5.44	1.00	0.35	0.18
Reach #1	2050	PF 1	1.20	1200.50	1200.68	1200.68	1200.76	0.004701	1.30	0.93	5.44	1.00	0.35	0.18
Reach #1	2000	PF 1	1.20	1199.72	1200.08		1200.10	0.000447	0.62	1.95	5.90	0.34	0.35	0.36
Reach #1	1950	PF 1	1.20	1199.63	1199.81	1199.81	1199.89	0.004701	1.30	0.93	5.44	1.00	0.20	0.18
Reach #1	1900	PF 1	1.20	1199.54	1199.72	1199.72	1199.8	0.004694	1.30	0.93	5.44	1.00	0.20	0.18
Reach #1	1850	PF 1	1.20	1198.24	1199.55		1199.55	0.000005	0.14	8.71	8.28	0.04	1.30	1.31
Reach #1	1800	PF 1	1.20	1199.28	1199.46	1199.46	1199.54	0.004727	1.30	0.92	5.44	1.01	0.28	0.18
Reach #1	1750	PF 1	1.20	1197.79	1198.02		1198.07	0.002116	1.01	1.19	5.56	0.70	0.20	0.23
Reach #1	1700	PF 1	1.20	1197.74	1197.92	1197.92	1198.00	0.004727	1.30	0.92	5.44	1.01	0.20	0.18
Reach #1	1650	PF 1	1.20	1196.14	1196.32	1196.32	1196.40	0.004727	1.30	0.92	5.44	1.01	0.20	0.18
Reach #1	1600	PF 1	1.20	1192.91	1193.09	1193.09	1193.17	0.004701	1.30	0.93	5.44	1.00	0.20	0.18
Reach #1	1550	PF 1	1.31	1192.27	1192.59		1192.62	0.000753	0.75	1.75	5.81	0.44	0.32	0.32
Reach #1	1500	PF 1	1.31	1192.05	1192.43		1192.45	0.000436	0.63	2.08	5.95	0.34	0.35	0.38
Reach #1	1450	PF 1	1.31	1192.02	1192.43		1192.45	0.000343	0.58	2.25	6.02	0.30	0.41	0.41
Reach #1	1400	PF 1	1.63	1191.82	1192.04	1192.04	1192.14	0.004450	1.43	1.14	5.54	1.00	0.20	0.22

Reach	Canal Station	Profile	Q Total	Min Ch Elev	W.S. Elev	Crit W.S.	E.G. Elev	E.G. Slope	Vel Chnl	Flow Area	Top Width	Froude # Chnl	Measured Depth	Simulated Depth
Reach #1	1350	PF 1	1.63	1186.95	1187.35		1187.38	0.000579	0.74	2.19	6.00	0.39	0.40	0.40
Reach #1	1300	PF 1	1.63	1186.85	1187.07	1187.07	1187.17	0.00445	1.43	1.14	5.54	1.00	0.22	0.22
Reach #1	1250	PF 1	1.63	1186.45	1186.88		1186.90	0.000459	0.69	2.36	6.07	0.35	0.40	0.43
Reach #1	1200	PF 1	1.83	1186.37	1186.6	1186.6	1186.72	0.004349	1.48	1.24	5.59	1.00	0.22	0.23
Reach #1	1150	PF 1	1.83	1184.29	1184.79		1184.81	0.000342	0.65	2.80	6.25	0.31	0.50	0.50
Reach #1	1100	PF 1	1.83	1184.06	1184.29	1184.29	1184.41	0.004349	1.48	1.24	5.59	1.00	0.22	0.23
Reach #1	1050	PF 1	1.83	1183.08	1183.49		1183.52	0.000669	0.81	2.25	6.02	0.42	0.40	0.41
Reach #1	1000	PF 1	1.90	1183.03	1183.27	1183.27	1183.38	0.004323	1.50	1.27	5.60	1.00	0.20	0.24
Reach #1	950	PF 1	1.90	1182.06	1182.38		1182.44	0.001676	1.11	1.71	5.80	0.65	0.32	0.32
Reach #1	900	PF 1	1.90	1181.47	1181.95		1181.98	0.00042	0.71	2.69	6.20	0.34	0.45	0.48
Reach #1	850	PF 1	2.00	1181.37	1181.62	1181.62	1181.74	0.004315	1.53	1.31	5.62	1.01	0.25	0.25
Reach #1	800	PF 1	2.00	1178.80	1179.31		1179.33	0.000387	0.70	2.85	6.27	0.33	0.50	0.51
Reach #1	750	PF 1	2.00	1178.72	1179.00	1179.00	1179.14	0.004185	1.61	1.24	4.71	1.00	0.30	0.28
Reach #1	700	PF 1	2.00	1176.78	1177.29		1177.33	0.000583	0.85	2.36	5.28	0.40	0.50	0.51
Reach #1	650	PF 1	2.00	1176.70	1176.98	1176.98	1177.12	0.004185	1.61	1.24	4.71	1.00	0.28	0.28
Reach #1	600	PF 1	2.00	1175.81	1176.3	1176.1	1176.34	0.000686	0.89	2.24	5.22	0.44	0.48	0.49
Reach #1	550	PF 1	2.00	1175.75	1176.04	1176.04	1176.17	0.004148	1.61	1.24	4.71	1.00	0.30	0.29
Reach #1	500	PF 1	2.00	1174.55	1175.28		1175.3	0.000167	0.55	3.61	5.84	0.22	0.70	0.73
Reach #1	450	PF 1	3.30	1174.52	1175.23		1175.28	0.000503	0.95	3.49	5.79	0.39	0.70	0.71
Reach #1	400	PF 1	3.30	1174.37	1174.76	1174.76	1174.94	0.003844	1.87	1.76	4.99	1.00	0.40	0.39
Reach #1	350	PF 1	3.30	1173.09	1173.78		1173.83	0.000562	0.98	3.36	5.73	0.41	0.65	0.69
Reach #1	300	PF 1	3.30	1172.99	1173.38	1173.38	1173.56	0.003872	1.88	1.76	4.98	1.01	0.40	0.39
Reach #1	250	PF 1	3.50	1171.90	1172.76	1172.31	1172.79	0.000300	0.81	4.34	6.14	0.31	0.85	0.86
Reach #1	0	PF1	3.50										1.00	0.98

Appendix 5: As built cross-sections

Table A4: As-built canal cross-section interpolation

Slope				0.0003		**Drop 1**	
Ch	**0**		**155**	**355**	**480**	**487**	**491**
dx			155	200	125	7	4
	x	y	y	y	y	yu	yd
	0	1205.7065	1205.662	1205.602	1205.5645	1205.527	1205.077
	1.1327	1204.6765	1204.6	1204.54	1204.5025	1204.465	1204.015
	2.577	1203.6465	1203.6	1203.54	1203.5025	1203.465	1203.015
	8.577	1203.6465	1203.6	1203.54	1203.5025	1203.465	1203.015
	9.827	1204.6765	1204.6	1204.54	1204.5025	1204.465	1204.015
	11.154	1205.7065	1205.662	1205.602	1205.5645	1205.527	1205.077
Chainage 0 +000 to 0+491							

Slope	0.0005		**Drop 2**		**Drop 3**	**Drop 4**		
Ch	**600**		**613**	**624**	**852**	**858**	**1157**	**1329**
dx	109		13	11		6	299	172
	x	y	yu	yd	yu	yd	y	y
	0	1204.7005	1204.694	1203.774	1202.75	1202.24	1201.46	1201.374
	1.0875	1203.8305	1203.824	1202.904	1201.88	1201.37	1200.59	1200.504
	2.175	1202.9605	1202.954	1202.034	1201.01	1200.5	1199.72	1199.634
	7.175	1202.9605	1202.954	1202.034	1201.01	1200.5	1199.72	1199.634
	8.2625	1203.8305	1203.824	1202.904	1201.88	1201.37	1200.59	1200.504
	9.35	1204.7005	1204.694	1203.774	1202.75	1202.24	1201.46	1201.374
Chainage 0+491 to 1+329								

Slope		**Drop 5**		**Drop 6**		0.000635	**Drop 7**	
		1520	**1530**	**1944**	**1954**	**2031**	**2051**	**2211**
dx		191	10	414	10	77	20	160
	x	yu	yd	yu	yd	yu	yd	yu
	0	1201.2785	1199.9785	1201.0156	1199.5256	1199.4767	1197.8767	1194.65
	1.0875	1200.4085	1199.1085	1200.1456	1198.6556	1198.6067	1197.0067	1193.78
	2.175	1199.5385	1198.2385	1199.2756	1197.7856	1197.7367	1196.1367	1192.91
	7.175	1199.5385	1198.2385	1199.2756	1197.7856	1197.7367	1196.1367	1192.91
	8.2625	1200.4085	1199.1085	1200.1456	1198.6556	1198.6067	1197.0067	1193.78
	9.35	1201.2785	1199.9785	1201.0156	1199.5256	1199.4767	1197.8767	1194.65
Chainage 1+329 to 2+211								

		Drop 8	0.000635	**Drop 9**	**Drop 10**	0.000483		**Drop 11**
Ch		**2231**	**2575**	**2585**	**2896**	**3060**	**3220**	**3243**
dx		20	344	10	311	164	160	23
	x	yd	yu	yd	yu	yd	yu	yd
	0	1194.01	1193.7916	1193.7616	1193.5641	1188.6941	1188.5925	1188.1925
	1.0875	1193.14	1192.9216	1192.8916	1192.6941	1187.8241	1187.7225	1187.3225
	2.175	1192.27	1192.0516	1192.0216	1191.8241	1186.9541	1186.8525	1186.4525
	7.175	1192.27	1192.0516	1192.0216	1191.8241	1186.9541	1186.8525	1186.4525
	8.2625	1193.14	1192.9216	1192.8916	1192.6941	1187.8241	1187.7225	1187.3225
	9.35	1194.01	1193.7916	1193.7616	1193.5641	1188.6941	1188.5925	1188.1925
Chainage 2+211 to 3+406								

	0.000483	**Drop 12**			**Drop 13**		**Drop 14**
Ch	**3406**		**3407**	**3880**	**3884**	**3978**	**3986**
dx	163		1	473	4	94	8
	yu	x	yd	yu	yd	yu	yd
	1188.1137	0	1186.0297	1185.8013	1184.8203	1184.7749	1183.8049
	1187.2437	1.0875	1185.1597	1184.9313	1183.9503	1183.9049	1182.9349
	1186.3737	2.175	1184.2897	1184.0613	1183.0803	1183.0349	1182.0649
	1186.3737	7.175	1184.2897	1184.0613	1183.0803	1183.0349	1182.0649
	1187.2437	8.2625	1185.1597	1184.9313	1183.9503	1183.9049	1182.9349
	1188.1137	9.35	1186.0297	1185.8013	1184.8203	1184.7749	1183.8049
	Chainage 3+406 to 3+986						

			0.000421	Drop 15		**Drop 16**	0.0005	**Drop 17**
Ch	0.00081	**4720**	**4953**	**4960**	**5151**	**5160**	**5321**	**5326**
dx		734	233	7	191	9	161	5
	x	yu	yu	yd	yu	yd	yu	yd
	0	1183.2103	1183.1123	1180.5403	1180.4598	1178.5198	1178.4393	1177.5493
	1.0875	1182.3403	1182.2423	1179.6703	1179.5898	1177.6498	1177.5693	1176.6793
	2.175	1181.4703	1181.3723	1178.8003	1178.7198	1176.7798	1176.6993	1175.8093
	6.175	1181.4703	1181.3723	1178.8003	1178.7198	1176.7798	1176.6993	1175.8093
	7.2625	1182.3403	1182.2423	1179.6703	1179.5898	1177.6498	1177.5693	1176.6793
	8.35	1183.2103	1183.1123	1180.5403	1180.4598	1178.5198	1178.4393	1177.5493
Chainage 3+986 to 5+326								

			Drop 18			**Drop 19**		**Drop 20**
Ch		**5441**	**5443**	**5502**	**5802**		**6018**	**6028**
dx		115	2	59	298	2	216	10
	x	yu	yd	yu	yu	yd	yu	yd
	0	1177.4918	1176.2918	1176.2623	1176.1133	1174.8343	1174.7263	1173.6363
	1.0875	1176.6218	1175.4218	1175.3923	1175.2433	1173.9643	1173.8563	1172.7663
	2.175	1175.7518	1174.5518	1174.5223	1174.3733	1173.0943	1172.9863	1171.8963
	6.175	1175.7518	1174.5518	1174.5223	1174.3733	1173.0943	1172.9863	1171.8963
	7.2625	1176.6218	1175.4218	1175.3923	1175.2433	1173.9643	1173.8563	1172.7663
	8.35	1177.4918	1176.2918	1176.2623	1176.1133	1174.8343	1174.7263	1173.6363
Chainage 5+326 to 6+028								

		Drop 21		**Drop 22**	0.00258	Drop 23		**Drop 24**
Ch		**6270**	**6273**	**6639**	**6644**	**6927**	**6932**	**7175**
dx		242	3	366	5	283	5	
	x	yu	yd	yu	yd	yu	yd	y
	0	1172.8208	1171.8008	1170.5674	1169.3474	1168.6172	1168.2972	1167.6703
	1.0875	1171.9508	1170.9308	1169.6974	1168.4774	1167.7472	1167.4272	1166.8003
	2.175	1171.0808	1170.0608	1168.8274	1167.6074	1166.8772	1166.5572	1165.9303
	6.175	1171.0808	1170.0608	1168.8274	1167.6074	1166.8772	1166.5572	1165.9303
	7.2625	1171.9508	1170.9308	1169.6974	1168.4774	1167.7472	1167.4272	1166.8003
	8.35	1172.8208	1171.8008	1170.5674	1169.3474	1168.6172	1168.2972	1167.6703
Chainage 6+028 to 7+175								

Appendix 6: Cross-sections

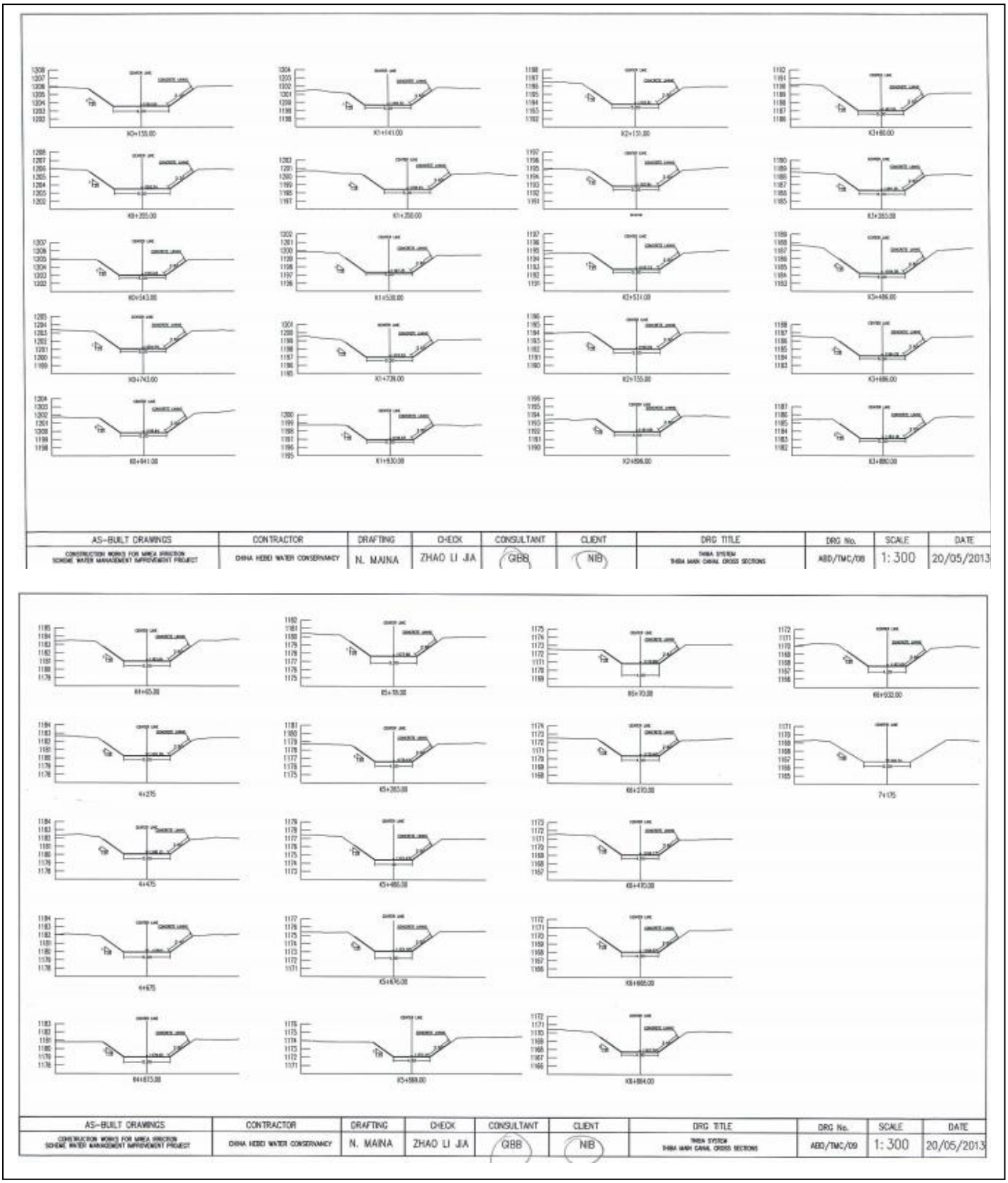

Figure A3: As-build cross-sections

Appendix 7: Profiles

Figure A4: Canal design capacities and profile plots

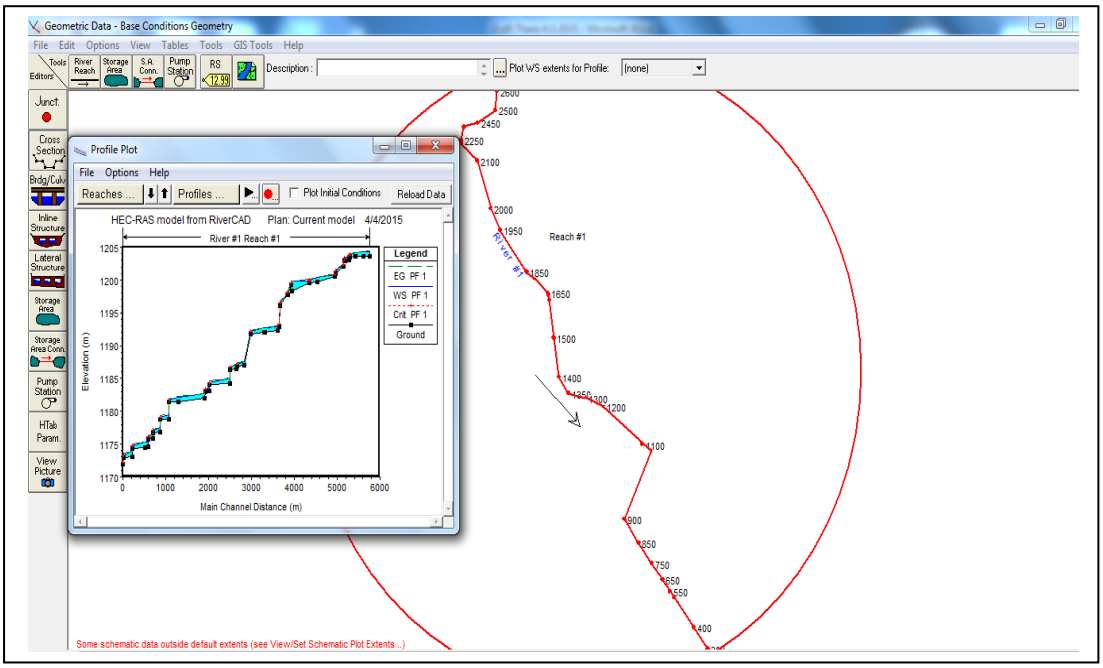

TMC canal alignment

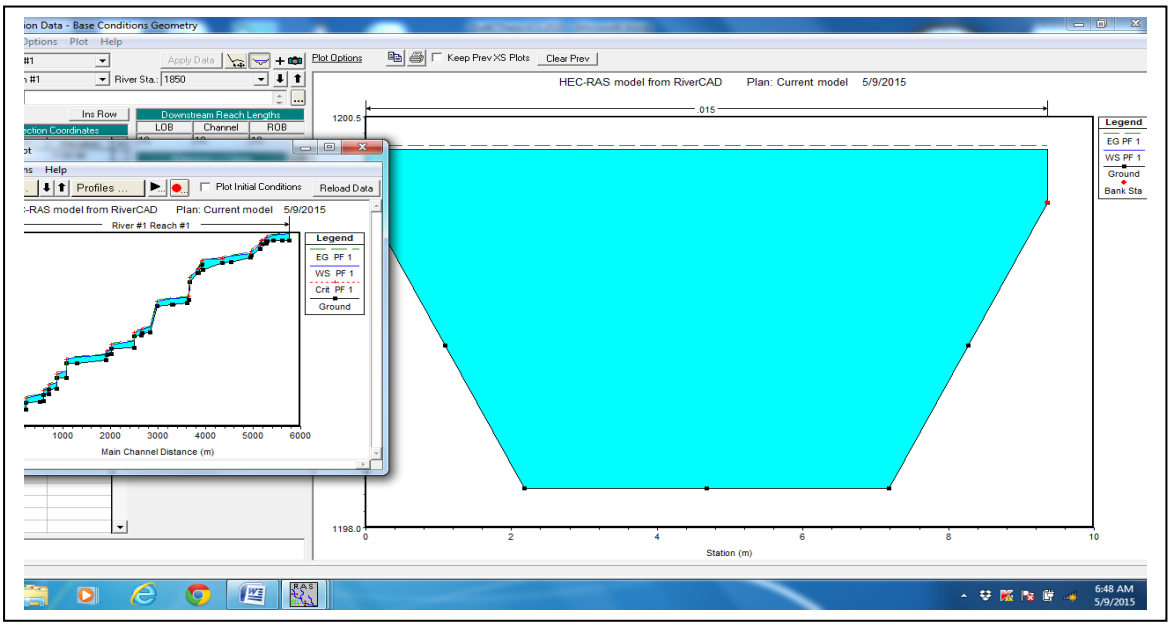

Canal Station 1850: Lined canal at design Q=6.4 m^3/s

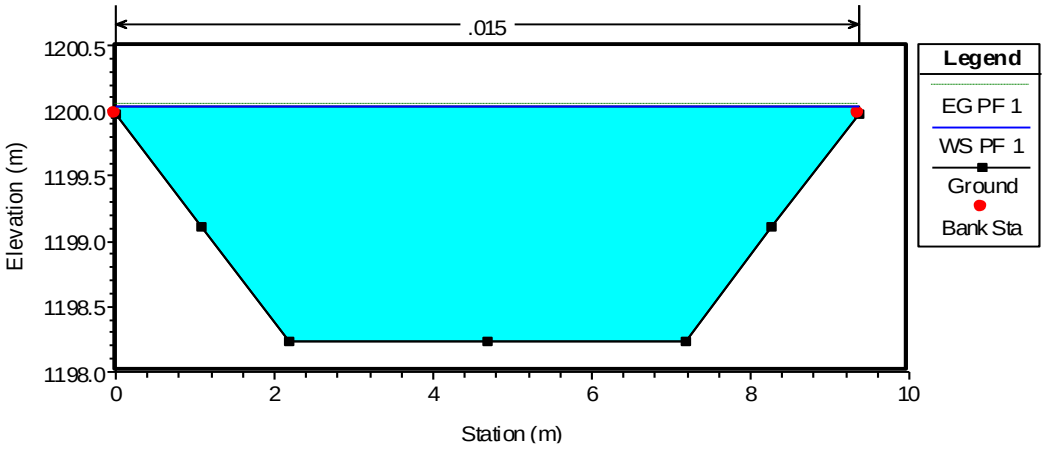

Canal station 1850: Lined canal with Q = 5.8m^3/s as a 8% reduction

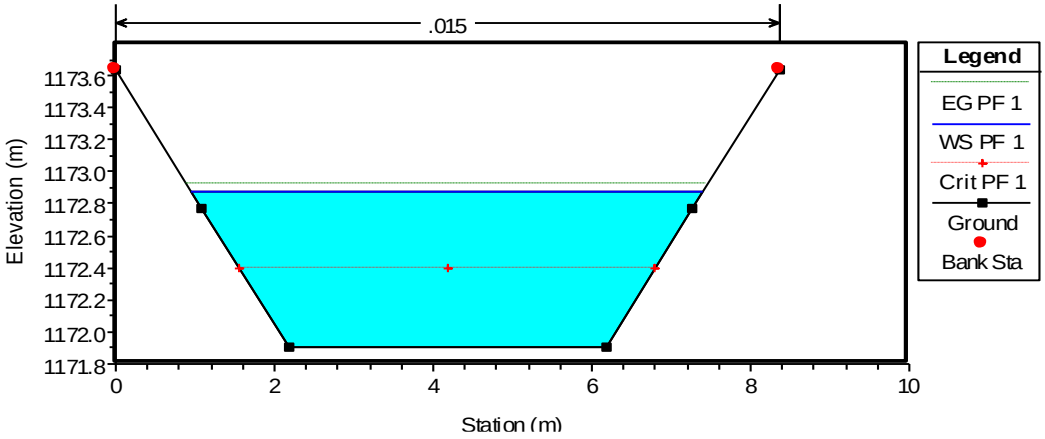

Canal station 250: Lined canal with Q = 4.7m^3/s as a 8% reduction

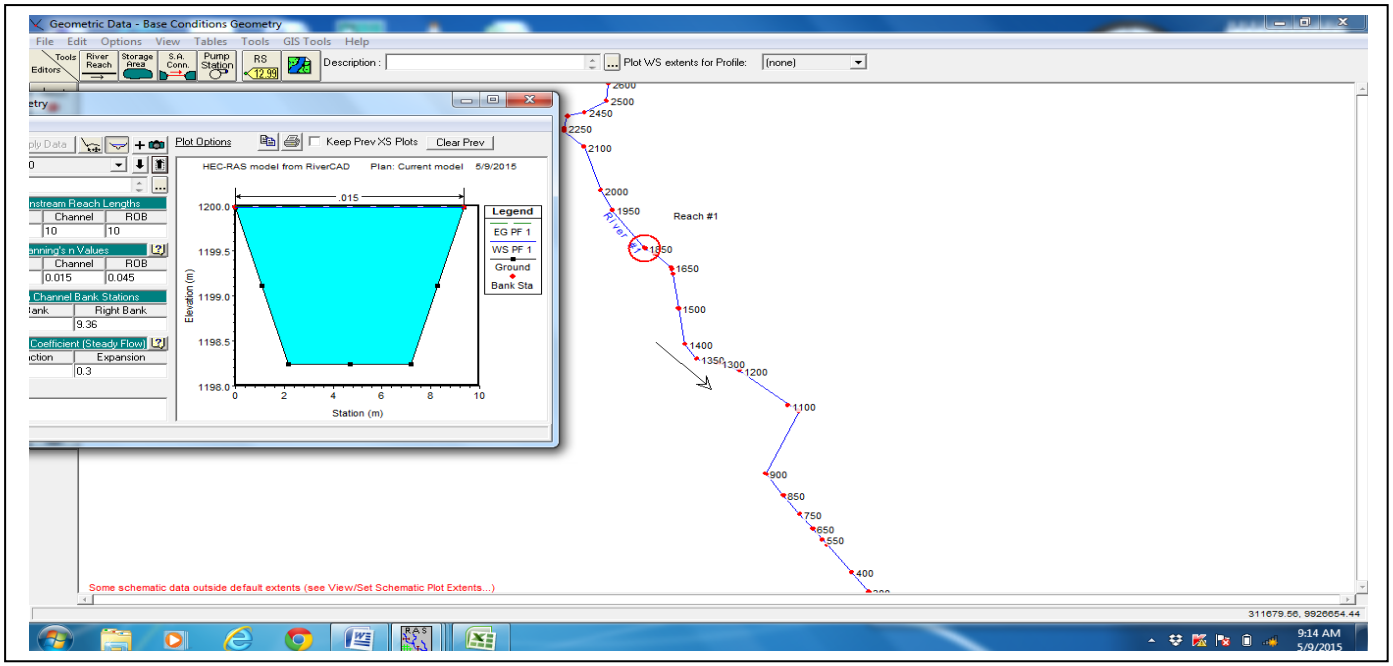

Location of canal station 1850 on TMC alignment

LCII profiles

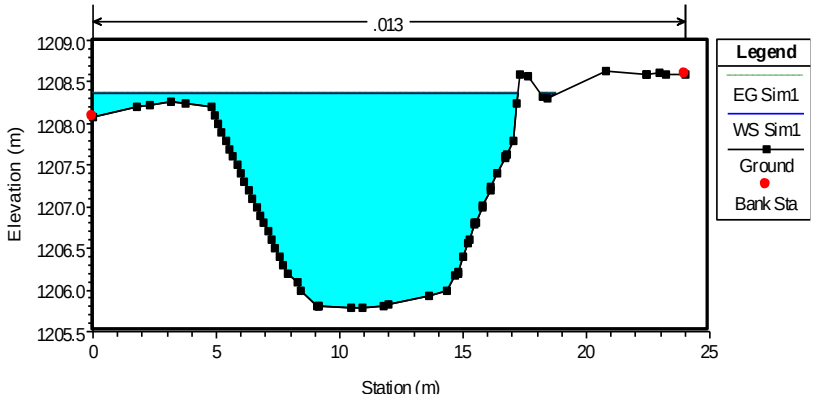

Canal station 1490: Earth canal overflowing the LHS bank at 9.9m^3/s flow

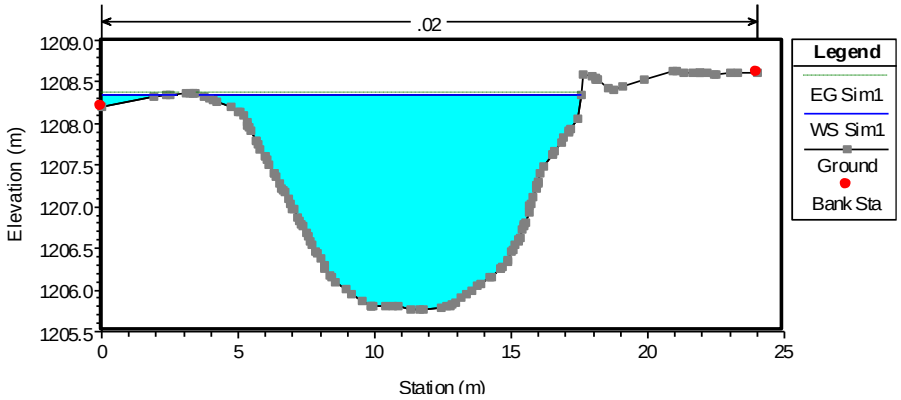

Canal station 1293: Interpolated cross-section

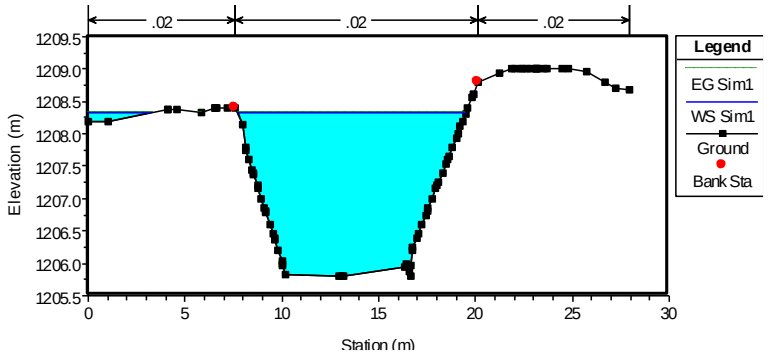

Canal station 840: Submerged bank on LCII

Figure A5: Complete set of cross-sections for the LCII model

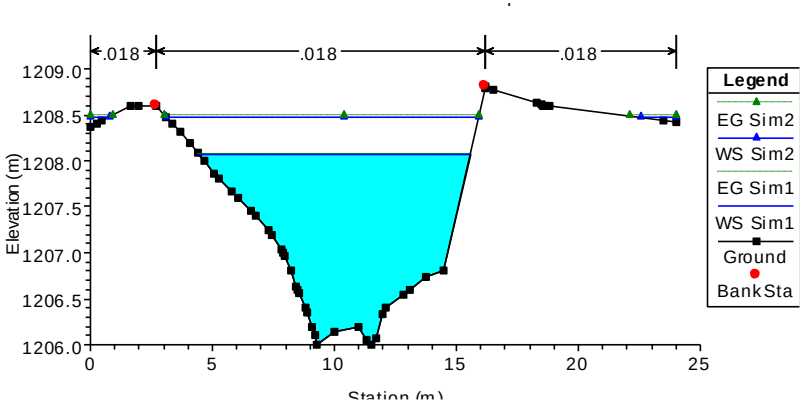

Canal station 1740: Unlined earth canal

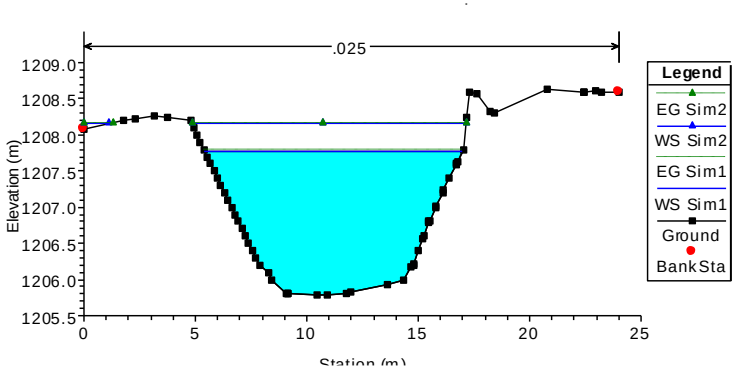

Canal station 1490: Unlined earth canal

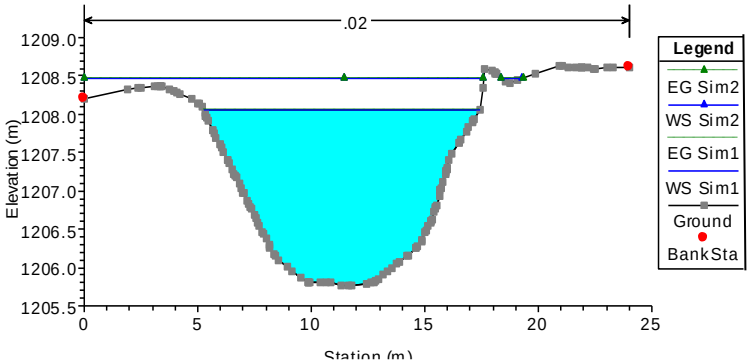

Canal station 1293: Interpolated canal section

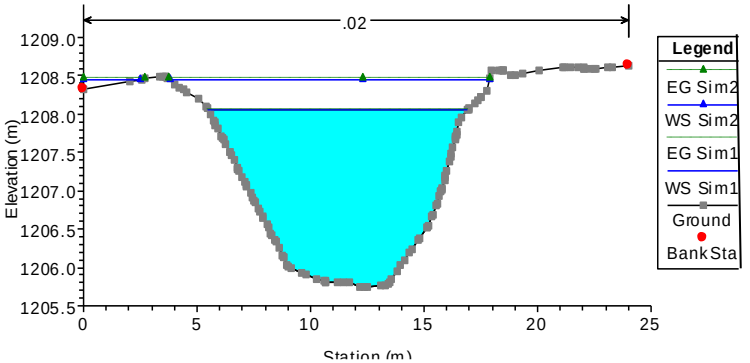

Canal station 1096: Interpolated canal section

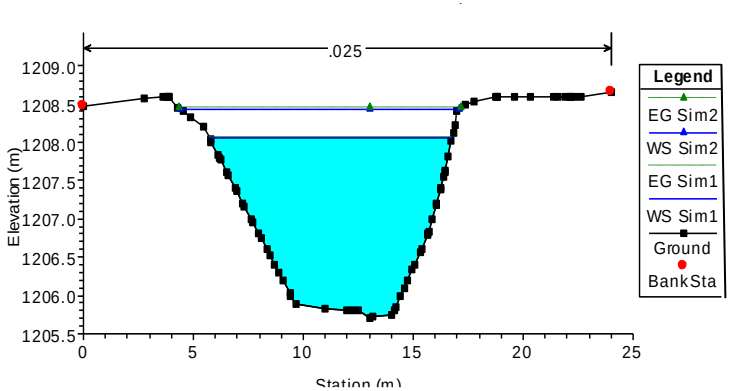

Canal station 900: Unlined earth canal

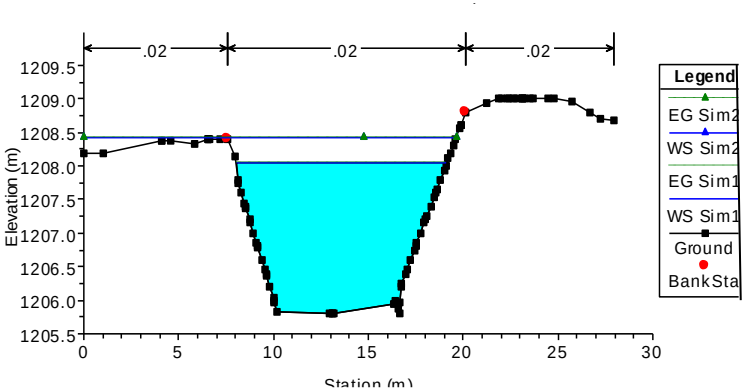

Canal station 640: Unlined earth canal

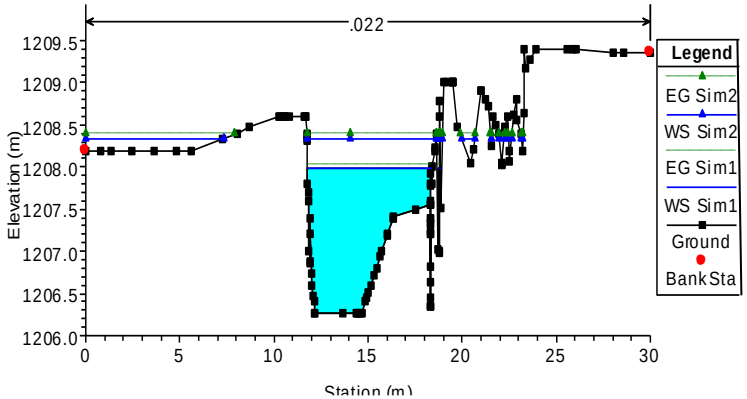

Canal station 380: At a drop structure

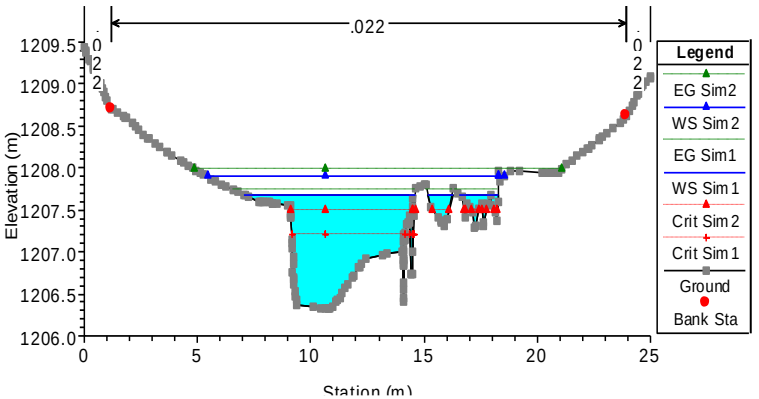

Canal station 190: Interpolated section near a drop structure

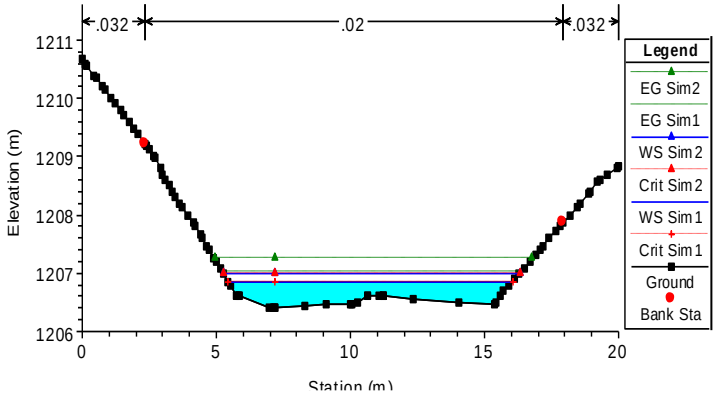

Canal station 000: At the beginning of the canal

Figure A6: Complete Set of Cross-Sections for the TMC Model

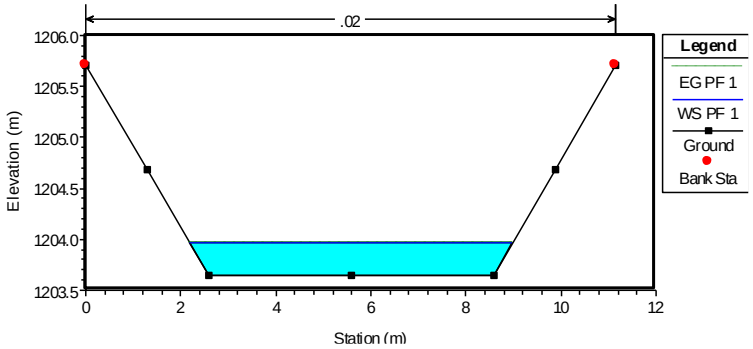

Canal station 2600: Lined canal

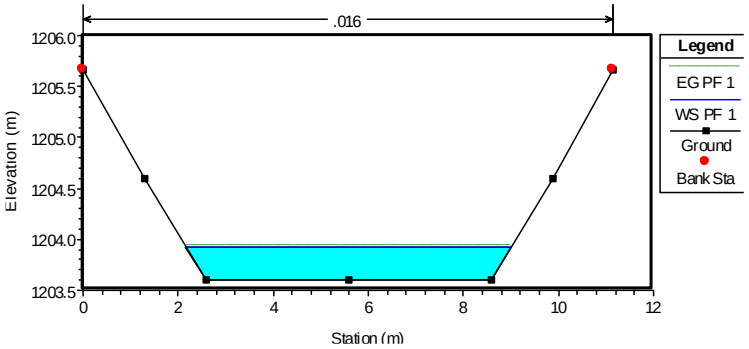

Canal station 2500: Lined canal

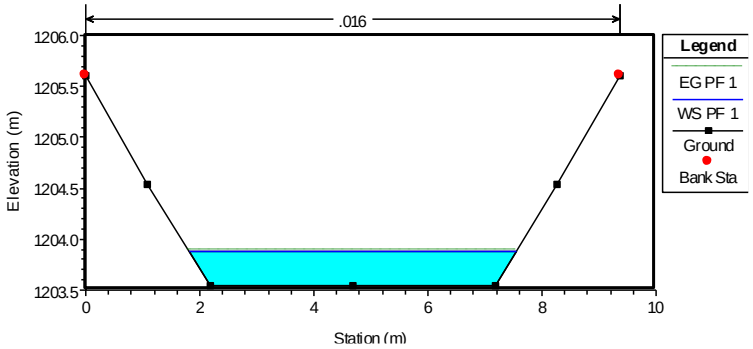

Canal station 2450: Lined canal

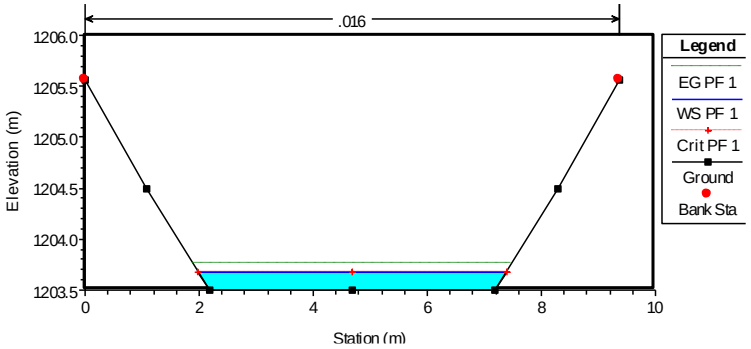

Canal station 2400: Lined canal

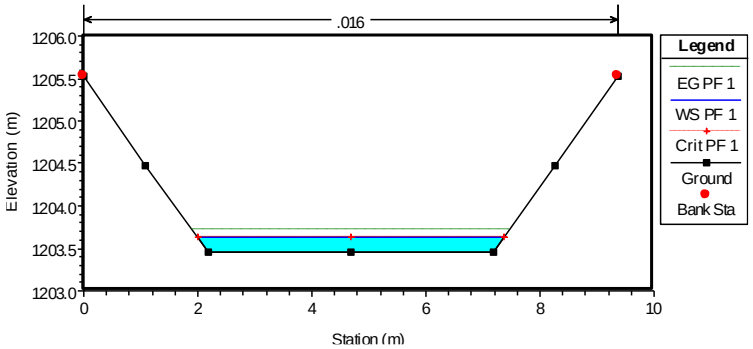

Canal station 2350: Lined section

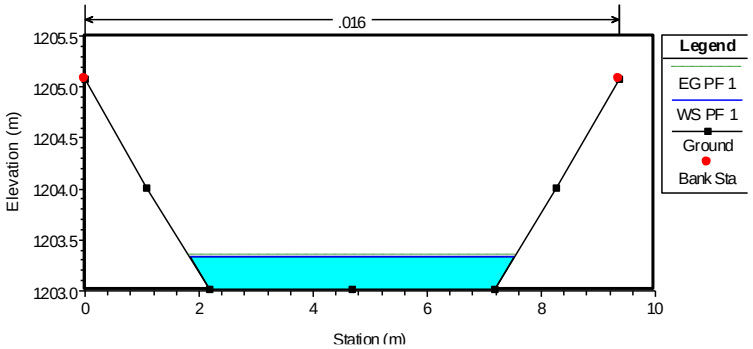

Canal station 2300: Lined canal section

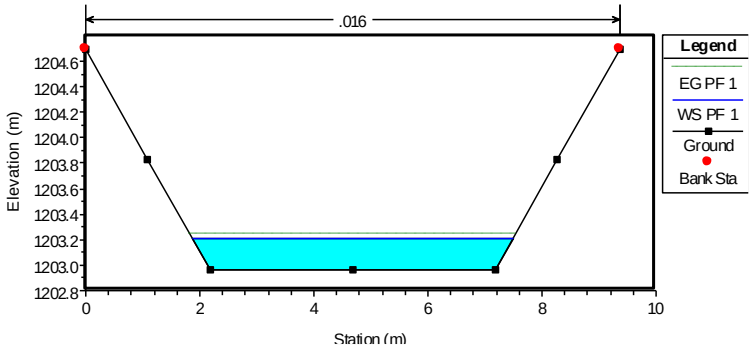

Canal station 2250: Lined canal

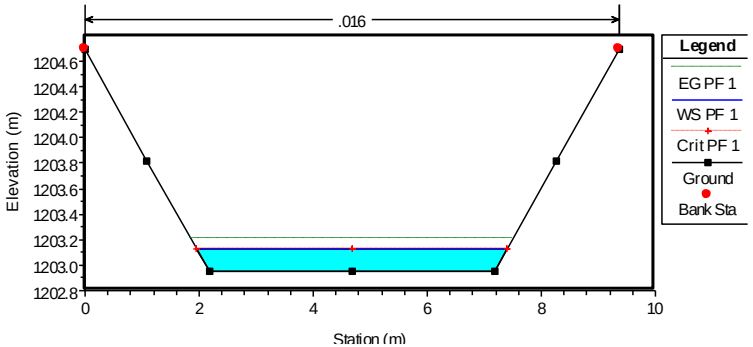

Canal Station 2200: Lined canal

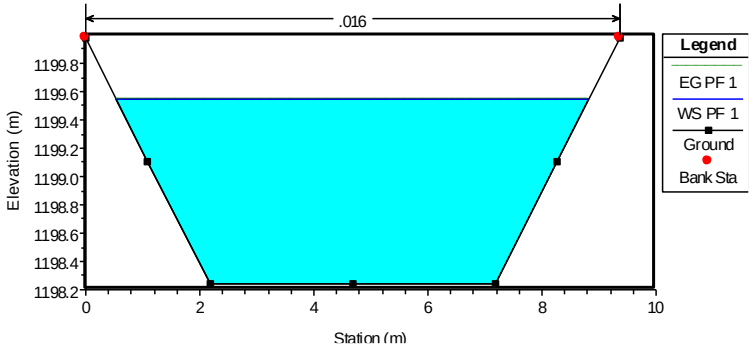

Canal station 1850: Increased flow volume at the section

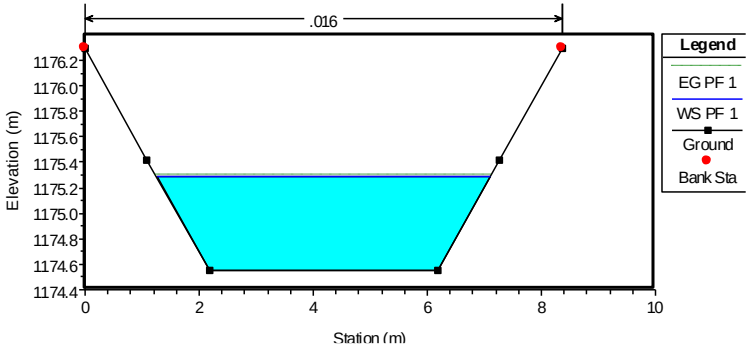

Canal station 500: Lined canal section

Appendix 8: Maximum canal flow capacity model outputs

Table A5: Maximum canal flow capacity estimation outputs - TMC

Reach	Canal Station	Profile	Q Total	Min Ch Elev	W.S. Elev	Crit W.S.	E.G. Elev	E.G. Slope	Vel Chnl	Flow Area	Top Width	Froude # Chnl	Depth (1)	Canal H (2)	= (1-2)
			(m^3/s)	(m)	(m)	(m)	(m)	(m/m)	(m/s)	(m^2)	(m)		(m)	(m)	(m)
Reach #1	2600	PF 1	10.20	1203.65	1204.81		1204.88	0.000371	1.19	8.60	8.89	0.38	1.16	1.74	0.58
Reach #1	2500	PF 1	10.20	1203.60	1204.75		1204.82	0.000376	1.19	8.58	8.94	0.39	1.15	1.74	0.59
Reach #1	2450	PF 1	10.20	1203.54	1204.58		1204.71	0.000783	1.60	6.39	7.27	0.54	1.04	1.74	0.7
Reach #1	2400	PF 1	10.20	1203.50	1204.21	1204.21	1204.52	0.002911	2.49	4.10	6.56	1.01	0.71	1.74	1.03
Reach #1	2350	PF 1	10.20	1203.46	1204.17	1204.17	1204.49	0.002895	2.49	4.10	6.53	1.00	0.71	1.74	1.03
Reach #1	2300	PF 1	10.20	1203.02	1204.00		1204.15	0.000957	1.71	5.97	7.16	0.60	0.98	1.74	0.76
Reach #1	2250	PF 1	10.20	1202.96	1203.66	1203.66	1203.97	0.002878	2.46	4.14	6.77	1.00	0.70	1.37	0.67
Reach #1	2200	PF 1	6.40	1202.95	1203.47	1203.47	1203.71	0.003087	2.16	2.97	6.31	1.00	0.52	1.37	0.85
Reach #1	2150	PF 1	6.40	1202.03	1202.55	1202.55	1202.79	0.00309	2.16	2.97	6.31	1.00	0.52	1.37	0.85
Reach #1	2100	PF 1	6.40	1201.01	1201.53	1201.53	1201.77	0.003117	2.16	2.96	6.31	1.01	0.52	1.37	0.85
Reach #1	2050	PF 1	6.40	1200.50	1201.02	1201.02	1201.26	0.003095	2.16	2.97	6.31	1.01	0.52	1.37	0.85
Reach #1	2000	PF 1	6.40	1199.72	1200.55		1200.64	0.000634	1.27	5.04	7.09	0.48	0.83	1.37	0.54
Reach #1	1950	PF 1	6.40	1199.63	1200.15	1200.15	1200.39	0.003104	2.16	2.96	6.31	1.01	0.52	1.37	0.85
Reach #1	1900	PF 1	6.40	1199.54	1200.06	1200.06	1200.3	0.003101	2.16	2.96	6.31	1.01	0.52	1.37	0.85
Reach #1	1850	PF 1	6.40	1198.24	1200.04		1200.05	0.000042	0.49	13.03	9.36	0.13	1.80	1.35	-0.45
Reach #1	1800	PF 1	6.20	1199.28	1199.79	1199.79	1200.03	0.003108	2.14	2.90	6.29	1.00	0.51	1.35	0.84
Reach #1	1750	PF 1	6.20	1197.79	1198.35	1198.3	1198.54	0.002294	1.93	3.21	6.41	0.87	0.56	1.35	0.79
Reach #1	1700	PF 1	6.20	1197.74	1198.25	1198.25	1198.49	0.003132	2.14	2.89	6.28	1.01	0.51	1.35	0.84
Reach #1	1650	PF 1	6.20	1196.14	1196.65	1196.65	1196.89	0.003127	2.14	2.89	6.29	1.01	0.51	1.35	0.84
Reach #1	1600	PF 1	6.20	1192.91	1193.42	1193.42	1193.66	0.003134	2.14	2.89	6.28	1.01	0.51	1.35	0.84
Reach #1	1550	PF 1	6.20	1192.27	1193.06		1193.15	0.000712	1.31	4.75	6.98	0.51	0.79	1.35	0.56
Reach #1	1500	PF 1	6.20	1192.05	1192.86		1192.94	0.000656	1.27	4.88	7.03	0.49	0.81	1.35	0.54
Reach #1	1450	PF 1	6.20	1192.02	1192.86		1192.94	0.000583	1.22	5.08	7.10	0.46	0.84	1.35	0.51

Reach	Canal Station	Profile	Q Total	Min Ch Elev	W.S. Elev	Crit W.S.	E.G. Elev	E.G. Slope	Vel Chnl	Flow Area	Top Width	Froude # Chnl	Depth (1)	Canal H (2)	= (1-2)
Reach #1	1400	PF 1	6.20	1191.82	1192.33	1192.33	1192.57	0.003106	2.14	2.90	6.29	1.00	0.51	1.35	0.84
Reach #1	1350	PF 1	6.20	1186.95	1187.73		1187.82	0.00074	1.32	4.68	6.96	0.52	0.78	1.35	0.57
Reach #1	1300	PF 1	6.20	1186.85	1187.37	1187.37	1187.6	0.003092	2.13	2.91	6.29	1.00	0.52	1.35	0.83
Reach #1	1250	PF 1	6.20	1186.45	1187.24		1187.33	0.000709	1.30	4.75	6.99	0.51	0.79	1.35	0.56
Reach #1	1150	PF 1	6.10	1184.29	1185.19		1185.26	0.000438	1.10	5.54	7.26	0.40	0.90	1.35	0.45
Reach #1	1100	PF 1	6.10	1184.06	1184.57	1184.57	1184.8	0.003113	2.13	2.87	6.27	1.00	0.51	1.35	0.84
Reach #1	1050	PF 1	6.10	1183.08	1183.82		1183.92	0.000864	1.39	4.40	6.86	0.55	0.74	1.35	0.61
Reach #1	1000	PF 1	6.10	1183.03	1183.54	1183.54	1183.77	0.003129	2.13	2.86	6.27	1.01	0.51	1.35	0.84
Reach #1	950	PF 1	6.10	1182.06	1182.74		1182.86	0.001163	1.53	3.98	6.7	0.64	0.68	1.31	0.63
Reach #1	900	PF 1	5.90	1181.47	1182.29		1182.37	0.000563	1.19	4.97	7.06	0.45	0.82	1.31	0.49
Reach #1	850	PF 1	5.90	1181.37	1181.87	1181.87	1182.09	0.003144	2.11	2.80	6.25	1.01	0.50	1.31	0.81
Reach #1	800	PF 1	5.90	1178.80	1179.68		1179.74	0.000447	1.10	5.37	7.21	0.41	0.88	1.31	0.43
Reach #1	750	PF 1	5.90	1178.72	1179.29	1179.29	1179.54	0.003103	2.21	2.67	5.42	1.00	0.57	1.31	0.74
Reach #1	700	PF 1	5.80	1176.78	1177.64		1177.73	0.000705	1.32	4.38	6.16	0.50	0.86	1.31	0.45
Reach #1	650	PF 1	5.80	1176.70	1177.26	1177.26	1177.51	0.003112	2.20	2.64	5.41	1.01	0.56	1.21	0.65
Reach #1	600	PF 1	5.80	1175.81	1176.64		1176.74	0.000814	1.39	4.17	6.07	0.54	0.83	1.21	0.38
Reach #1	550	PF 1	5.80	1175.75	1176.31	1176.31	1176.56	0.003132	2.20	2.63	5.4	1.01	0.56	1.21	0.65
Reach #1	500	PF 1	5.80	1174.55	1175.48		1175.55	0.000546	1.21	4.79	6.32	0.44	0.93	1.21	0.28
Reach #1	450	PF 1	5.80	1174.52	1175.44		1175.52	0.000552	1.22	4.77	6.32	0.45	0.92	1.21	0.29
Reach #1	400	PF 1	5.80	1174.37	1174.93	1174.93	1175.18	0.003099	2.20	2.64	5.41	1.00	0.56	1.21	0.65
Reach #1	350	PF 1	5.80	1173.09	1173.97		1174.06	0.000648	1.29	4.51	6.21	0.48	0.88	1.21	0.33
Reach #1	300	PF 1	5.60	1172.99	1173.54	1173.54	1173.78	0.003143	2.18	2.57	5.37	1.01	0.55	1.27	0.72
Reach #1	250	PF 1	5.10	1171.90	1172.92	1172.42	1172.97	0.0003	0.95	5.39	6.56	0.33	1.02	1.27	0.25

Table A6: Maximum canal flow capacity estimation outputs - LCII

Reach	Canal Station	Profile	Q Total	Min Ch Elev	W.S. Elev	Crit W.S.	E.G. Elev	E.G. Slope	Vel Chnl	Flow Area	Top Width	Froude # Chnl	Depth (1)	Canal H (2)	=(1-2)
			(m^3/s)	(m)	(m)	(m)	(m)	(m/m)	(m/s)	(m^2)	(m)		(m)		
LC II Alignment	1740	Sim1	8.00	1206	1208.36		1208.37	0.000056	0.47	16.88	12.28	0.13	2.36	2.50	-0.14
LC II Alignment	1490	Sim1	8.00	1205.79	1208.36		1208.36	0.000014	0.33	24.43	17.83	0.09	2.57	2.50	0.07
LC II Alignment	1293.33*	Sim1	8.50	1205.76	1208.35		1208.36	0.000042	0.37	22.80	16.74	0.10	2.59	2.50	0.09
LC II Alignment	1096.66*	Sim1	8.50	1205.74	1208.34		1208.35	0.000039	0.39	21.58	13.78	0.10	2.60	2.50	0.10
LC II Alignment	900	Sim1	9.00	1205.71	1208.33		1208.34	0.000066	0.43	20.98	12.15	0.10	2.62	2.50	0.12
LC II Alignment	640	Sim1	9.00	1205.8	1208.32		1208.33	0.000035	0.40	22.47	14.96	0.09	2.52	2.50	0.02
LC II Alignment	380	Sim1	9.00	1206.26	1208.26		1208.3	0.001401	0.89	10.13	14.25	0.34	2.00	2.20	-0.20
LC II Alignment	190.*	Sim1	9.90	1206.33	1207.84	1207.42	1207.92	0.002787	1.25	7.91	12.46	0.50	1.51	1.60	-0.09
LC II Alignment	0	Sim1	9.90	1206.4	1206.97	1206.97	1207.19	0.005443	2.08	4.76	10.95	1.01	0.57	0.80	-0.23

1207.42 and 1206.97 in Critical water surface column are the elevations for the set boundary conditions

Appendix 9: List of publications

1. A Paper Review on Hydraulic Analysis of Irrigation Canals Using HEC-RAS Model: A Case Study of Mwea Irrigation Scheme, Kenya. Journal of Hydrology December, 2014
2. Calibration of Channel roughness coefficient for Thiba Main canal Reach in Mwea Irrigation scheme, Kenya. Journal of Hydrology, September 2015